
Tome 20

Mai 1982

Numéro 2

La mer

うみ

昭和 57 年 5 月

日 仏 海 洋 学 会

La Société franco-japonaise
d'océanographie
Tokyo, Japon

日 仏 海 洋 学 会

編 集 委 員 会

委員長	富永政英 (鹿児島大学)		
委員	有賀祐勝 (東京水産大学)	半沢正男 (神戸商船大学)	井上 実 (東京水産大学)
	神田献二 (東京水産大学)	増田辰良 (東京水産大学)	森田良美 (東京水産大学)
	西村 実 (東海大学)	高木和徳 (東京水産大学)	高野健三 (筑波大学)
	宇野 寛 (東京水産大学)	柳川三郎 (東京水産大学)	

投 稿 規 定

1. 報文の投稿者は本会会員に限る。
2. 原稿は簡潔にわかりやすく書き、図表を含めて印刷ページで10ページ以内を原則とする。原稿（正1通、副1通）は、(〒101) 東京都千代田区神田駿河台2-3 日仏会館内 日仏海洋学会編集委員会宛に送ること。
3. 編集委員会は、事情により原稿の字句の加除訂正を行うことがある。
4. 論文（欧文、和文とも）には必ず約200語の欧文（原則として仏語）の要旨をつけること。欧文論文には欧文の要旨のほかにも必ず約500字の和文の要旨をつけること。
5. 図及び表は必要なもののみに限る。図はそのまま版下になるように縮尺を考慮して鮮明に黒インクで書き、論文の図及び表には必ず英文（又は仏文）の説明をつけること。
6. 初校は原則として著者が行う。
7. 報文には1編につき50部の別刷を無料で著者に進呈する。これ以上の部数に対しては、実費（送料を含む）を著者が負担する。

Rédacteur en chef Masahide TOMINAGA (Kagoshima University)
Comité de rédaction Yusho ARUGA (Tokyo University of Fisheries) Masao HANZAWA (Kobe University of Mercantile Marine) Makoto INOUE (Tokyo University of Fisheries) Kenji KANDA (Tokyo University of Fisheries) Tatsuyoshi MASUDA (Tokyo University of Fisheries) Yoshimi MORITA (Tokyo University of Fisheries) Minoru NISHIMURA (Tokai University) Kazunori TAKAGI (Tokyo University of Fisheries) Kenzo TAKANO (University of Tsukuba) Yutaka UNO (Tokyo University of Fisheries) Saburo YANAGAWA (Tokyo University of Fisheries)

RECOMMANDATIONS A L'USAGE DES AUTEURS

1. Les auteurs doivent être des membres de la Société franco-japonaise d'océanographie.
2. Les notes ne peuvent dépasser dix pages. Les manuscrits à deux exemplaires, dactylographiés sur papier fort, doivent être envoyés au Comité de rédaction de la Société franco-japonaise d'océanographie, c/o Maison franco-japonaise, 2-3, Kanda Surugadai, Chiyoda-ku, Tokyo, 101 Japon.
3. Le Comité de rédaction se réserve le droit d'apporter, le cas échéant, des modifications mineuses aux manuscrits ainsi que de demander aux auteurs de les corriger.
4. Des résumés en langue japonaise ou langue française sont obligatoires.
5. Les figures au trait seront tracées à l'encre de Chine noire sur papier blanc ou sur calque. Les légendes des figures et des tableaux sont indispensables.
6. Les premières épreuves seront corrigées, en principe, par les auteurs.
7. Un tirage à part des articles en cinquante exemplaires est offert gratuitement aux auteurs. Ceux qui en désirent un plus grand nombre peuvent les faire établir à leurs frais.

Estimation of the Kuroshio Mass Transport Flowing out of the East China Sea to the North Pacific*

Junichi NISHIZAWA**, Eturo KAMIHIRA**, Kumio KOMURA**,
Ryoji KUMABE** and Masamori MIYAZAKI**

Abstract: Geostrophic transport of the Kuroshio referred to 1,000 db surface is estimated at a section near the southeast end of Kyushu Island using data of more than twenty years. The section is between Cape Toi and 30°N, 133°E. The geostrophic transport varies seasonally; largest in summer and smallest in winter, with a mean value of $46.5 \times 10^6 \text{ m}^3/\text{sec}$. Year-to-year change is also appeared. A relationship between the large Kuroshio transport and its meander is pointed out.

1. Introduction

The Kuroshio is a western boundary current in the North Pacific. It starts from the North Equatorial Current near the coast of the Philippine Islands, passes through the East China Sea and flows eastward along the south coast of Japan. A branch also flows from the East China Sea into the Japan Sea. The volume transport of the Kuroshio is likely to be related with a water mass formation in these areas, but its absolute value is not well-known.

We estimate geostrophic transport of the Kuroshio at the entrance of a region near the exit to the East China Sea to compare with previous ones obtained in the neighbouring areas.

Figure 1 shows the location of the sections as well as depth contours in meters. The estimation is made at Section I off Cape Toi at the southeast end of Kyushu Island. Another estimation made by the Nagasaki Marine Observatory at Section PN in the East China Sea is shown by a solid line. The third estimation is made at Section G off Kii Peninsula for the 90 nautical mile width crossing the maximum velocity area. Most of the data are given by MINAMI *et al.* (1978, 1979), though some additional recent data are supplemented.

The Kuroshio flows across Section PN on the trough west of the Riukiu Islands, changes its direction to the east in the vicinity of Tokara Islands, flowing out of the East China Sea into the North Pacific, changes again its direction to the north, and flows across Section I and across Section G along the south coast of Japan.

2. Methods

The Kuroshio has been observed by the Japan Meteorological Agency for a long time. The data are published in "Results of Marine Meteorological and Oceanographical Observations". The present estimation is mainly based on the data in these reports with some recent data which are not yet published. They span more than twenty years as a whole though there are some periods of no data.

Figure 2 shows a detailed view of Section I. Because no observational stations are kept permanently, the stations figured are only an example. In many cases four or five stations are located on Section I. The farthest one from the coast is usually located at about 30°N, 133°E. Except for the stations nearest to the coast, all the stations are deep enough to carry out geostrophic calculation referred to 1,000 db surface. Only for some shallow stations, extrapolation is done. In other cases where no reasonable extrapolation is possible, data are omitted. Geostrophic velocity and volume transport are calculated by the standard method.

* Received August 31, 1981

Presented at the First JECSS Workshop, June 1981 (cf. La mer, 20: 37-40, 1982).

** Kobe Marine Observatory, Chuo-ku, Kobe, 650 Japan

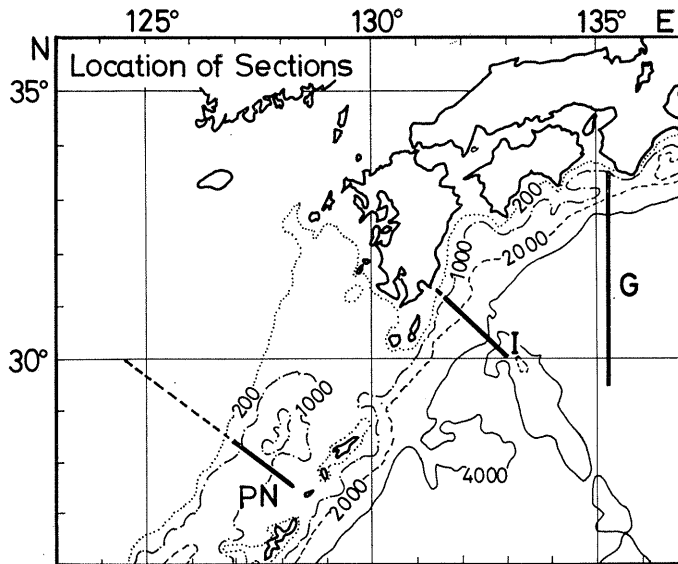


Fig. 1. Location of Sections I, PN and G. Sea floor depth in meters.

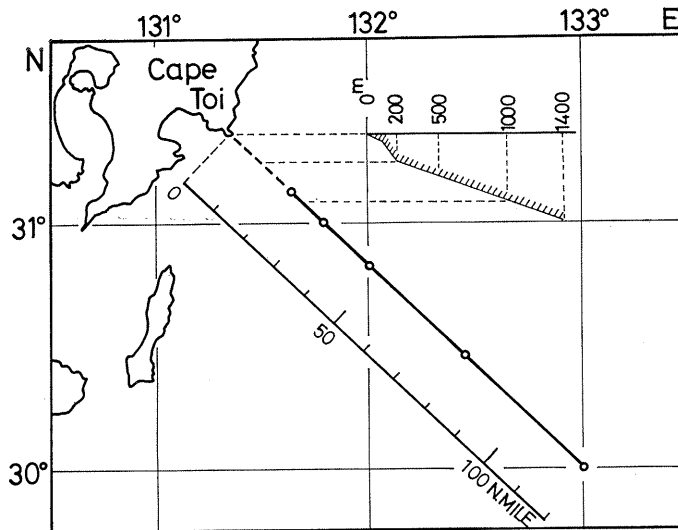


Fig. 2. A detailed view of Section I. Open circles are hydrographic stations. Distance from Cape Toi is shown in nautical miles. Sea floor depths north of 31°N specified for extrapolation are shown in meters.

Based on data in "Prompt Reports of the Sea Conditions of Maritime Safety Agency of Japan", it is inferred that the southern edge of the Kuroshio is sufficiently covered by this section, while its northern edge is covered not enough. So another extrapolation is made to estimate the total transport as follows. First we specify

the sea floor near Cape Toi as shown in the insert of Fig. 2. Then it is assumed that the geostrophic velocity along the coast is the same as that calculated from the northernmost pair of stations. This assumption might not hold good in some cases, especially when the nearest station is far from the coast. For three tenths

of all the cases the nearest stations are at around 30°50'N, 132°00'E. The northernmost stations are nearer in the rest cases.

Total volume transport of the Kuroshio through the cross section between Cape Toi and the station at about 30°N, 133°E is calculated under the conditions mentioned above.

3. Results

Values of total transport through Section I referred to 1,000 db surface are calculated for 59 cases. Mean values and standard deviations are calculated for each season; winter (January-March), spring (April-June), summer (July-September) and fall (October-December). The results are shown in Fig. 3. Annual mean transport is $46.5 \times 10^6 \text{ m}^3/\text{sec}$. The transport varies seasonally, largest ($50.1 \times 10^6 \text{ m}^3/\text{sec}$) in summer and smallest ($43.1 \times 10^6 \text{ m}^3/\text{sec}$) in winter. It is 48.0 and $44.2 \times 10^6 \text{ m}^3/\text{sec}$ in spring and fall, respectively. Standard deviation consists of two kinds of deviations. One is the deviation of transport itself and the other is that due to errors in each estimation.

Mean transport for each season at Section PN referred to 700 db is shown in Fig. 4. This is calculated for 80 cases and annual mean transport is $19.7 \times 10^6 \text{ m}^3/\text{sec}$. Seasonal variation of the transport at Section PN is not apparent. Mean transport for each season at Section G referred to 1,000 db is shown in Fig. 5. This is

calculated for 92 cases. The transport changes seasonally in the same way as that at Section I, but each value of mean transport at Section G is about 10% less than that at Section I.

In order to see year-to-year change of the transport, it is better to represent the transport in percent of the seasonal mean and efface the effect of the seasonal variation. Percent transport and yearly mean for the three sections are shown in Fig. 6. The period in which the Kuroshio meander is present south of Japan (off Tokaido) is also shown in the figure.

In Fig. 6 it is found that the periodic change of the transport is not apparent at Section I because of lack of observations in some periods, but the change at Section I resembles that at Section PN. The periodic change of the trans-

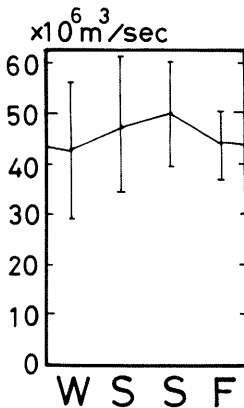


Fig. 3. Mean transport at Section I referred to 1,000 db surface for winter (W), spring (S), summer (S) and fall (F). Standard deviation is also shown.

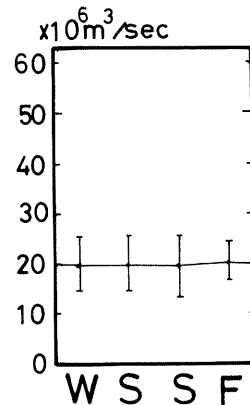


Fig. 4. Mean transport at Section PN referred to 700 db surface.

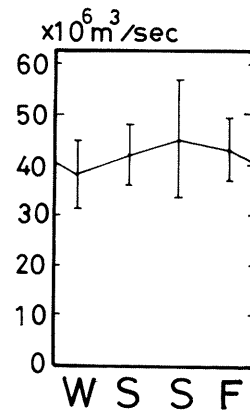


Fig. 5. Mean transport at Section G referred to 1,000 db surface.

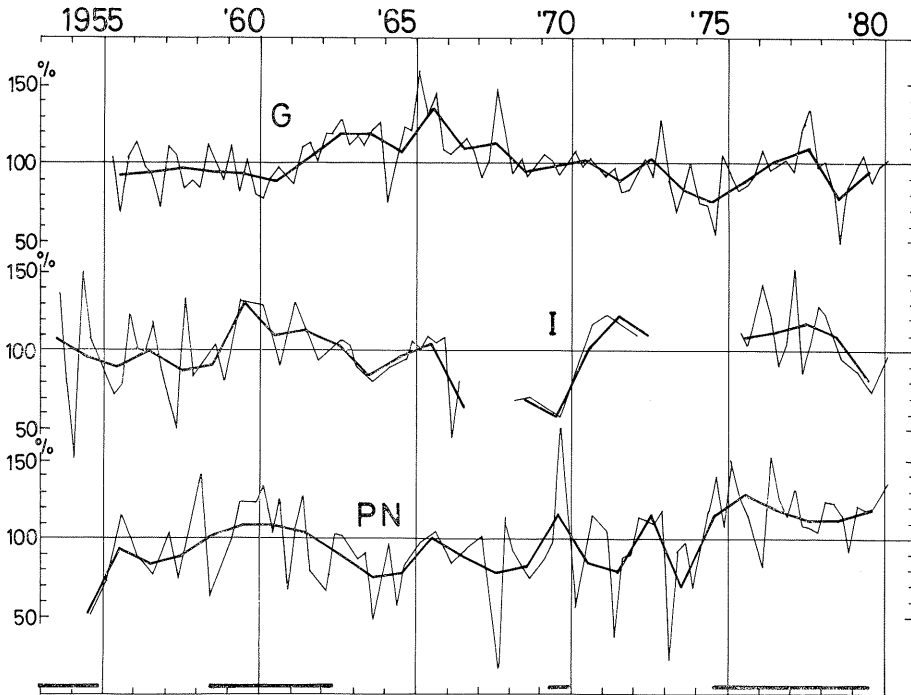


Fig. 6. Year-to-year change of the estimated transport. Percent to each seasonal mean at each section (thin lines) and its yearly mean (thick lines). The periods in which the Kuroshio is meandering are shown with bar at the bottom.

port at Section PN is found not to be very apparent (at about 4 and 10 or 20 year interval?), but the transport is large when the Kuroshio is meandering. It is also found that the transport at Section G varies with periods of about 7 and 20 years.

4. Discussion

Seasonal change of the volume transport of the Kuroshio is estimated at Section I. This is the case with Section G. However, no seasonal change is found at Section PN in the East China Sea. The reason for this difference is not known. The value of geostrophic transport at Section PN is rather small comparing with that at Section I. This is partly because the reference level (700 db) at Section PN is shallower than that at Section I. But, on considering the fact that a part of the Kuroshio flows into the Japan Sea, the probability of existence of a current or a flow east of the Riukiu Islands is not small, which might give some reason for the seasonal change of the transport at Section I.

On the other hand, the year-to-year change of the transport at Section I resembles that at Section PN, but does not resemble that at Section G. Large transport is found at Section PN when the Kuroshio is meandering. Probably the situation is the same at Section I. But the reasons for these facts are not known. Although it is unsuccessful to estimate the Kuroshio transport at the boundary between the East China Sea and the North Pacific, our results should be helpful to improve knowledge of the Kuroshio in the East China Sea.

Acknowledgements

The authors wish to thank Mr. Akira SANO and other members of the Oceanographical Division of the Kobe Marine Observatory for many valuable advice and discussions. The data at Section PN are offered by Mr. Ipeei EGUCHI of the Nagasaki Marine Observatory. We also thank him and the staff of the Nagasaki Marine Observatory.

References

- MINAMI, [H., E. KAMIHIRA, H. EGUCHI and J. NISHIZAWA (1978): Statistical features of the oceanographic conditions south of Honshu, Japan (Part 1; Summer and Winter off Kii Peninsula). Umi to Sora, **53**, 147-156.
- MINAMI, H., E. KAMIHIRA, K. KOMURA, H. EGUCHI and J. NISHIZAWA (1979): Statistical features of the oceanographic conditions south of Honshu, Japan (Part 2; In spring and autumn off Kii Peninsula). Bull. Kobe Mar. Observatory, **197**, 1-11.

東シナ海から北太平洋へ流出する黒潮流量の見積り

西沢純一, 上平悦朗, 小村久美男, 隈部良司, 宮崎正衛

要旨: 20年余りの資料を用いて, 九州南東の都井岬沖で, 1,000 db 面を基準にした黒潮の地衡流量を計算した。計算は, 都井岬側の陸岸と 30°N , 133°E とを両端とする断面について行われた。この断面を通過する流量の平均値として $46.5 \times 10^6 \text{m}^3/\text{sec}$ の値が得られた。流量は季節的に変化し, 夏に多く冬に少ない。この様相は潮岬沖で計算された結果と同様である。経年変化の様子は, 東シナ海における流量変化に似ており, 東海道沖の黒潮大蛇行が存在する期間は東シナ海での流量が多い。

On the Outflow Modes of the Tsugaru Warm Current*

Dennis M. CONLON

Abstract: The Tsugaru Warm Current displays two principal circulation modes. The first mode is characterized by the presence of a warm-core anticyclonic gyre that extends as far east as longitude 143° (gyre mode). In the second mode, the Tsugaru Warm Current is generally confined near the Honshu coast (coastal mode). The occurrence of these modes is consistent with the laboratory findings of WHITEHEAD and MILLER (1979), which suggests that inertial-rotational dynamics govern the Tsugaru Warm Current.

1. Introduction

Sea straits which connect basins of different water mass characteristics are typically characterized by a two-layer flow regime, with lighter water flowing into one basin at the surface and denser water flowing in the opposite direction at depth. The flow of light water into a basin is of interest in the study of dynamics of rivers and estuaries, as well as sea straits, and it has generated a number of contributions to the oceanographic literature (e.g., TAKANO, 1954; NOF, 1978a, b; BEARDSLEY and HART, 1978). Research on buoyant outflows has primarily emphasized deflection and spreading of the outflow jet. Basic considerations of the dynamics of flow in a rotating system lead to the natural conclusion that a buoyant jet will be deflected *cum sole* and most investigations substantiate such behavior.

More recent work by WHITEHEAD and MILLER (1979, hereafter referred to as WM), however, suggests that an outflow jet can assume several different flow modes, depending on the buoyancy of the outflow, the geometry of the basin, and latitude. In their experiments, WM employed two semi-circular connecting basins, filled with water of different densities and mounted on a rotating turntable. After spinning up the fluids, the connection was opened and the resulting buoyant outflow was examined using photographs of pellets floating on the surface. The natural

length scale of such a density-driven process is the internal Rossby radius of deformation, $R = (g\Delta\rho h/\rho f^2)^{1/2}$, which was varied by adjusting the rotation period of the turntable. The results of the WM experiments can be summarized as follows: When R was relatively small the outflow jet showed pronounced instability, but as R was increased the jet veered to the right,

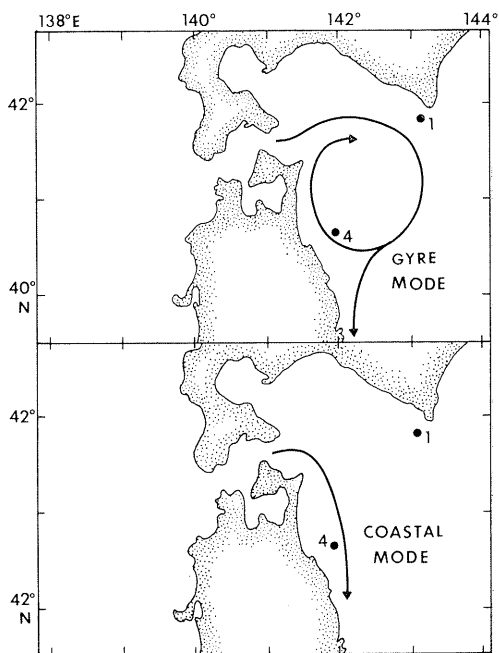


Fig. 1. Schematic representation of principal modes of outflow jet from the Tsugaru Strait. Upper picture: gyre mode of warmer months. Lower picture: coastal mode of colder months. Positions of USNS SILAS BENT current moorings of November 1975-January 1976 also shown. (See Fig. 4)

* Received January 14, 1982

Presented at the First JECSS Workshop, June 1981 (cf. La mer, 20: 37-40, 1982).

** U.S. Office of Naval Research, NSTL Station, MS 39529, USA

hugging the coast. Where R was increased still further, however, the jet separated from the wall; a return flow was generated at the separation point, and in time a fully-developed gyre was generated. WM argued that their results showed that the gyre in the Alboran Sea is produced by the same inertial-rotational dynamics which governed their laboratory experiments.

2. Modes of the Tsugaru Warm Current

Interestingly, the Tsugaru Warm Current displays certain characteristics which suggest that it, too, may be governed by the inertial-rotational dynamics examined in the WM experiments.

Previous investigations (SUGIURA, 1958; HATA, 1975; and others) have documented the extreme seasonal variation of the eastward extent of the Tsugaru Warm Current. In the warmer months of summer and fall the Current extends as far as longitude 143°E, whereas during the colder months of winter and spring the Current appears to be confined to a narrow band adjacent

to the coast of Honshu. Significantly, a gyre is typically present during the warmer months that is suggestive of the laboratory gyre of WM.

Table 1. Seasonal Variation of Internal Rossby Radius.

	Upper Layer Density (σ_t)*	Rossby Radius (Est.)** (km)
January	26.2	8.2
February	26.4	4.7
March	26.4	4.7
April	26.3	6.7
May	26.0	10.6
June	25.8	12.5
July	25.0	18.4
August	24.1	23.2
September	24.0	23.7
October	24.2	22.7
November	25.1	17.7
December	25.6	14.2

* From surveys of RMS OYASHIO MARU, 1949-1952.

** Based on lower layer density of $\sigma_t=26.5$ (SUGIURA, 1958) and upper layer mean thickness of 210 m (HATA, 1975).

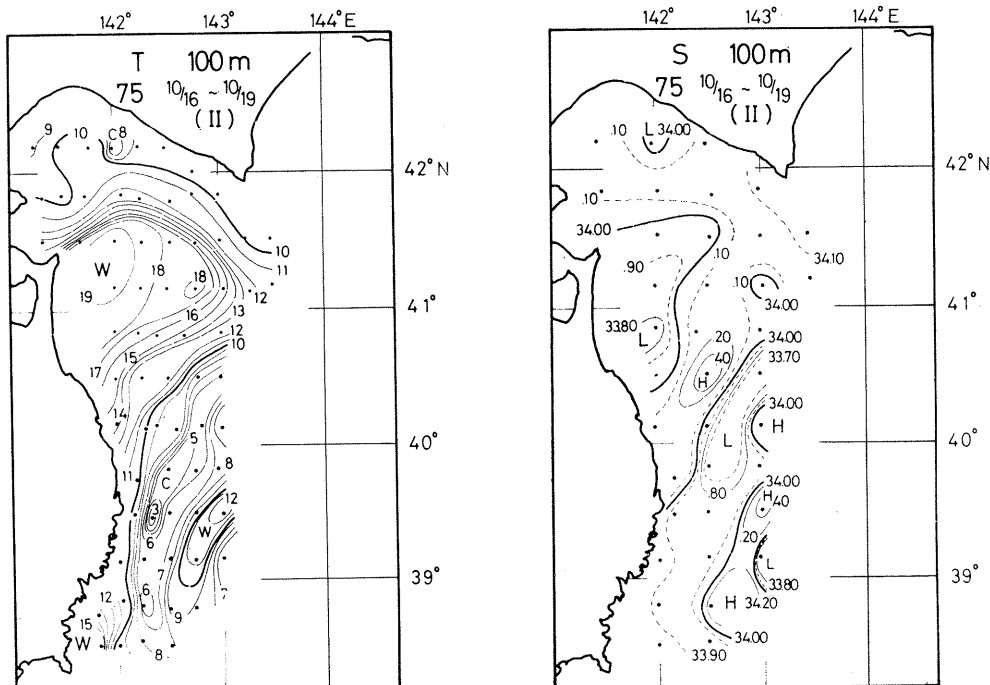


Fig. 2. The outflow region of the Tsugaru Strait in October 1975, showing the gyre mode. (Hakodate Marine Observatory, Oceanographic Observatory Report, Vol. 14, No. 1.)

A simplified model of the WM results is depicted in Fig. 1, in which two of the WM modes are shown: a gyre mode (high R) and a coastal mode (low R). The question to be addressed, then, is whether the Tsugaru Warm Current shows a pronounced seasonal variation in R that is consistent with the existence of these two modes. To answer this question, the interannual variability of the internal deformation on radius R must be calculated.

The monthly variation of the upper layer density in the Tsugaru Warm Current region was obtained from data gathered by the RMS OYASHIO MARU in 97 transects run eastward from the Honshu coast at latitude $40^{\circ}32.5'$ north during the years 1949-1952 (Table 1). The station occupied at longitude 142° east on each transect is central to the flow regions of both gyre and coastal modes; measurements at the 25m level at this station were used to avoid transient surface effects such as rain. The underlying water in this region is of Oyashio origin and is stable throughout the year; the transition

to the lower layer occurs roughly at the $\sigma\tau=26.5$ isopycnal (SUGIURA, 1958), from which $\Delta\rho$ can be computed. HATA (1975) estimates the thickness of the Tsugaru Warm Current to be about 180 m during the cold months and 240 m during late summer and fall; because R varies as $h^{1/2}$, a general estimate of 210 m for the surface layer thickness should then be adequate within about 10%. Using the above data, average values of R were calculated for each month of the year, and the results are shown in the accompanying table. The internal Rossby deformation radius shows an extremely large interannual variation (a factor of 5), and indeed, R is large when a gyre is usually present and small when it is not. Further, a comparison of this table with the maps of HATA (1975) suggests that R values of less than 10 km represent the coastal mode, while the gyre mode appears to be established when R exceeds 15 km. If these values are to be believed, then the table suggests that a transition from gyre mode to coastal mode should occur sometime between

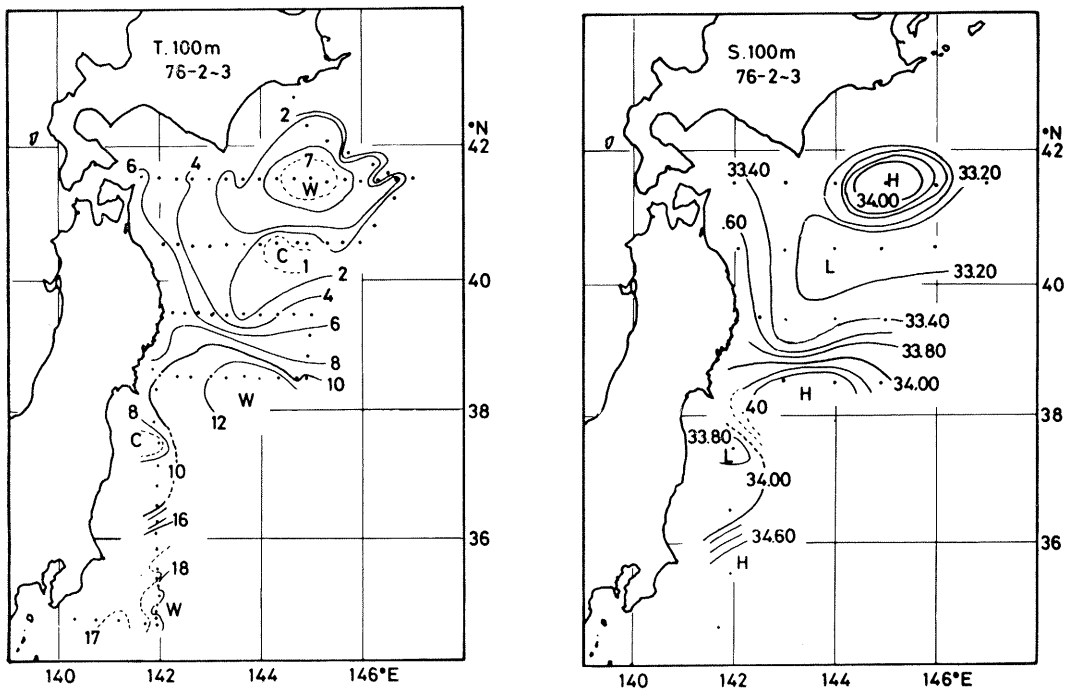


Fig. 3. The outflow region in February-March 1976, showing flow confined near the Honshu coast. The eddy at 145°E is of Kuroshio origin. (Hakodate Marine Observatory, Oceanographic Observation Report, Vol. 14, No. 1)

October ($R > 20$ km) and February ($R < 5$ km).

3. An Observation of Modal Transition

Attention is focused on the Tsugaru Warm Current during the period October 1975–February 1976, using data obtained by the research vessels KOFU MARU, SHUMPU MARU and USNS SILAS BENT.

In October 1975 the gyre is clearly seen in the temperature distribution at 100 m (Fig. 2). Concurrent GEK data show that the outflow jet initially deflects to the left, then moves in an arc clockwise out to longitude 143° east, turns back to the coast at latitude 41° north, and bifurcates near $40^\circ 30'N$, $142^\circ E$. The Rossby radius of the jet approximated from the hydrographic data is about 25 km; sectional profiles of T , S , and ρ indicate that the jet is between 20 km and 40 km wide, so the data are in rough agreement with Rossby adjustment ideas.

By late February 1976 the picture has changed completely (Fig. 3). The anticyclonic gyre has disappeared, and now the flow appears to be in the coastal mode. (TS data show that the eddy at $145^\circ E$ is a spinoff eddy from the Kuroshio).

Fortuitously, moored current meters deployed from November 1975 to January 1976 by the SILAS BENT were in an excellent position to monitor the change of modes (see Fig. 1). Current meter 1 (northern location, Fig. 4b) lies between Erimo Misaki and the core of the Tsugaru Warm Current. The measurements show weak currents of about 20 cm/sec or less, but the direction of the current is remarkably uniform on a bearing of 320° – 340° from the beginning of the record until about December 19. The direction of the current and its steadiness during this period strongly suggest the presence of a coastal countercurrent generated

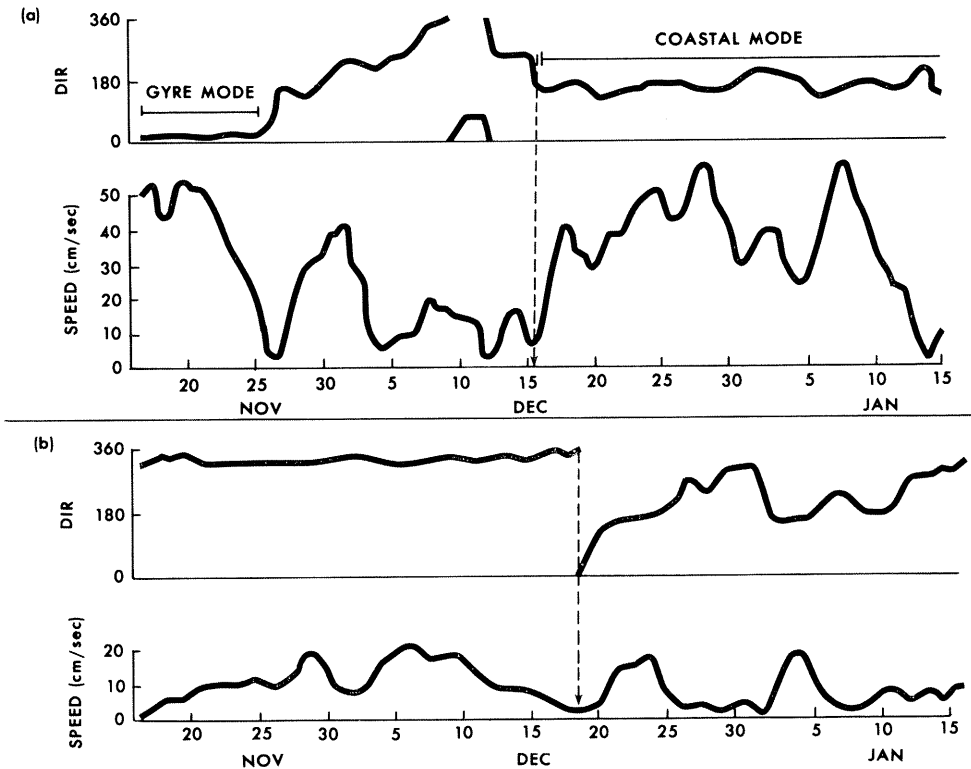


Fig. 4. Currents in the outflow region of the Tsugaru Strait, November 1975–January 1976, from survey of USNS SILAS BENT. Current data have been averaged by 72-hour running mean. (a) Southern location, position 4, 45-m depth (see Fig. 1). (b) Northern location, position 1, 225-m depth.

by the infilling of the adjacent bight by the Tsugaru Warm Current. Current meter 4 (southern location, Fig. 4a) is located within the zone of influence of both gyre and coastal modes. From November 17 to November 25, the currents are strong (up to 50 cm/sec) and very steady on a bearing of 20° , which indicates that the gyre is still active. The period between November 27 and December 14 appears to be a time of instability. The direction alternates from roughly southerly (November 27–December 4) to near northerly (around December 10) to easterly (December 14), with a trend toward decreasing current speeds. Sometime on December 15 or 16, however, the current speed increases sharply and the direction swings to the south, remaining between 140° and 200° for the remainder of the record. The coastal mode appears to have been firmly established.

A maximum estimate of the time of transition in this case is about three weeks (November 25–December 15). The close agreement between the abrupt direction changes at locations 1 and 4, however, indicate that the actual transition might be more rapid (order days instead of weeks).

It may be appropriate to add one speculative note. It has been suggested that during colder months, the penetration of the Oyashio into this region acts to "push" the Tsugaru Warm Current against the coast of Honshu. Note, however, that the significant direction shift in

current at the southern location occurs a few days *before* the major shift at the northern location (December 15 versus December 19). An alternative hypothesis, therefore, is that the gyre mode prevents Oyashio intrusion, and only when the gyre collapses is the Oyashio able to penetrate this region. The Tsugaru Warm Current could therefore play an important role in the shifting of the Oyashio Front.

References

- BEARDSLEY, R. C. and J. HART (1978): A simple model for the flow of an estuary onto a continental shelf. *J. Geophys. Res.*, **53**(C2): 873–883.
- HATA, K. (1975): Variations in hydrographic conditions in the seas adjacent to the Tsugaru Straits. *Bull. Hakodate Mar. Observ.*, **18**: 17–29 (in Japanese).
- NOF, D. (1978a): On geostrophic adjustment in sea straits and wide estuaries; theory and laboratory experiments. Part I, One-layer system. *J. Phys. Oceanogr.*, **8**: 690–702.
- NOF, D. (1978b): On geostrophic adjustment in sea straits and wide estuaries: theory and laboratory experiments. Part II, Two-layer system. *J. Phys. Oceanogr.*, **8**: 861–872.
- SUGIURA, J. (1958): On the Tsugaru Warm Current. *Geophys. Mag.*, **28**: 399–409.
- TAKANO, K. (1954): On the velocity distribution off the mouth of a river. *J. Oceanogr. Soc. Japan*, **10**: 60–64.
- WHITEHEAD, J. A. and A. R. MILLER (1979): Laboratory simulation of the gyre in the Alboran Sea. *J. Geophys. Res.*, **84**(C7): 3733–3742.

津軽暖流の流出モード

Dennis M. CONLON

要旨: 津軽暖流は2つのおもな流出モードを示す。その1つは東経 143° にまで及ぶ高気圧性暖水渦(渦モード)である。もう1つのモードでは、津軽暖流は本州海岸におしつけられている(海岸モード)。これら2つのモードの存在はWHITEHEAD and MILLER (1979)の室内実験の結果—慣性—渦力学が津軽暖流を支配しているという示唆—と一致する。

Note on Currents Driven by a Steady Uniform Wind Stress on the Yellow Sea and the East China Sea*

Byung Ho CHOI**

Abstract: A two-dimensional hydrodynamical model of the Yellow Sea and the East China Sea is used to derive the currents driven by steady wind stresses on the shelf. Experiments have been performed with the model to determine the responses of the shelf to stationary wind stress fields suddenly imposed on the shelf for various wind directions of uniform NW, N, SW, SE winds and wind stresses of 1.6 dyn/cm^2 and 10 dyn/cm^2 , respectively. Circulation patterns thereby deduced are presented and discussed.

1. Introduction

This paper describes the continuing model studies in the Yellow Sea and the East China Sea. The previously developed sea model of the Yellow Sea and the East China Sea shelf (CHOI, 1980) was satisfactorily utilized to compute M_2 tidal distribution in the system. As a subsequent model development step, the shelf model is used to derive the wind-induced currents in the shelf sea and the preliminary results of studies are presented and discussed here. Numerical experiments carried out with the model were to determine response of the shelf sea produced by steady uniform wind stress fields suddenly imposed on the sea area. In this respect, the separate effects of steady uniform winds have been investigated and in each case circulation patterns have been deduced. The underlying objective of this work is to build up fundamental knowledge of the system for the eventual development of a surge forecasting model of the Yellow Sea and the East China Sea. In the present study, the currents computed are the average values of water column and along the open-sea boundaries at the shelf edge radiation condition is employed which allows disturbances from the interior of the model to pass outwards.

2. Yellow Sea and the East China Sea model

The bottom topography in the study area is shown in Fig. 1. The model grid, with a resolution of $1/5^\circ$ latitude by $1/4^\circ$ longitude, is shown in Fig. 2. Computations are two-dimensional and solve the vertically-integrated equations of motion formulated on spherical polar

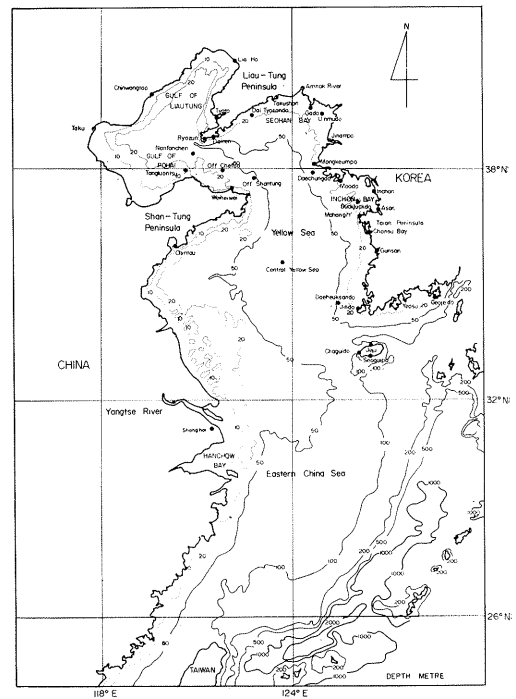


Fig. 1. The bottom topography of the the Yellow Sea and the East China Sea.

* Received October 27, 1981

** Department of Civil Engineering, Sung Kyun Kwan University Suwon Campus, Kyonggi-do, Korea

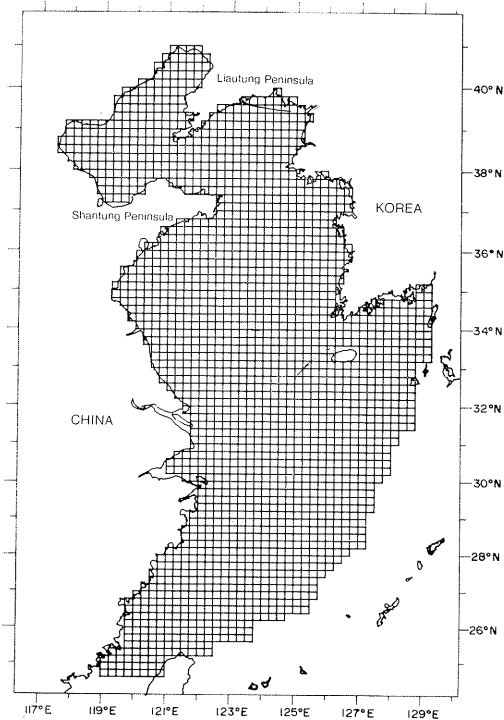


Fig. 2. The Yellow Sea and the the East China Sea model finite difference grid.

coordinates yielding elevations and depth-mean currents at the centres of the mesh elements. Nonlinear terms are included and a quadratic law of bottom friction is assumed. Ignoring variations in water density, the influence of temperature and salinity stratification upon the movement of water is not resolved. A coefficient of bottom friction, 0.0025, was assumed over the whole shelf.

The finite difference scheme, which advances the surface elevation, ξ , and the eastward and northward component of the velocity, u and v , over the entire network at time t to the values of these variables at time $t + \Delta t$ is explicit: employing central space difference and a combination of forward and backward time difference in the manner described by FLATHER and HEAPS (1975). In generating the wind driven surge fields, a time step of 4 minutes was used. As an open sea boundary condition for wind-driven surge computation a radiation condition (REID and BODINE, 1968) was employed along the

edge of continental shelf. Applying a radiation condition to the internally generated surge gives

$$hq_n' = (gh)^{1/2} \xi,$$

where q_n' is the associated outward going current velocity across the boundary. It was assumed that the transmission of energy outward across the boundary may be represented as a simple progressive wave travelling at right angles to the boundary (HEAPS, 1974).

3. Numerical experiments

A uniform steady wind was blown for four tidal cycles from the state of rest. Northerly type winds of N and NW direction were chosen for representing the winter condition and southerly type winds of SW and SE direction were chosen for representing the summer condition. Wind stress of 1.6 dyn/cm² applied may represent a wind speed of 10 m s⁻¹ and wind stress of 10 dyn/cm² was also applied to represent rather strong wind forces. Series of numerical experiment performed are as follows;

Numerical experment 1, uniform northwesterly wind stress of 1.6 dyn/cm²

Numerical experiment 2, uniform northerly wind stress of 1.6 dyn/cm²

Numerical experment 3, uniform southeasterly wind stress of 1.6 dyn/cm²

Numerical experiment 4, uniform southwesterly wind stress of 1.6 dyn/cm²

Numerical experiment 5, uniform northwesterly wind stress of 10 dyn/cm²

Nnumerical experiment 6, uniform northerly wind stress of 10 dyn/cm²

Numerical experiment 7, uniform southeasterly wind stress of 10 dyn/cm²

Numerical experiment 8, uniform southwesterly wind stress of 10 dyn/cm²

The computed spatial distribution of steady wind-induced surface elevation over the shelf is represented as contour elevation. The spatial distributions of vectors of wind-induced currents are also accompanied by a diagrammatic interpretation in term of flow lines.

4. Discussion of results

Under the northwesterly wind, the sea surface slopes upwards from lowest values in the

Gulfs of Pohai and Liautung to increasing values in the direction of east by southeast down to Pohai Strait and then in the direction of south-east down to southward shelf edge (Fig. 3(a) and Fig. 4(a)). This longitudinal set-up being

accompanied by a marked transverse slope may be due to the earth's rotation. The patterns of depth-mean currents shown in Fig. 5 and Fig. 6 indicate that there are relatively strong southerly flow down both sides of the Chinese

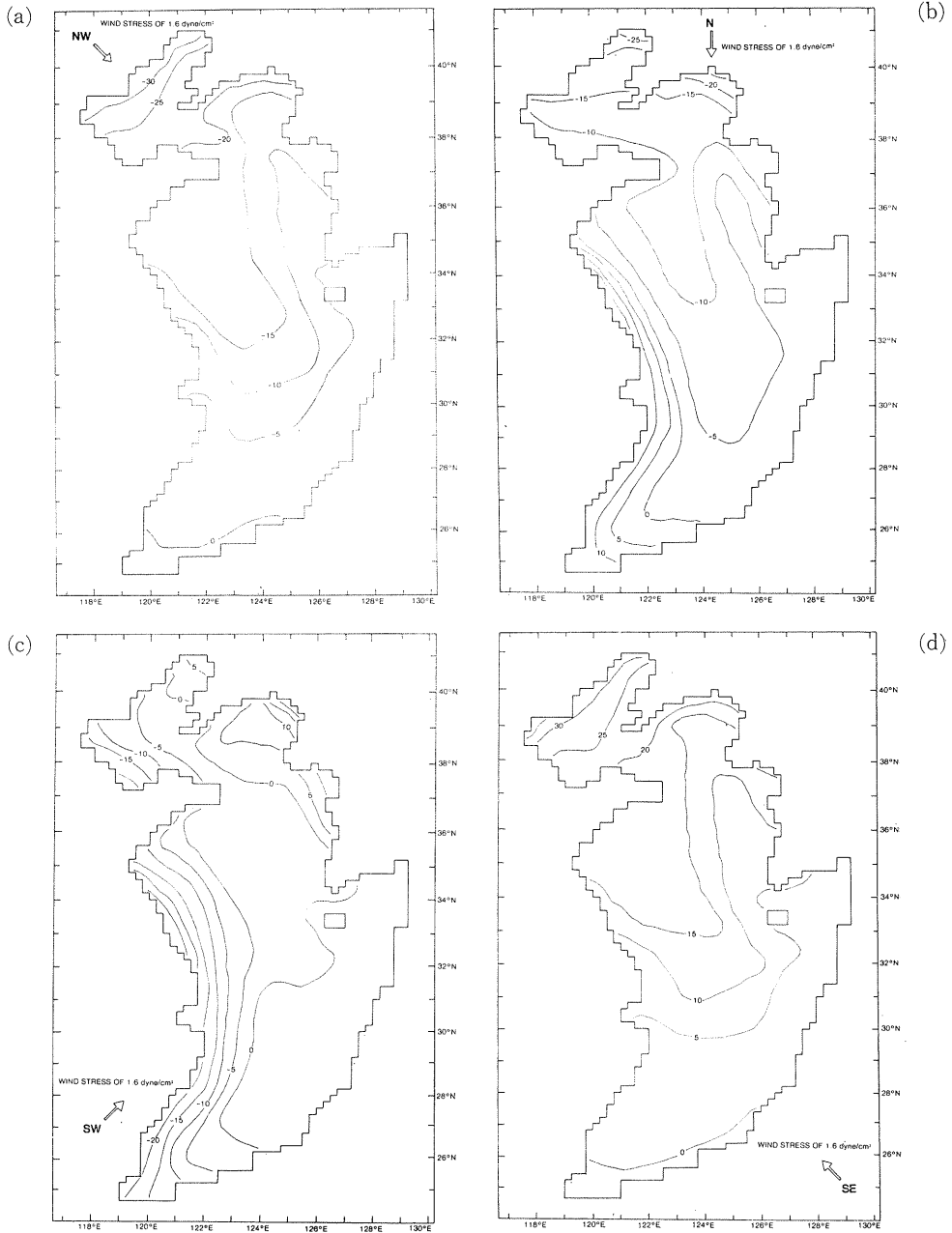


Fig. 3. Surface elevations produced by a uniform wind stress of 1.6 dyn/cm² from NW, N, SW and SE winds.

coast and the west coast of Korea and northerly flow up in the middle of the Yellow Sea. This north-going flow along the deeper part of the Yellow Sea may be due to return flow at depth contrasting to coastal situation where cur-

rent tends to be south-going along the shallow water depth contours in direction of the wind. The variation of longitudinal flows accounts for the transverse variation of surface gradient.

Under the northerly wind condition, the sea

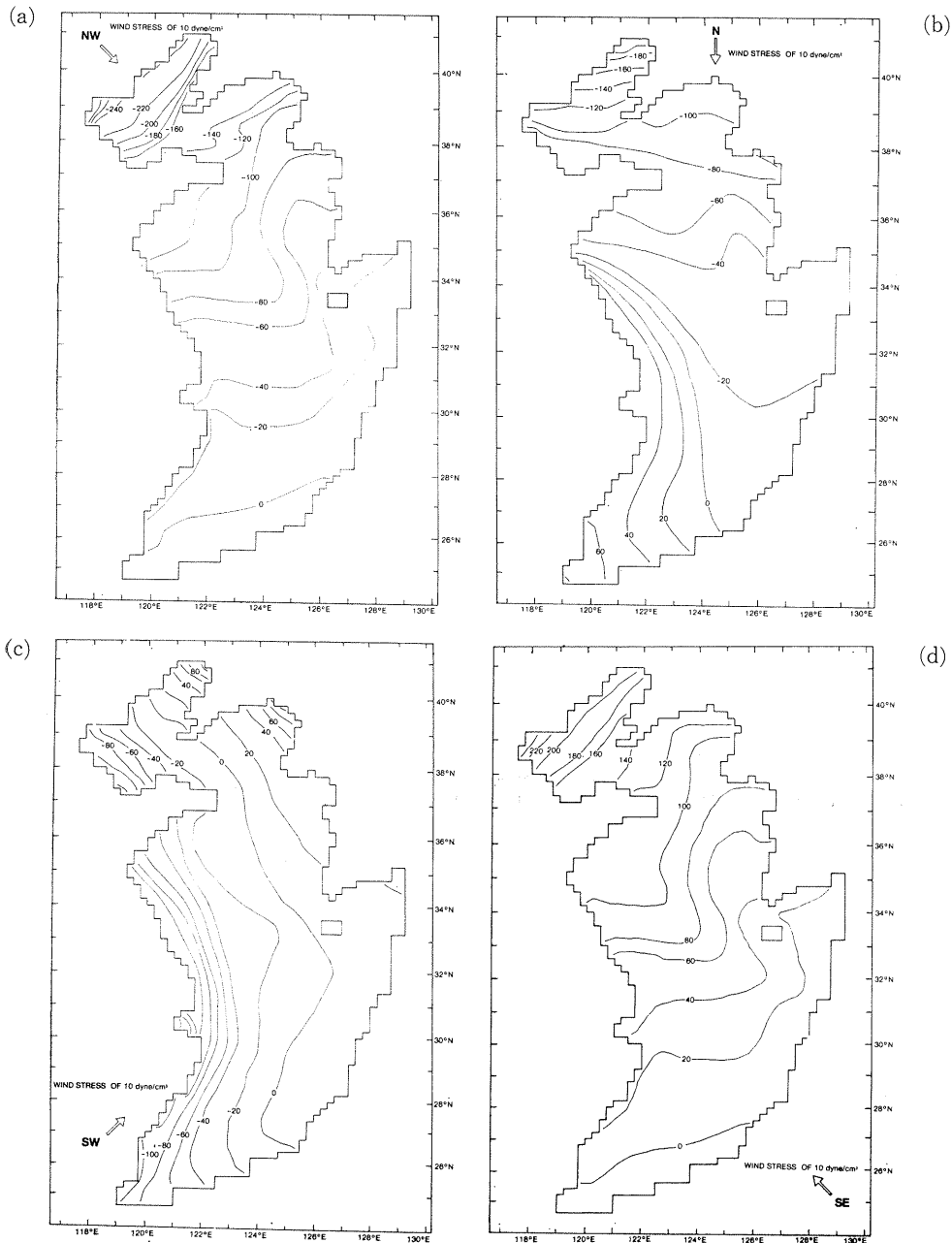


Fig. 4. Surface elevations produced by a uniform wind stress of 10 dyn/cm² from NW, N, SW and SE winds.

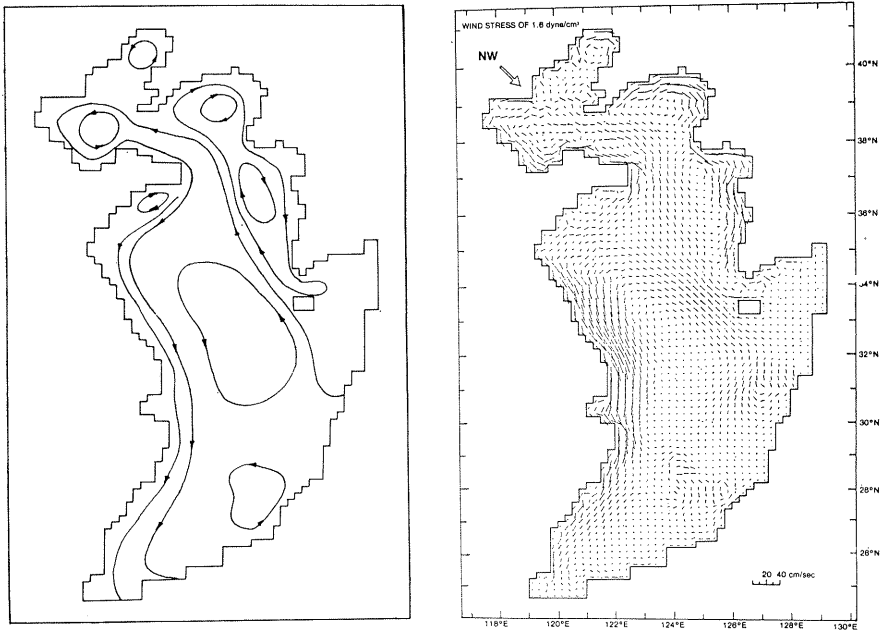


Fig. 5. The wind driven currents produced by a uniform NW wind stress of 1.6 dyn/cm^2 and corresponding flow lines.

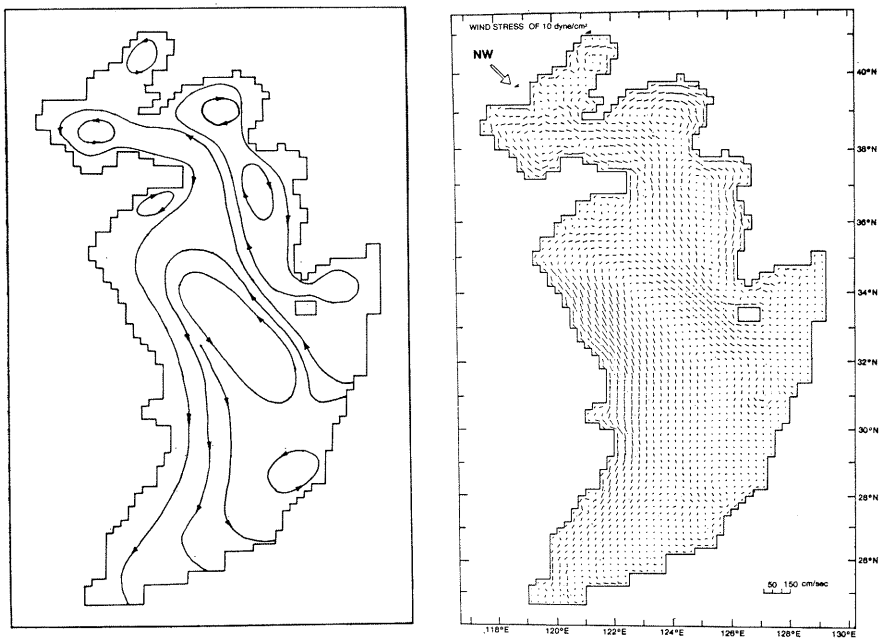


Fig. 6. The wind driven currents produced by a uniform NW wind stress of 10 dyn/cm^2 and corresponding flow lines.

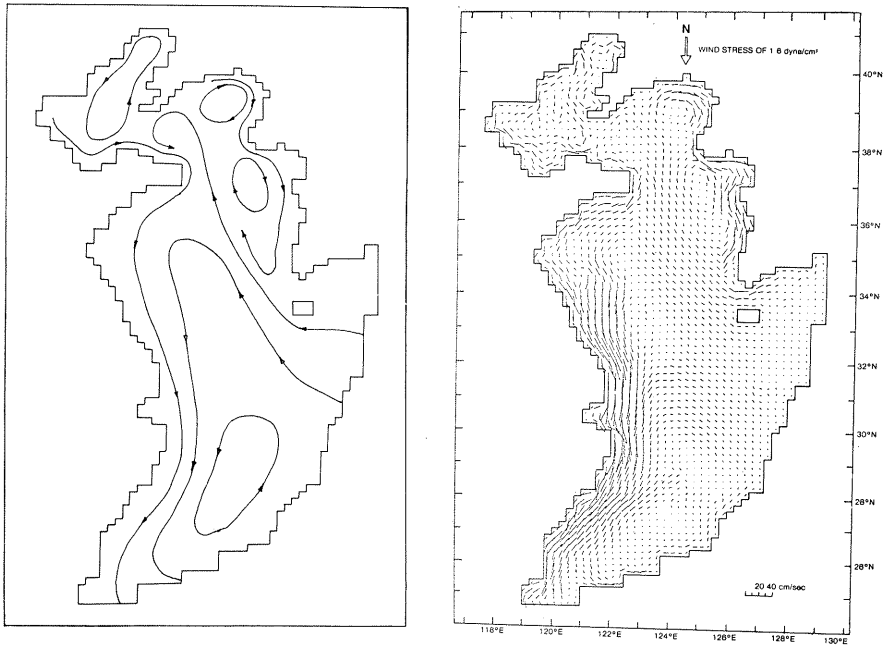


Fig. 7. The wind driven currents produced by a uniform N wind stress of 1.6 dyn/cm^2 and corresponding flow lines.

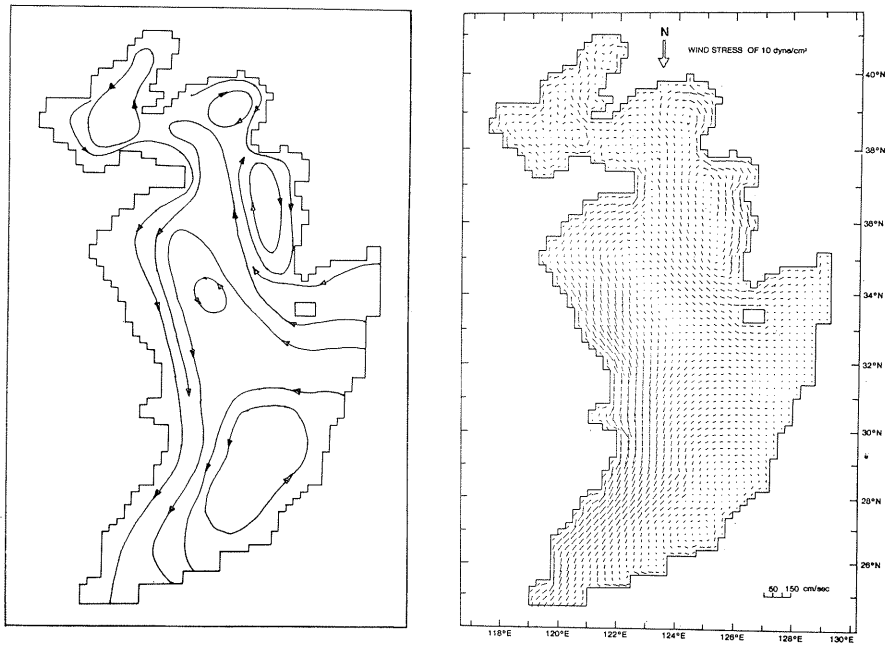


Fig. 8. The wind driven currents produced by a uniform N wind stress of 10 dyn/cm^2 and corresponding flow lines.

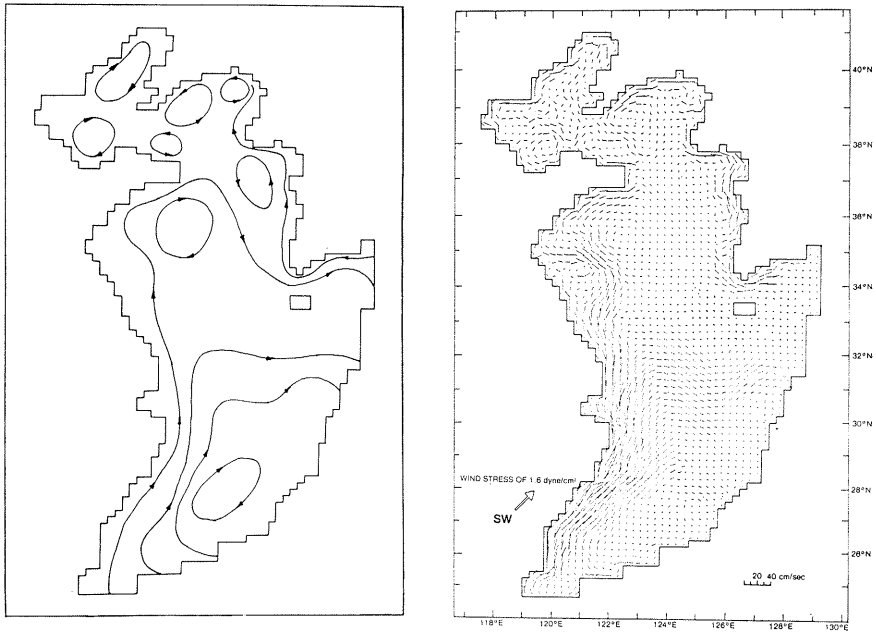


Fig. 9. The wind driven currents produced by a uniform SW wind stress of 1.6 dyn/cm^2 and corresponding flow lines.

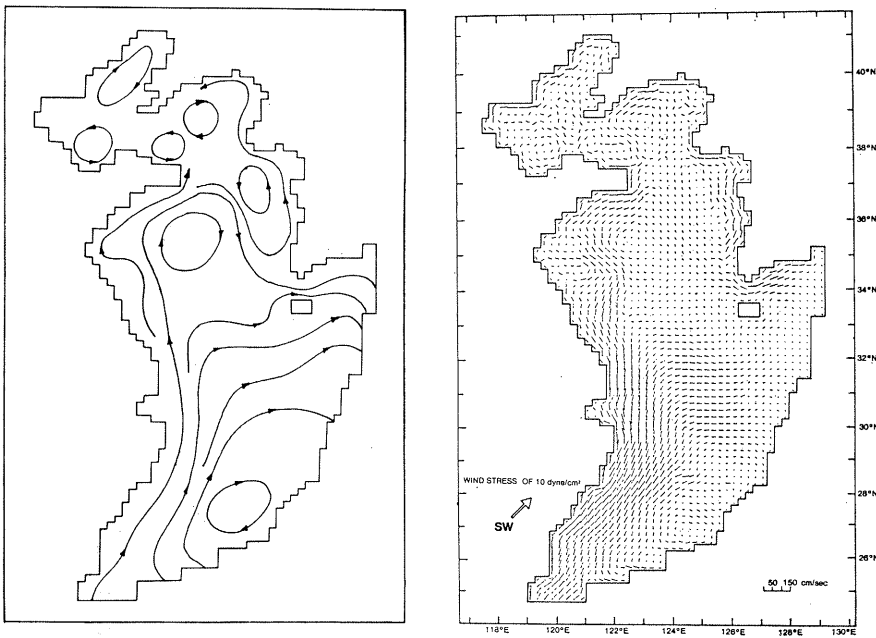


Fig. 10. The wind driven currents produced by a uniform SW wind stress of 10 dyn/cm^2 and corresponding flow lines.

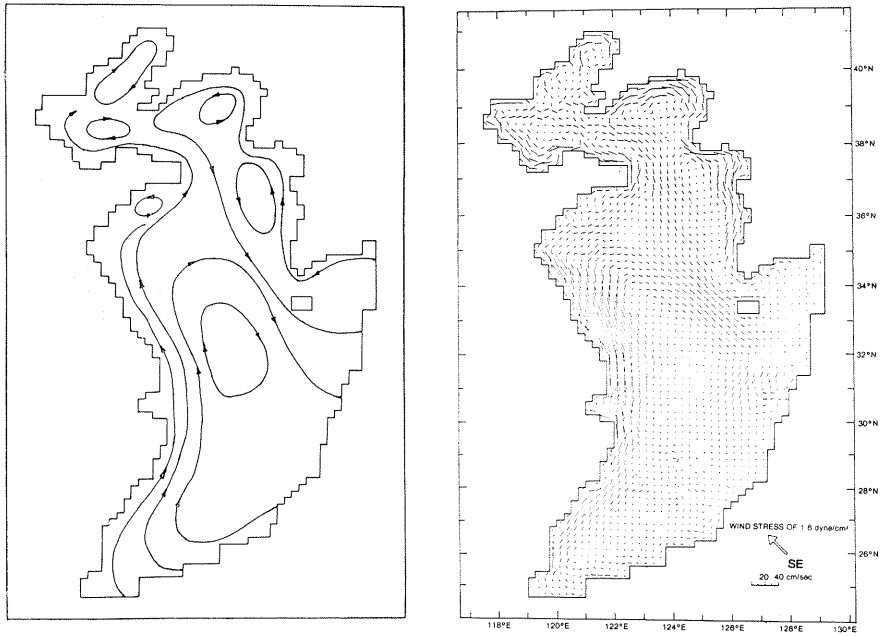


Fig. 11. The wind driven currents produced by a uniform SE wind stress of 1.6 dyn/cm^2 and corresponding flow lines.

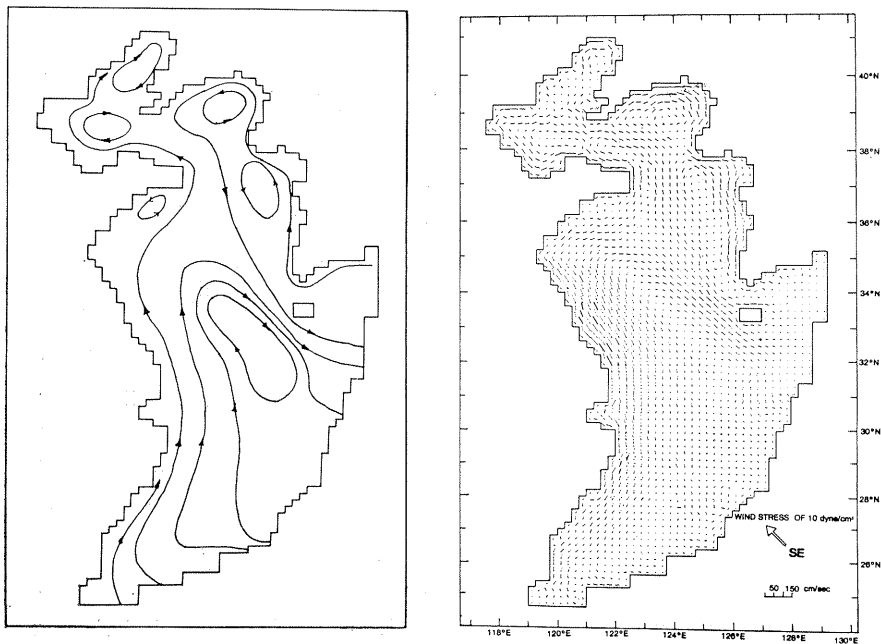


Fig. 12. The wind driven currents produced by a uniform SE wind stress of 10 dyn/cm^2 and corresponding flow lines.

surface slopes upwards from lower values in the upper part of the Yellow Sea to increasing values in the direction of south down to the south border of the Yellow Sea and then in the direction of southwest down to the Taiwan Strait (Fig. 3(b) and Fig. 4(b)). The patterns of depth-mean currents shown in Fig. 7 and Fig. 8 indicate that flow pattern induced due to a uniform northerly wind is somewhat similar to those due to northwesterly wind.

Under the southwesterly wind direction, the sea surface slopes upwards from lower values along the Chinese coast to increasing values in the direction of northeast over the shelf (Fig. 3(c) and Fig. 4(c)). The patterns of depth-mean currents shown in Fig. 9 and Fig. 10 indicate that there are relatively strong northerly flow up along the both sides of the Chinese coast and the west coast of Korea and southwesterly flow down in the middle of the Yellow Sea in contrast to the condition of uniform northerly type winds.

Under the southeasterly wind direction, the sea surface slopes upwards from lowest values along the shelf edge to increasing values in the direction of northwest throughout the shelf region (Fig. 3(d) and Fig. 4(d)). The patterns of depth-mean currents shown in Fig. 11 and Fig. 12 indicate that flow pattern due to a uniform southeasterly wind is somewhat similar to those due to southwesterly wind in the region of the Yellow Sea. Northerly-type winds maintain a southward flow along the Chinese coast and along the west coast of Korea inducing clockwise flow gyres in Seohan Bay and the west coast of South Korea and anticlockwise flow gyres in the Gulfs of Liautung and Pohai, and in the middle part of the East China Sea. Southerly-type winds maintain a northward flow along the Chinese coast and along the west coast of Korea inducing anticlockwise flow gyres in Seohan Bay and the west coast of South Korea and clockwise flow gyres in the

Gulfs of Liautung and Pohai and in the middle of the Yellow Sea and the East China Sea.

5. Concluding remarks

This paper has presented a short account of some of the numerical experiments from the Yellow Sea and the East China Sea model. Numerical experiments performed with the model to determine the response of the Yellow Sea and the East China Sea have shown that circulation patterns thereby deduced exhibit significant spatial variation of currents, and also have shown the complexity of the wind-driven circulation on the continental shelf.

Further studies may eventually be necessary to construct a three-dimensional shelf sea model since three-dimensional studies of the North Sea (DAVIES, 1980) indicate that both the magnitude and direction of the wind-induced current change significantly with depth and consequently depth-mean currents derived from two-dimensional model may not adequately describe the wind-induced circulation on the shelf.

References

- CHOI, B. (1980): A tidal model of the Yellow Sea and the Eastern China Sea. *Korea Ocean Res. Develop. Inst. Report* 80-02.
- DAVIES, A. M. (1980): Application of numerical models to the computation of the wind-induced circulation of the North Sea during JONSDAP '76. *Meteor. Forsch. Ergebn., Reihe A*, **22**: 53-68.
- FLATHER, R. A. and N. S. HEAPS (1975): Tidal computations for Morecambe Bay. *Geophys. J. Royal Astronom. Soc.*, **42**: 489-517.
- HEAPS, N. S. (1974): Development of a three-dimensional numerical model of the Irish Sea. *Rapp. Proc. Verb. Reun. Cons. int. Explor. Mer*, **167**: 147-162.
- REID, R. O. and B. R. BODINE (1968): Numerical model for storm surges in Galveston Bay. *J. Hydraul. Div. Proc. Am. Soc. Civ. Engrs.*, **94**: 33-57.

黄海と東シナ海で定常均一風によつてひきおこされる海流

Byung Ho CHOI

要旨: 黄海と東シナ海の上を吹く定常風によつておきる海流を二次元数値モデルを使って調べた。風の強さとしては2種類, 1.6 dyn/cm^2 と 10 dyn/cm^2 , 向きとしては4種類, 北西, 北, 南西, 南東の風を用い, 合計8つの場合について計算した。計算結果を図示し, 考察を加えた。

Variations of Chlorophyll *a* Concentration and Photosynthetic Activity of Phytoplankton in Tokyo Bay*

Yoshiaki SHIBATA** and Yusho ARUGA**

Abstract: Phytoplankton biomass (chlorophyll *a*) was investigated together with some environmental conditions mainly at 15 stations in Tokyo Bay including Uruga Strait from December 1975 through December 1978. Photosynthetic and respiratory rates were measured under various light intensities and temperatures with phytoplankton samples taken from the surface water off Haneda. Generally, the chlorophyll *a* concentration was higher in the northwestern part and lower in the southern part of the inner bay. In Uruga Strait the chlorophyll *a* concentration was apparently lower than that in the inner bay. Seasonal changes of the chlorophyll *a* concentration and the photosynthetic activity of phytoplankton considerably differed from those observed ten or more years ago. Both the chlorophyll *a* concentration and the light-saturated photosynthetic rate on a chlorophyll *a* basis remained high throughout the year with the highest values being observed ordinarily in summer; however neither the spring bloom nor the autumn increase in standing crop of phytoplankton was remarkable. Water temperature and salinity seemed to play important roles in controlling both standing crop and photosynthetic activity of phytoplankton. The changes of phytoplankton biomass and distribution seemed to be dependent on such meteorological or physical factor as tide or drift current brought about by strong wind rather than on such chemical factors as nutrient concentrations. In Tokyo Bay high productivity of the phytoplankton community is maintained throughout the year and productivity does not appear to be limited by nutrients provided that physical conditions are favorable.

1. Introduction

Tokyo Bay covers an area of about 1,500 km² including Uruga Strait by which the inner part of the bay is connected to the Pacific Ocean. Around the bay, especially around the inner bay, there are many cities and industrial areas, and a large amount of sewage flows into it. Because of these conditions, Tokyo Bay is one of the most polluted bays in Japan. The red tide in Tokyo Bay was first reported early in this century and is now observed almost always throughout the year. Many investigations have been done on red tide formation, species composition and its succession. MARUMO and MURANO (1973) and MARUMO *et al.* (1974) determined the species composition of red tide in the bay with special attention to diatom succession. HOGETSU *et al.* (1959) was the first to investigate the photosynthetic rate of blooming *Skeletonema*

obtained from the area off Haneda in the bay. Since the first intensive investigation of the primary production in Tokyo Bay (cf. MATSUDAIRA 1964), there have been many other investigations conducted on primary production. ICHIMURA and KOBAYASHI (1964) and ICHIMURA and ARUGA (1964) reported the seasonal changes of chlorophyll and photosynthetic rate of phytoplankton. ICHIMURA (1967) investigated primary production with special reference to environmental gradients. FUNAKOSHI *et al.* (1974), TERADA *et al.* (1974) and YAMAGUCHI and ICHIMURA (1976) reported that the primary productivity of Tokyo Bay is highest of all the inshore regions in Japan. These works were, however, limited spatially in the bay or by time of the year.

The present work was carried out to determine the variations of standing crop and photosynthetic activity of the phytoplankton community in Tokyo Bay in relation to environmental factors and in comparison with previously reported data.

* Received August 28, 1981

** Laboratory of Phycology, Tokyo University of Fisheries, Konan-4, Minato-ku, Tokyo, 108 Japan

2. Material and methods

Observations were carried out at 15 stations in Tokyo Bay (Fig. 1) from December 1975 through December 1978. Monthly observations were intended initially, but each year a few of the monthly observations could not be carried out mainly due to the inavailability of a research ship. Water samples were taken from various depths by a PVC bucket and a Van Dorn type water sampler, and used for the measurements of chlorophyll *a*, photosynthesis, respiration, salinity and nutrients. At the same time, measurements of Secchi disk depth and water temperature were conducted. Water temperature was measured with a standard thermometer and/or a bathythermograph. Salinity was measured with a recording S-T meter attached to the T/S Seiyu Maru or an Autolab portable T-S meter.

An aliquot of each water sample was immediately filtered through a 47 mm Whatman GF/C glassfiber filter, and the filters, wrapped in

aluminum foil, were stored in a freezer until pigment analyses could be conducted. Pigments were extracted with 90% acetone, absorbances of the extract were measured with a Hitachi 101 spectrophotometer and the concentrations of chlorophylls were calculated by the formulae of SCOR-Unesco (1966).

Photosynthesis and respiration of phytoplankton were measured both in the laboratory and on the deck using the light and dark bottle method under various light intensities and temperatures, followed by the Winkler titration technique for dissolved oxygen determination. The light intensities on the bottles were regulated by varying the distance of the light source from the bottles in the laboratory experiments or by changing the number of neutral vinyl sheets rolled around the transparent acrylic cylinders in which the bottles containing water samples were placed under natural sunlight in the deck experiments. The measurements were carried out at *in situ* surface water temperature regulated either by pumping surface water over the bottles or by a cooling device (Taiyo Coolnit CL-15).

Phosphate, nitrate, nitrite and silicate concentrations were determined using the procedures described by STRICKLAND and PARSONS (1972).

3. Results and discussion

(1) Distribution of chlorophyll *a*

Chlorophyll *a* has usually been used as an index of phytoplankton biomass (ARUGA and MONSI 1963, ARUGA 1966). Horizontal distributions of chlorophyll *a* in the surface water are shown in Fig. 2. The area of the shaded circles is proportional to the concentration of chlorophyll *a*. Usually the level of surface chlorophyll *a* concentration was markedly higher in the inner bay than in Uraga Strait. In some cases the higher chlorophyll *a* concentrations observed in the northern part of the strait can be related with the water flowing out of the inner bay to the strait at low tide as will be described in detail later. At Stn. T-9 in an oceanic area off Tateyama, the chlorophyll *a* concentration was always quite low as compared with that in the strait. In the inner bay, the surface chlorophyll *a* concentration varied greatly

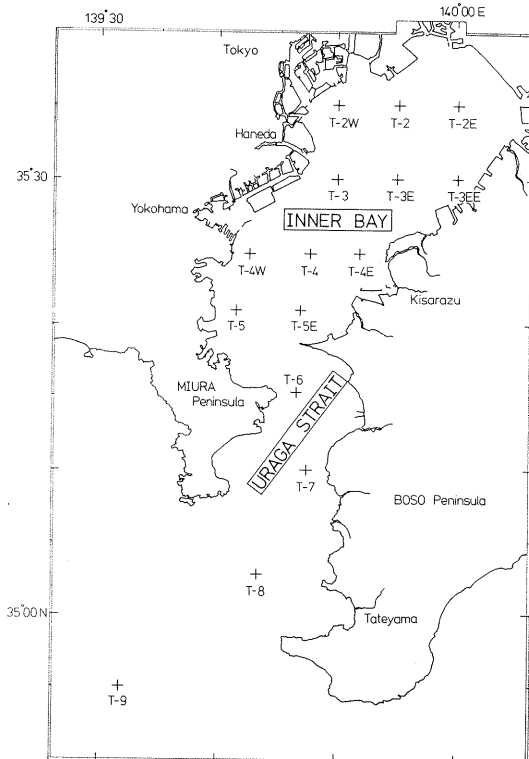


Fig. 1. Map of Tokyo Bay showing the location of stations.

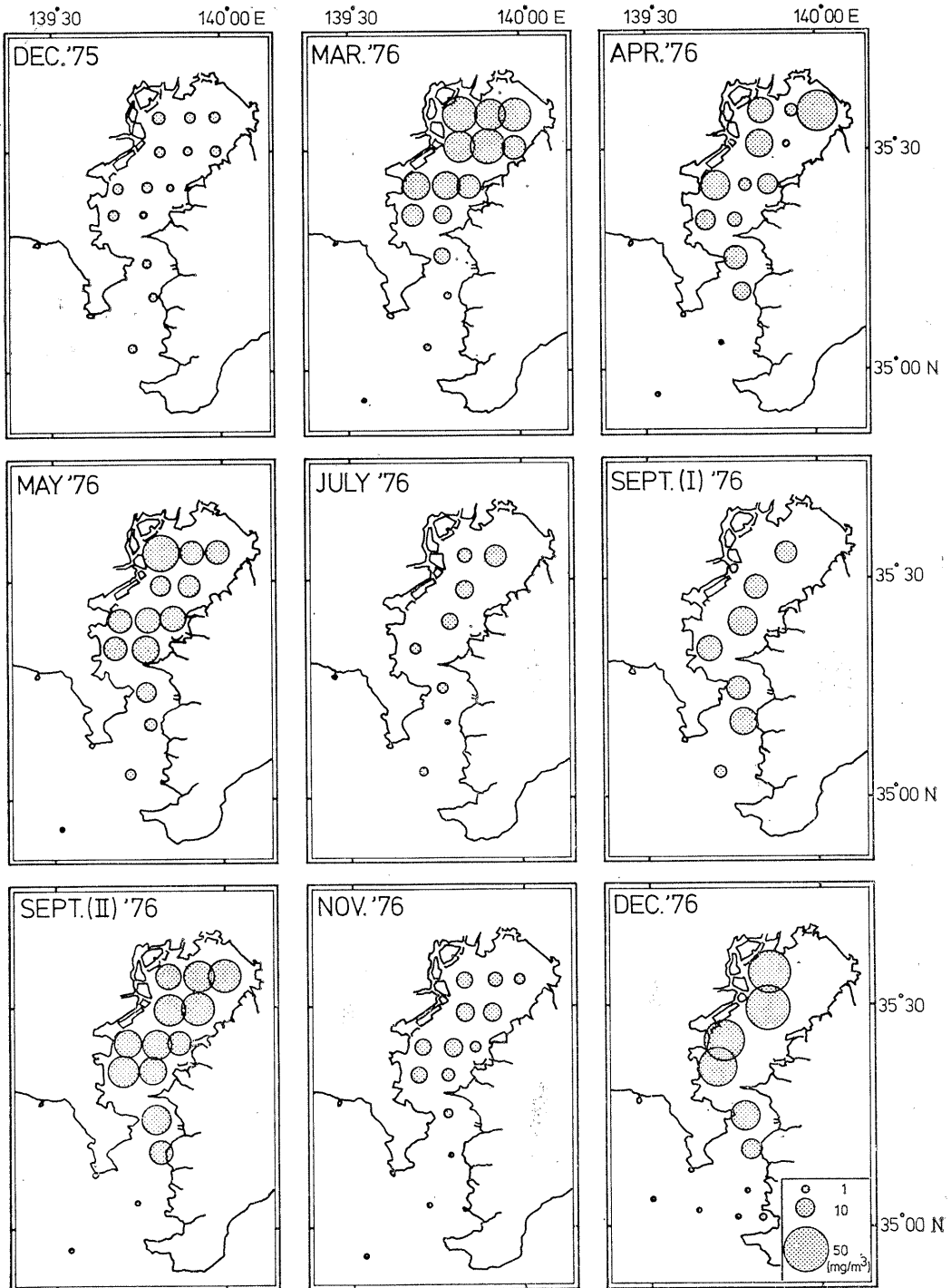


Fig. 2. Distribution of chlorophyll *a* concentration in the surface water of Tokyo Bay from December 1975 through December 1978.

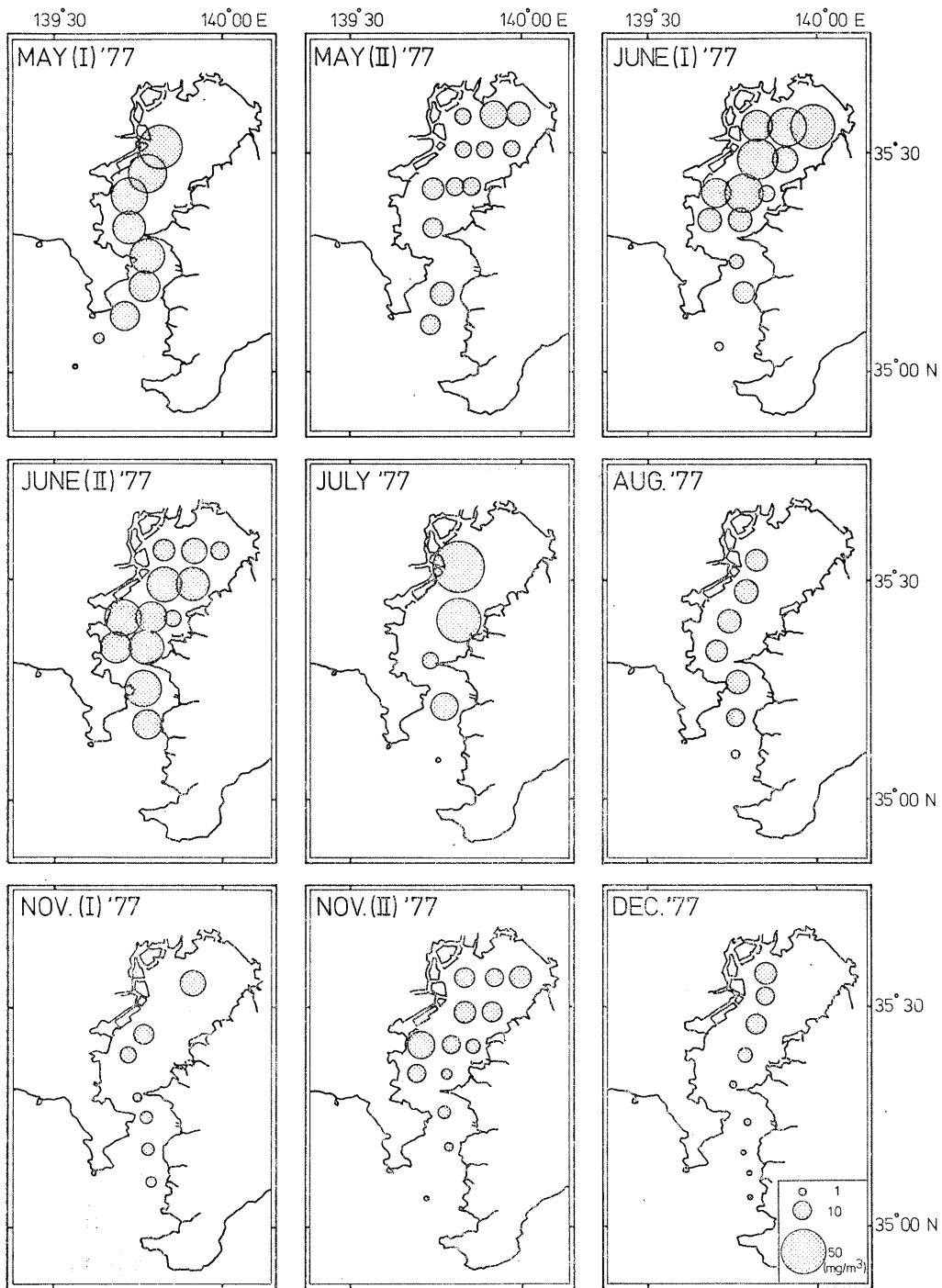


Fig. 2. (Continued)

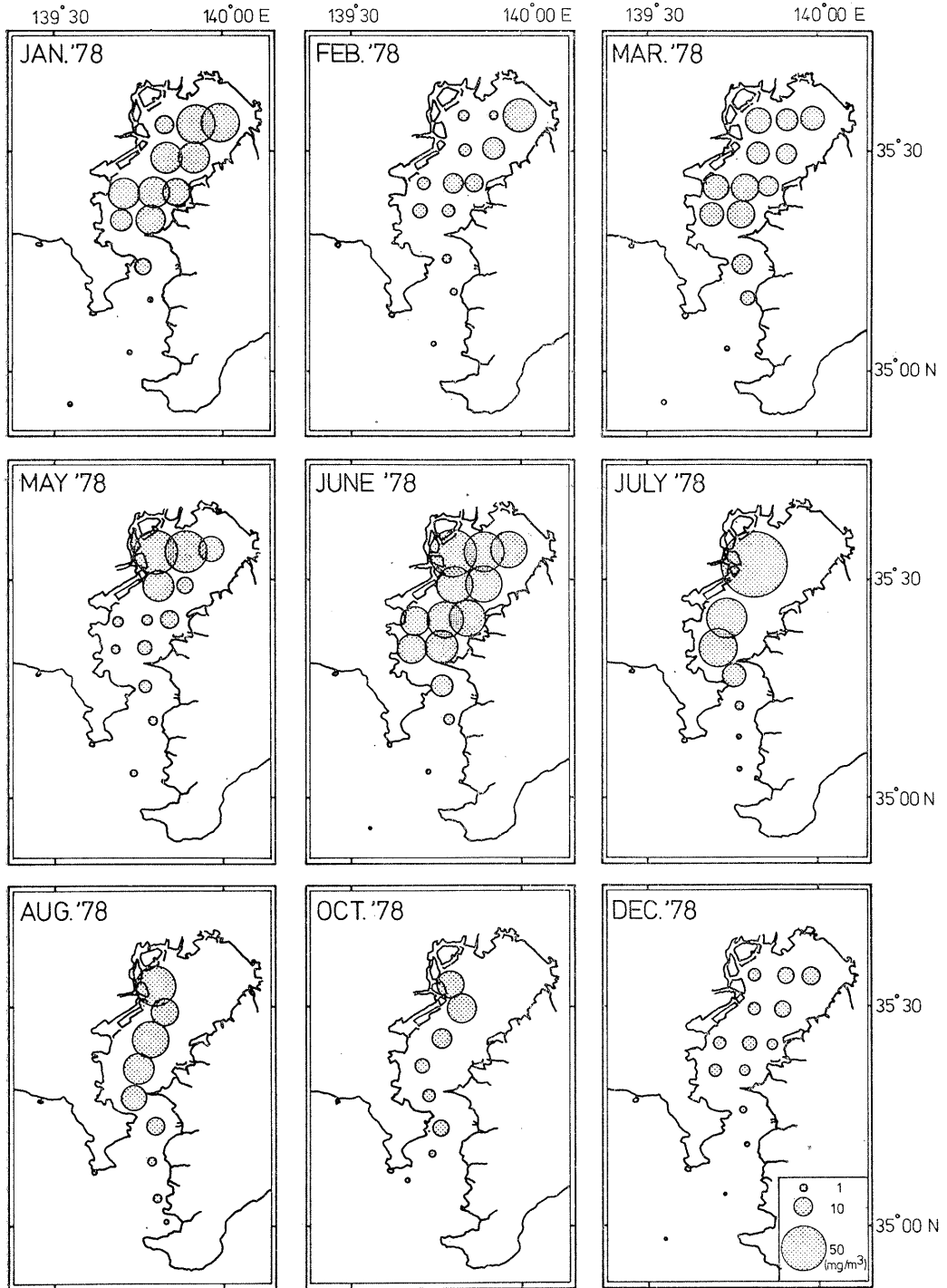


Fig. 2. (Continued)

from station to station and with the time of year as can be seen in Fig. 2. Both in the northern and central regions of the inner bay the chlorophyll *a* concentrations remained at levels higher than 10 mg/m³ throughout most the year. The highest chlorophyll *a* concentration of 104.7 mg/m³ was obtained in the region off Haneda in July 1978.

The most typical type of distribution can be seen in the case of May 1978 (Fig. 2) with higher chlorophyll *a* values in the northwestern inner bay and lower values in the southeastern inner bay and in Uraga Strait. This type of distribution has been observed frequently (ICHIMURA 1967, TERADA *et al.* 1974, YAMAGUCHI and ICHIMURA 1976), and has been explained as related to environmental gradients, especially to nutrient gradients. During the present investigation, such a situation was also observed on some occasions.

The second type of distribution is represented by that of February 1978, in which the surface chlorophyll *a* concentration was higher in the northeastern part than in the southwestern part of the inner bay. This type of distribution was rather rare and found in April 1976, May (II)

1977 and February 1978. It is of interest to note that such high chlorophyll *a* concentrations were not reported before in the eastern part of the inner bay. The third type of distribution is characterized by a rather homogeneous distribution of chlorophyll *a* concentration in the inner bay as seen in the case of March 1976. This type of chlorophyll *a* distribution was often obtained throughout the year irrespective of the seasons.

In general, the trend of the surface chlorophyll *a* distribution is concluded to be similar to that of ten or more years ago with higher chlorophyll *a* concentrations in the northwestern part of the inner bay and with a decrease of the concentrations to the southeast. During the past ten years, however, the area of higher chlorophyll *a* concentrations has extended further to the southeast.

Seasonal changes of the surface chlorophyll *a* concentration at each station are shown in Fig. 3. Although sometimes measurements were not made every month, comparisons can be made. The concentrations of chlorophyll *a* remained at very high levels throughout the year at the stations in the inner bay. Generally, the chloro-

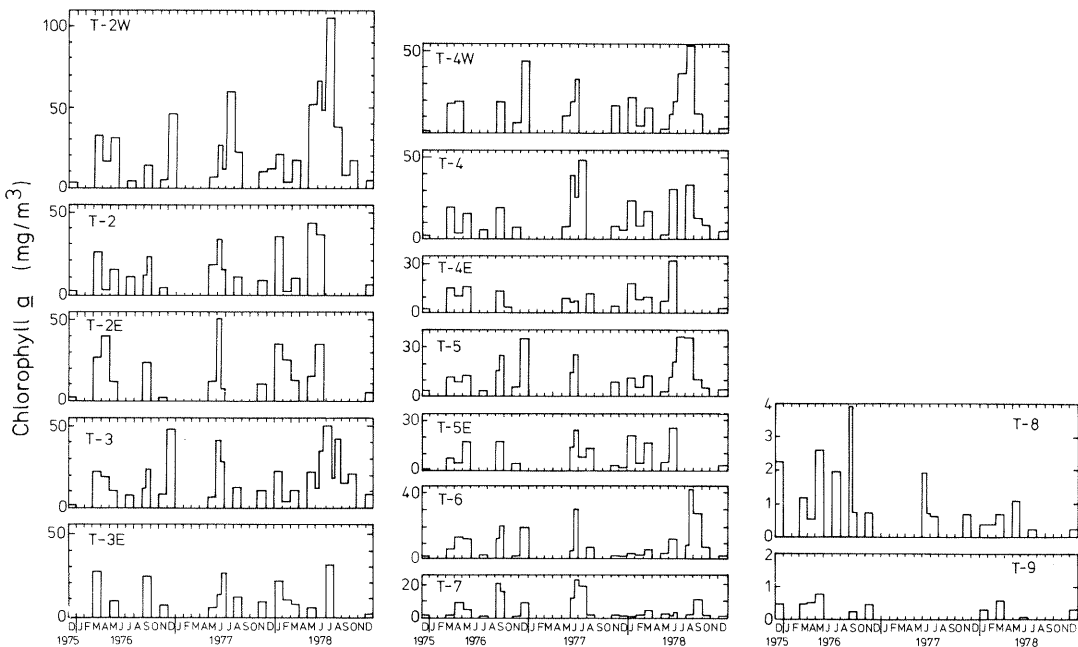


Fig. 3. Seasonal changes of the surface chlorophyll *a* concentration at 14 stations (Stns. T-2W~T-9).

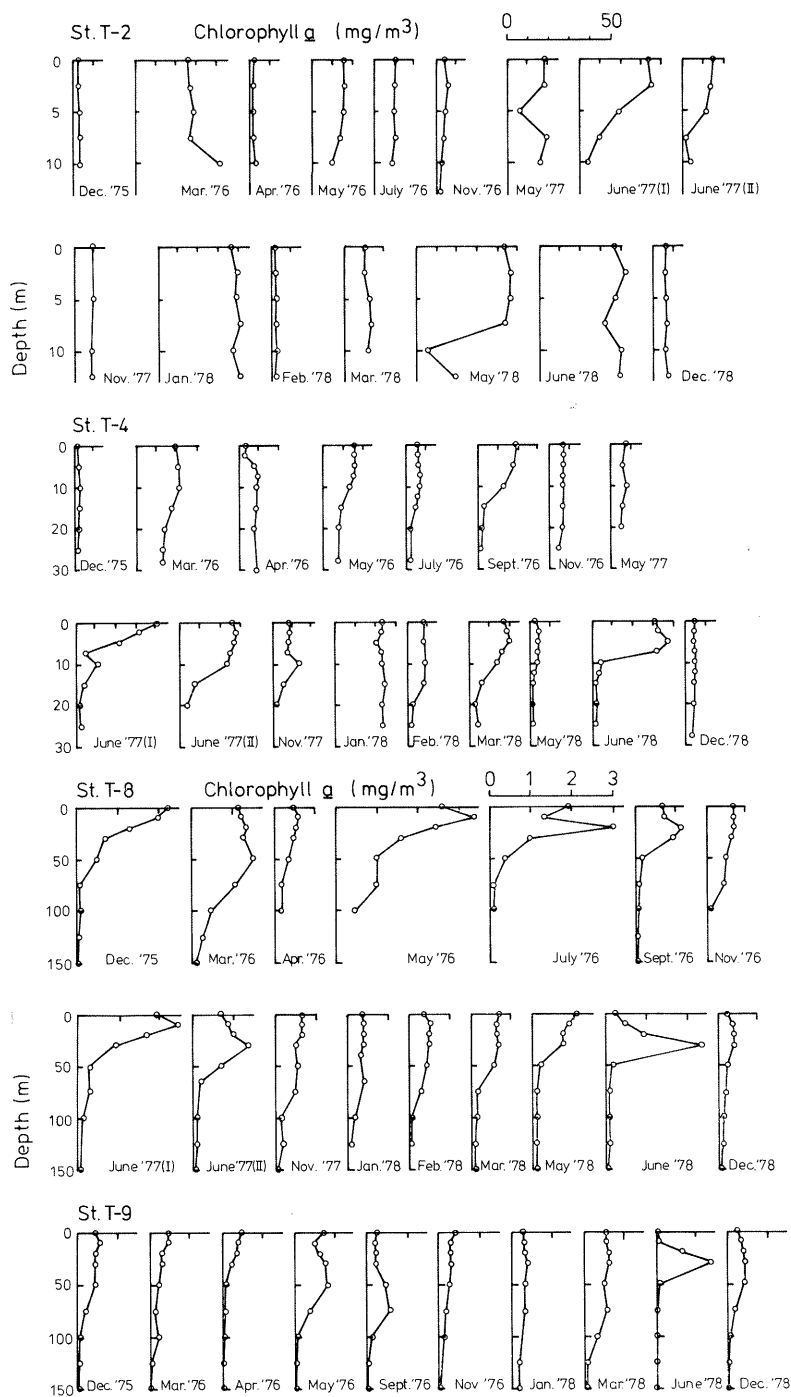


Fig. 4. Vertical distributions of chlorophyll *a* at Stns. T-2, T-4, T-8 and T-9.

phyll *a* concentration began to increase from March and reached its maximum in August, sometimes with a small decrease observed during the rainy season (mainly in June). It decreased rapidly in autumn and remained comparatively low during winter until the following March with some short-term variations. This general pattern of variation is similar to those observed in Tokyo Bay ten or more years ago (ICHIMURA and ARUGA 1964, ICHIMURA 1967, YAMAGUCHI and ICHIMURA 1976). However, as generally observed by other investigators, the seasonal variations of chlorophyll *a* concentration with two or three remarkable peaks including the spring bloom, summer bloom and/or autumn increase were not clearly observed during the present investigation. It may be that these peaks were possibly hidden by a higher basal level of chlorophyll *a* concentration during these years in Tokyo Bay.

In the northwestern part of the inner bay (Stn. T-2W), the typical pattern of variations as mentioned above was obtained in the surface chlorophyll *a* concentration. On the contrary, in the northeastern part of the inner bay (Stn. T-2E), fairly high concentrations of chlorophyll *a* were observed during winter as compared with the concentrations in other parts of the bay. For example, the values obtained in January or February 1978 were approximately equal to those obtained in May or June 1978 in the northeastern part of the inner bay, whereas in the northwestern part values one half to one third the May or June values were obtained in winter (Fig. 3).

The fluctuations of the surface chlorophyll *a* concentrations at Stns. T-6 and T-7 in Uraga Strait were rather large with a range of 0.336-41.68 mg/m³ (Fig. 3). Water movement in the strait is strongly affected by tidal currents. The boundary between oceanic and neritic waters around the strait is shifted continually northwards or southwards, so that even if the observations were done on the same day the values obtained would change conspicuously from time to time. Thus, it is difficult to have a generalized trend of variations in the chlorophyll *a* concentrations in Uraga Strait.

The surface chlorophyll *a* concentrations at

Stns. T-8 and T-9 were considerably lower as compared with those at other stations in the bay and never exceeded 4 mg/m³ throughout the year (Fig. 3). The chlorophyll *a* concentrations at Stn. T-8 were always higher than those at Stn. T-9. This is possibly due to the fact that the area of Stn. T-8 is affected by neritic water from the bay more effectively than at Stn. T-9.

The seasonal changes in the vertical distribution of chlorophyll *a* at Stns. T-2, T-4, T-8 and T-9 are shown in Fig. 4. At Stn. T-2 the chlorophyll *a* concentration varied conspicuously and was sometimes stratified vertically in summer, whereas homogeneous distributions were observed in winter. When stratified, the chlorophyll *a* maximum was usually found within the upper 5 m layer and sometimes near the bottom. At Stn. T-4 the pattern of vertical distribution did not vary as much as that at Stn. T-2, and a stratified distribution was obtained almost throughout the year except for December 1975, January and December 1978 in which homogeneous distributions were observed. The chlorophyll *a* maximum was found within the upper 15 m layer, which was a little deeper than that at Stn. T-2.

The distinctive stratified vertical distribution of chlorophyll *a* was observed in the northwestern part of the inner bay by ICHIMURA (1967) and FUNAKOSHI *et al.* (1974). According to ICHIMURA (1967), the stratified distribution of chlorophyll *a* may possibly be due to special hydrographic conditions in the inshore region of the bay where the distinctive gradient of density has been produced by freshwater discharge. In the present investigation, the chlorophyll *a* distribution was well stratified during spring to autumn both at Stns. T-2 and T-4. In winter, however, no clear stratification was observed in the vertical distribution of chlorophyll *a*. This indicates that the phytoplankton cells were distributed almost homogeneously throughout the water column due to the vertical mixing of water caused by strong wind in this shallow part of the bay.

At Stns. T-8 and T-9, the chlorophyll *a* concentration in the surface water was very low and did not exceed 4 mg/m³ throughout the year as described above. The concentration of

chlorophyll *a* at each depth was almost always higher at Stn. T-8 than at Stn. T-9. The stratification of chlorophyll *a* distribution was observed throughout the year at both stations (Fig. 4). These patterns of stratification coincide well with those reported in the oceanic regions (ARUGA and MONSI 1962, LORENZEN 1967, ARUGA and ICHIMURA 1968), especially with those reported in summer. The chlorophyll *a* maximum was found at 10–50 m depth and 10–75 m depth at Stns. T-8 and T-9, respectively. The vertical distribution of chlorophyll *a* is usually characterized by the presence of a chlorophyll *a* maximum (LORENZEN 1967). The fact that the chlorophyll *a* maximum at Stn. T-9 was located deeper than that at Stn. T-8 suggests a strong influence of oceanic water at Stn. T-9. These chlorophyll *a* maxima were found mostly at the thermocline and in some cases above it.

(2) Photosynthetic activity

With the surface water samples collected near

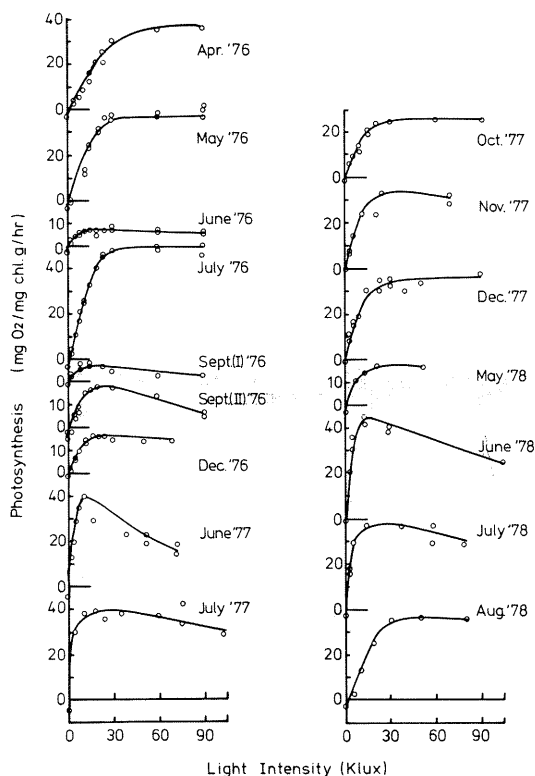


Fig. 5. Photosynthesis-light curves of phytoplankton from the surface water off Haneda in Tokyo Bay.

Tokyo Light off Haneda, the photosynthesis of phytoplankton was measured at nearly *in situ* temperatures under various light intensities. The photosynthesis-light curves thus obtained are shown in Fig. 5. The light intensity at which the light-saturation of photosynthesis occurred was about 10–30 klux, and the light-saturated net photosynthetic rates were in the range of 8.20–56.10 mgO₂/mg.chl.*a*/hr. The inhibition of photosynthesis by strong light was sometimes encountered within the range of light intensity up to 100 klux. This inhibition occurred particularly with those samples obtained during the period of high water temperature. According to ICHIMURA (1967), in most cases the light-saturation of photosynthesis occurred at a light intensity below 8 klux with phytoplankton samples taken from the northwestern part of Tokyo Bay, and no inhibition by strong light

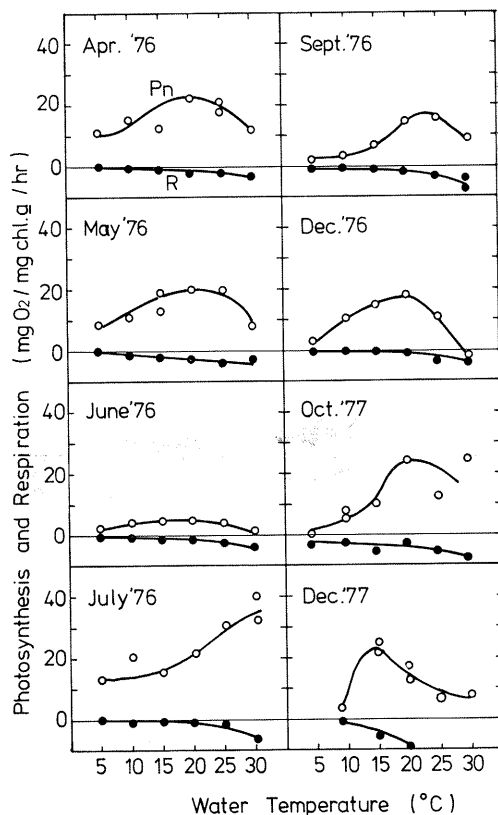


Fig. 6. Photosynthesis- and respiration-temperature curves of phytoplankton from the surface water off Haneda in Tokyo Bay.

was observed at light intensities up to 20 klux. A similar photosynthesis-light curve was reported with a bloom of *Skeletonema costatum* which showed no inhibition by strong light even at 140 klux (HOGETSU *et al.* 1959). FUNAKOSHI (1973) also reported no inhibition of photosynthesis in *Skeletonema costatum* under a strong light of 150 klux in summer. On the other hand, many observations about the inhibition of photosynthesis by strong light were reported by many investigators (RYTHER 1956, RYTHER and MENZEL 1959, ICHIMURA *et al.* 1962, ICHIMURA and ARUGA 1964, ARUGA 1965b). It is noteworthy that both types of photosynthesis-light curves with or without inhibition by strong light were obtained in the present investigation. This suggests that the subsurface phytoplankton cells photosynthesize at somewhat higher rates than the surface ones in Tokyo Bay, at least in summer.

Photosynthesis-temperature relations of phytoplankton have been scarcely studied from the ecological and physiological points of view, and in these respects the information about natural phytoplankton communities is especially scarce (ARUGA 1965a, ARUGA and ICHIMURA 1968). Seasonal changes in the photosynthesis-temperature curves and the respiration-temperature curves obtained with the samples taken from the surface water near Tokyo Light off Haneda are shown in Fig. 6. In most cases the net photosynthetic rate increased gradually with a rise in temperature to reach a maximum and decreased gradually with a further rise in temperature. The maximum photosynthetic rates mostly occurred at temperatures between 20 and 25°C except in July 1976 and December 1977. Significant seasonal changes in the temperature optimum for photosynthesis were not observed. According to ARUGA (1965b), in laboratory cultures the photosynthesis-temperature relation of algae varied to some extent with the temperature conditions under which they had been grown. Under natural conditions ARUGA (1965a) observed that the optimum temperature for photosynthesis of freshwater phytoplankton shifted adaptively; the higher the environmental temperature, the higher the optimum temperature for photosynthesis. How-

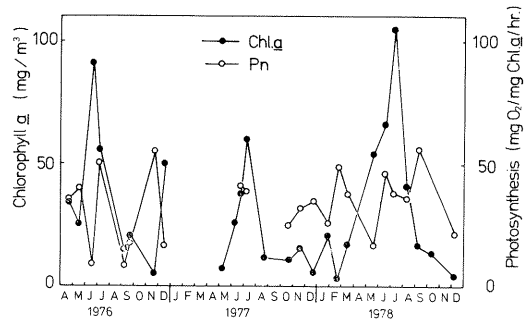


Fig. 7. Seasonal changes of the concentration of chlorophyll *a* and the light-saturated net photosynthetic rate per unit amount of chlorophyll *a* of phytoplankton in the surface water off Haneda in Tokyo Bay.

ever, even though the data were limited, such a relationship was not observed in the present study. The respiratory rate of phytoplankton gradually increased with a rise in temperature within the temperature range of the present measurements.

Seasonal changes in the light-saturated net photosynthetic rate per unit amount of chlorophyll *a* and the chlorophyll *a* concentration of surface water off Haneda are illustrated in Fig. 7. The light-saturated net photosynthetic rate varied in the range of 8.20–56.01 mgO₂/mg.chl. *a*/hr with the highest value in September 1978 and the lowest in September 1976. Such a definite trend as already reported in Tokyo Bay by ICHIMURA and ARUGA (1964) and ICHIMURA (1967) was not observed in the changes of the photosynthetic rate. In those reports the photosynthetic rate on a chlorophyll *a* basis increased from the end of spring and showed a peak in early summer, thereafter it decreased in early autumn but increased again showing a small peak in late autumn. In the present investigation, however, the seasonal changes in the photosynthetic activity as well as the chlorophyll *a* concentrations of surface water considerably differed from those obtained early in the 1960's in Tokyo Bay (ICHIMURA and KOBAYASHI 1964, ICHIMURA and ARUGA 1964, ICHIMURA 1967) as well as from those in eutrophic lakes (ICHIMURA and ARUGA 1964). The light-saturated net photosynthetic rate per unit volume of water in the same samples showed changes strongly related to the changes in chlorophyll *a* concen-

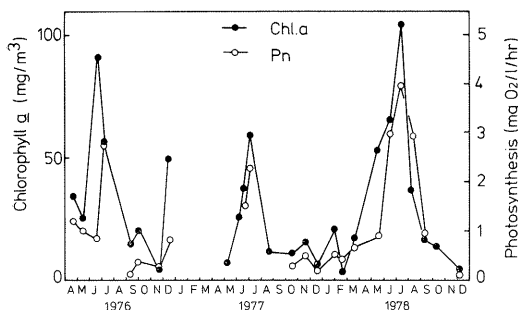


Fig. 8. Seasonal changes of the concentration of chlorophyll *a* and the light-saturated net photosynthetic rate per unit volume of water of phytoplankton in the surface water off Haneda in Tokyo Bay.

tration (Fig. 8). This would mean that the photosynthetic activity per unit volume of water is ordinarily dependent on the phytoplankton density or on the concentration of chlorophyll *a* in the water concerned.

The distribution of the light-saturated net photosynthetic rate of surface phytoplankton in November 1977 is illustrated in Fig. 9. Three regions of higher photosynthetic activity were clearly recognized. The photosynthetic rate was considerably higher in the northwestern part of the bay as reported by ICHIMURA (1967), TERADA *et al.* (1974) and FUNAKOSHI *et al.* (1974). Usually the photosynthetic rate of phytoplankton was higher in this region than elsewhere in the bay throughout the year. It is interesting to note that another area of high photosynthetic rate was identified between Yokohama and Kisarazu. Thus, an extension of the highly productive area in recent years is suggested.

There have been a large number of reports on phytoplankton production in which the photosynthesis of phytoplankton was measured either by the light and dark bottle oxygen technique or by the radioactive carbon (^{14}C) technique. With natural populations the agreement between the data obtained by the two techniques is often poor (RYTHER and YENTSCH 1958, McALLISTER 1961). The ^{14}C technique can give results much lower than those calculated from oxygen evolution (ANTIA *et al.* 1963). As reported by SHIMURA *et al.* (1978) with *Trichodesmium* populations, a suitable correction

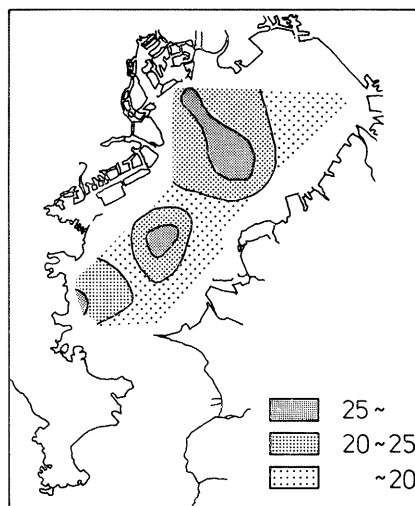


Fig. 9. Distribution of the light-saturated net photosynthetic rate ($\text{mg O}_2/\text{mg chl. } a/\text{hr}$) of surface phytoplankton in Tokyo Bay in December 1977.

must be made in certain situations for the extracellular release of photosynthates when the primary production is computed on the basis of the data obtained by the ^{14}C technique. McALLISTER (1961), however, found that the absolute ^{14}C uptake rates appear to exceed the absolute O_2 evolution rates at high light intensity for shade-adapted cells. When comparing the values obtained by the different techniques, therefore, certain corrections should be considered carefully. In the studies of phytoplankton productivity in Tokyo Bay, both of the techniques have been employed independently. Using the ^{14}C technique, ICHIMURA (1967) obtained light-saturated photosynthetic rates of 0.4–3.5 $\text{mgC}/\text{mg chl. } a/\text{hr}$ in the highly eutrophic inshore area off Haneda and 0.4–2.5 $\text{mgC}/\text{mg chl. } a/\text{hr}$ in the area off Kisarazu in Tokyo Bay during 1962–1963. Using the same technique, ICHIMURA and KOBAYASHI (1964) reported light-saturated photosynthetic rates of 0.46–5.18 $\text{mgC}/\text{mg chl. } a/\text{hr}$ for the surface water of the inner bay. YAMAGUCHI and ICHIMURA (1976) obtained high photosynthetic rates of 0.69–7.20 $\text{mgC}/\text{mg chl. } a/\text{hr}$ during the period of 1972–1974 in the bay. On the other hand, using the light and dark bottle oxygen technique, HOGETSU *et al.* (1959) obtained the light-saturated photo-

synthetic rates of 24–45 mgO₂/mg.chl./hr for the bloom of *Skeletonema costatum* off Haneda in Tokyo Bay. FUNAKOSHI *et al.* (1974) reported rates of 1.5–15 mgO₂/mg.chl./hr also for the *Skeletonema* bloom in the bay. In order to compare the data from the oxygen technique with those from the ¹⁴C technique, the amount of O₂ evolved was tentatively converted to the amount of carbon assimilated with the photosynthetic quotient as unity. As a result, the values obtained in the present work were 3.08–21.00 mgC/mg.chl./hr, indicating that the higher rates are extraordinarily high even if underestimation by the ¹⁴C technique is taken into consideration. However, at least, it is noted that the light-saturated photosynthetic rate of phytoplankton in Tokyo Bay is quite high when compared with the rates in productive Oyashio (3–6 mgC/mg.chl./hr) and coastal areas (2–7 mgC/mg.chl./hr), or with the rates in eutrophic lakes (2–6 mgC/mg.chl./hr) summarized by ICHIMURA and ARUGA (1964) for Japanese waters. Thus, it is concluded that the photosynthetic activity of phytoplankton in Tokyo Bay is as high as the highest level observed in natural waters (YAMAGUCHI and SHIBATA 1979).

(3) *Phytoplankton biomass and photosynthetic activity in relation to environmental factors*

Water temperature is one of the major environmental factors affecting phytoplankton produc-

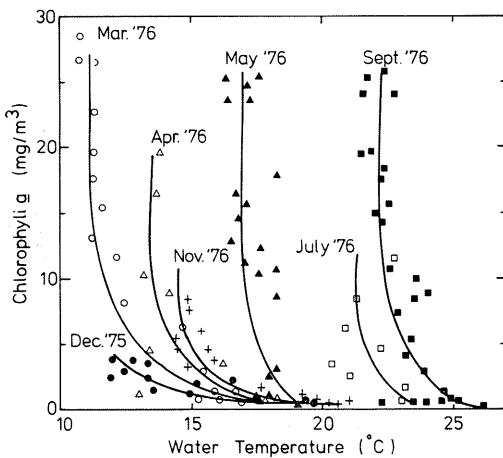


Fig. 10. Relationships between chlorophyll *a* concentration and temperature in the surface water of Tokyo Bay (December 1975–November 1976).

tion. The chlorophyll *a* concentrations obtained in December 1975–November 1976 for the surface water of Tokyo Bay and Uruga Strait were plotted in relation to *in situ* temperatures (Fig. 10). As can be seen in Fig. 10, the chlorophyll *a* concentration remained high irrespective of changes in water temperature, especially in the inner bay. In Fig. 11, the chlorophyll *a* concentrations in the surface water at Stn. T-2W is plotted in relation to the *in situ* water temperatures. The upper level of chlorophyll *a* concentration seemed to be related to water temperature to some extent although no significant correlation was observed.

The light-saturated net photosynthetic rates per unit amount of chlorophyll *a* of surface phytoplankton off Haneda were plotted in relation

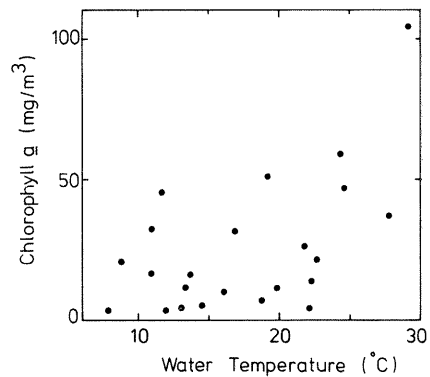


Fig. 11. Relationship between chlorophyll *a* concentration and temperature of the surface water at Stn. T-2W in Tokyo Bay.

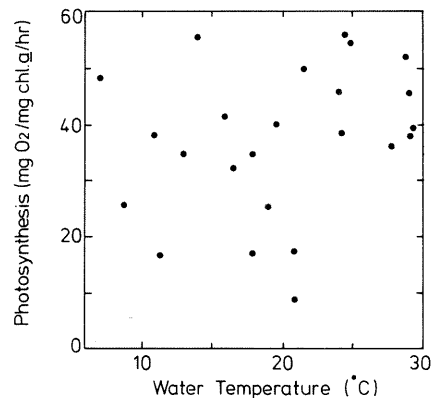


Fig. 12. Relationship between the light-saturated net photosynthetic rate of phytoplankton and temperature of the surface water off Haneda.

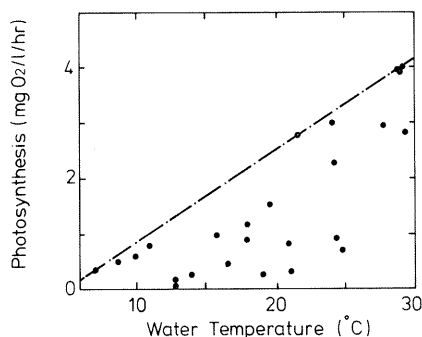


Fig. 13. Relationship between the light-saturated net photosynthetic rate of phytoplankton and temperature of the surface water off Haneda.

to the *in situ* water temperatures, but no correlation was found (Fig. 12). This would suggest that the water temperature does not limit the photosynthetic capacity of phytoplankton. However, as can be seen in Fig. 13, the upper level of the light-saturated net photosynthetic rate per unit volume of water seemed to be limited to a certain extent by temperature as was the case with chlorophyll *a* concentrations (Fig. 11). As the activity of the organisms increases in general with rise in temperature, it is expected that the photosynthetic rate of phytoplankton is higher during the period of higher water temperature. ICHIMURA (1967) obtained a linear relationship between the light-saturated photosynthetic rate per unit amount of chlorophyll and *in situ* water temperature at a station off Haneda in Tokyo Bay. In the present study, however, such a clear relationship was not obtained between the light-saturated photosynthetic rate or the chlorophyll *a* concentration and the *in situ* water temperature in the inner bay as shown above.

The relationships between the light-saturated net photosynthetic rate of phytoplankton and salinity and between the chlorophyll *a* concentration and salinity of the surface water are shown in Fig. 14, in which are included the data obtained in the inner part of the bay and Uruga Strait. The light-saturated net photosynthetic rate of phytoplankton from the low-salinity water of the inner bay was appreciably higher when compared with the low photosynthetic rate of phytoplankton from the high-salinity water of Uruga Strait. In Fig. 14(A)

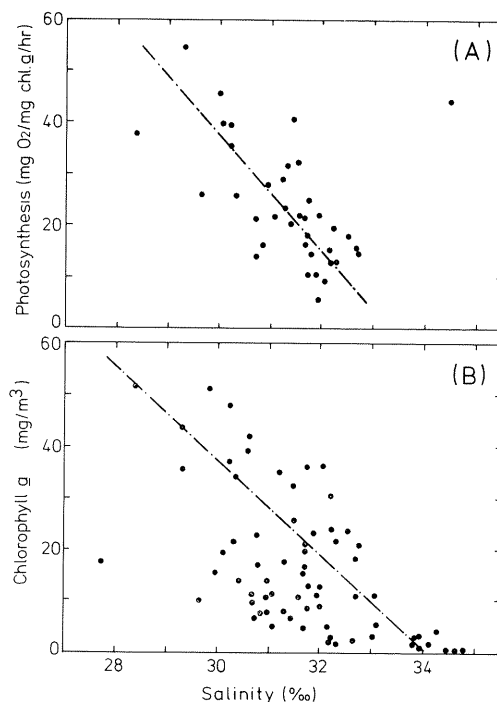


Fig. 14. Relationships of the light-saturated net photosynthetic rate and the chlorophyll *a* concentration to salinity in the surface water in Tokyo Bay.

it is clearly illustrated that the photosynthetic rate was lower in the samples from the high-salinity water even though the data scattered to a certain extent. A similar trend was also obtained between the chlorophyll *a* concentration and salinity as shown in Fig. 14(B), though the data scattered much more as compared to Fig. 4(A).

Salinity is also an important factor affecting phytoplankton production especially in the neritic and estuarine areas where a noticeable salinity gradient is often observed. There have been many investigations concerning the effect of salinity on phytoplankton production (NAKANISHI and MONSI 1965, MAEDA *et al.* 1973, SHIMURA *et al.* 1979, TERADA and ICHIMURA 1979a, b). According to NAKANISHI and MONSI (1965), phytoplankton in Tokyo Bay seemed to be tolerant to a rather wide range of salinity without appreciable decrease in their photosynthetic activity. TERADA and ICHIMURA (1979a) found that within the estuary the photo-

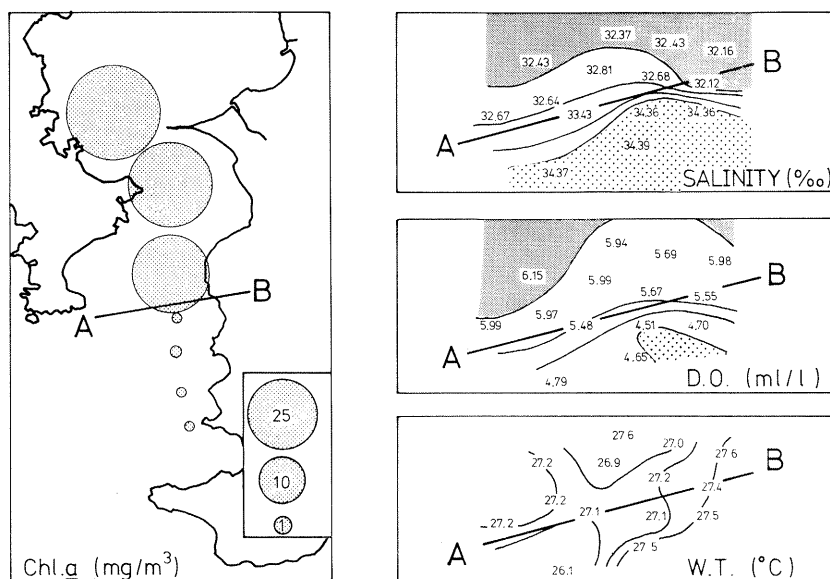


Fig. 15. Distributions of chlorophyll *a* concentration, salinity, dissolved oxygen concentration and temperature in the surface water at the entrance of Tokyo Bay obtained on August 26, 1978.

synthetic rate correlated linearly with salinity and inversely with nutrient concentration. The present data coincide fairly well with those reported by TERADA and ICHIMURA (1979b) in the salinity range above 30‰. In this range, the lower photosynthetic rate obtained in the present study may be not only due to higher salinity but also to lower concentrations of nutrients. The photosynthetic rate of phytoplankton was low in the southern part of the inner bay with high salinity. It may be possible to expect that inflowing freshwater stimulates in some way the phytoplankton photosynthesis in the innermost part of the bay where the photosynthetic rate was observed to be higher in water of lower salinity.

In Fig. 14(B) special attention is paid to the distinctive difference in the concentration of chlorophyll *a* around the salinity of 33.5‰, because the chlorophyll *a* concentration decreased with the increase in salinity and could not be found at any greater concentrations than 5 mg/m³ in the water with salinity of 33.5‰ or more. Fig. 15 shows the results of the observations on hydrographic conditions and chlorophyll *a* concentration in the surface water around the front at the entrance of Tokyo Bay on August

26, 1978. A marked difference was observed in the concentration of chlorophyll *a* around the front, the boundary of bay water and oceanic water. The boundary was quite clearly distinguished in salinity and dissolved oxygen concentration but not in water temperature. The boundary salinity was around 33.5‰ and agreed well with that mentioned above in reference with Fig. 14(B). Thus, the neritic phytoplankton community in Tokyo Bay is characterized by water with salinity of less than 33.5‰.

Transparency of water is dependent on the concentration of suspended substances and colored dissolved matter in the water. Fig. 16 shows the relationship between the chlorophyll *a* concentration in surface water and transparency (Secchi disk depth) measured in Tokyo Bay and its adjacent areas including Stns. T-8 and T-9 during the period from March to November 1976. The obtained hyperbolic relationship coincided fairly well with that reported by ICHIMURA (1956) for lake water in Japan. However, there is a distinctive difference between the present result and the results obtained for the Kuroshio and [Oyashio areas by SAJIO and ICHIMURA (1960). The difference is clearly seen when the

concentration of chlorophyll *a* is plotted on logarithmic scale (Fig. 17); in the present areas the Secchi disk depth does not increase much with decrease of the chlorophyll *a* concentration. This suggests that the proportion of suspended substances other than phytoplankton is high in water of Tokyo Bay, which would largely be concerned with defining the photosynthetic layer in the bay.

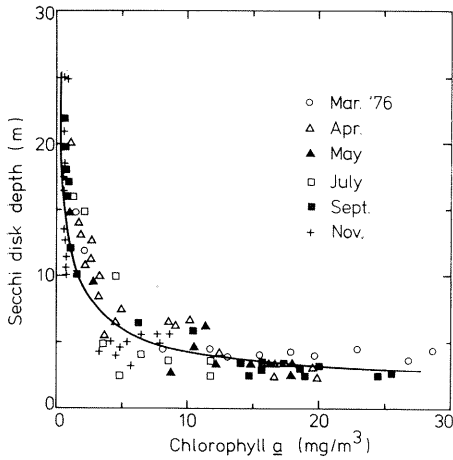


Fig. 16. Relationship between the concentration of surface chlorophyll *a* and Secchi disk depth in Tokyo Bay and adjacent areas (1976).

Figure 18 compares the horizontal distributions of chlorophyll *a*, light-saturated net photosynthetic rate, phosphate, nitrate, nitrite and silicate in the surface water of Tokyo Bay on December 11, 1978. The nutrient concentrations were higher in the northwestern part of the bay. Such a trend was already obtained in the early 1960's (ICHIMURA 1967) and seems not to have changed. The level of concentrations of these nutrients has not been changed very much although a slight decrease in nitrate was noticed.

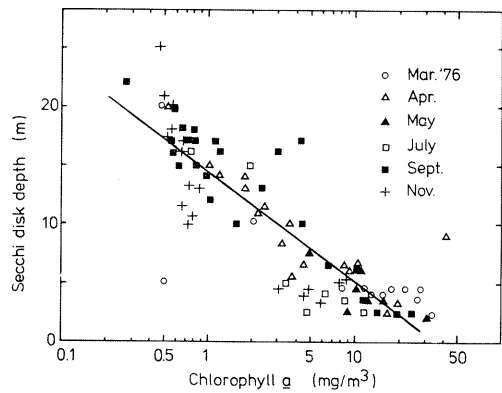


Fig. 17. Relationship between the concentration of surface chlorophyll *a* and Secchi disk depth in Tokyo Bay and adjacent areas (1976).

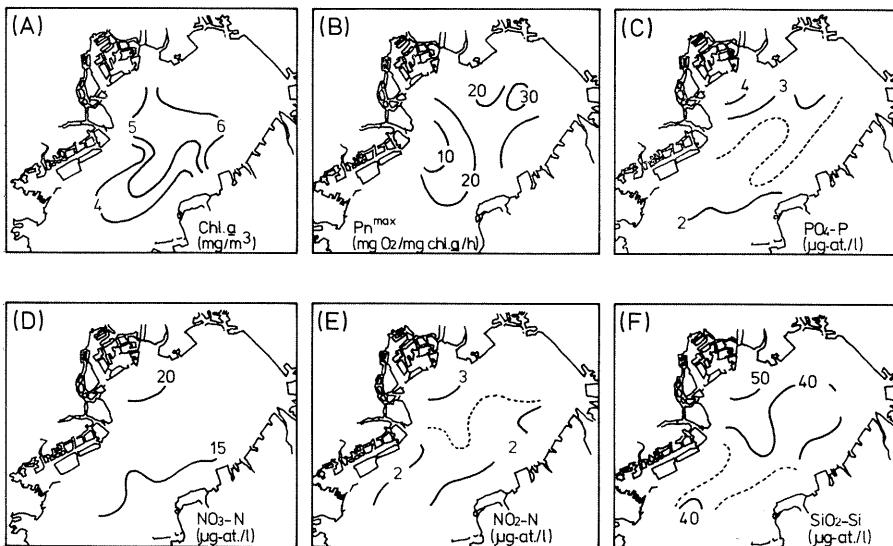


Fig. 18. Horizontal distributions of chlorophyll *a*, light-saturated net photosynthetic rate (P_n^{max}), phosphate, nitrate, nitrite and silicate in the surface water of Tokyo Bay on December 11, 1978.

It is generally said that the distribution of chlorophyll *a* is related to the distribution of nutrients and that the phytoplankton growth is greatly affected by nutrient concentrations. In the present investigation, the data supporting this generalization were obtained in May 1978, but in December 1978 the distribution of chlorophyll *a* did not coincide with that of the nutrients. A similar result was reported in the observation of the distribution of polluted water by SAITOH *et al.* (1979) when they analyzed the LANDSAT MSS data of 1972-1976 in Tokyo Bay. According to them, the chlorophyll *a* distribution might be dependent not on nutrient gradients but on such meteorological or physical factor as tide or drift current brought about by strong wind stress, which transports surface phytoplankton cells toward the northeastern part

of the bay. This situation could reasonably be used for explaining the distribution of chlorophyll *a* obtained in January and February 1978. In spite of these conditions it is said that phytoplankton chlorophyll *a* might be produced more vigorously in the northwestern water than in the southeastern water; in the former water appropriate nutrient supply is expected for phytoplankton growth.

Short-term variations of the concentrations of inorganic nutrients and chlorophyll *a* and the photosynthetic activity of phytoplankton in the surface water off Haneda are illustrated in Fig. 19. The variations of phosphate, nitrate and nitrite concentrations were almost independent of the variation of chlorophyll *a* concentration, while the variation of silicate concentration seemed to be inversely correlated with that of chlorophyll *a* concentration to a certain extent. Although the concentrations of phosphate and/or nitrate are usually considered to limit phytoplankton growth, it is hardly the case when the variation of phytoplankton biomass is independent of those of nutrient concentrations as seen in Fig. 19. It is reasonable to consider that the present concentrations of inorganic nutrients in Tokyo Bay are far above the levels to be limiting on phytoplankton growth (YAMAGUCHI and SHIBATA 1979).

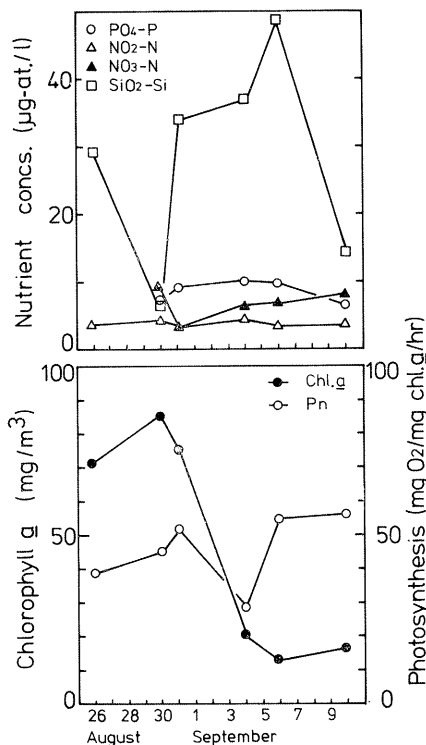


Fig. 19. Short-term changes in the concentrations of phosphate, nitrate, nitrite, silicate and chlorophyll *a* and in the light-saturated net photosynthetic rate of phytoplankton in the surface water off Haneda from August 26 to September 10, 1978.

4. Concluding remarks

In the inner part of Tokyo Bay, both the concentration of chlorophyll *a* and the photosynthetic activity of phytoplankton are very high almost throughout the year, so that a very high level of primary production by phytoplankton is expected all over the inner bay throughout the year. Especially in summer the light condition favors the maintenance of high primary productivity of phytoplankton, resulting in an increase of the phytoplankton standing crop and frequent occurrence of phytoplankton blooms. The highest productive area is found in the northwestern part of the inner bay, even though the highly productive area tended to expand southwards. A markedly high level of chlorophyll *a* concentration observed during the period other than summer and higher photosynthetic activity of phytoplankton in addition

to the extremely high levels of nutrient concentrations in water support the comparatively high level of primary productivity all over the inner part of Tokyo Bay provided that the meteorological and hydrological conditions are favorable.

Acknowledgements

We are very grateful to Captain T. ISOUCHI, officers and the crew of the T/S Seiyo Maru, Tokyo University of Fisheries, for their helpful cooperation during the cruises throughout the present investigations. Sampling work on board was carried out in cooperation with Professor M. MURANO and the member of his laboratory, to whom we express cordial thanks. We are also very much indebted to the members of our laboratory for their assistance throughout the investigations. We express our thanks to Ms. K. TORIKO for her kind help in revising the English of the manuscript.

References

- ANTIA, N. J., C. D. MCALLISTER, T. R. PARSONS, K. STEPHENS and J. D. H. STRICKLAND (1963): Further measurements of primary production using a large-volume plastic sphere. *Limnol. Oceanogr.*, **8**: 166-183.
- ARUGA, Y. (1965a): Ecological studies of photosynthesis and matter production of phytoplankton I. Seasonal changes in photosynthesis of natural phytoplankton. *Bot. Mag. Tokyo*, **78**: 280-288.
- ARUGA, Y. (1965b): Ecological studies of photosynthesis and matter production of phytoplankton II. Photosynthesis of algae in relation to light intensity and temperature. *Bot. Mag. Tokyo*, **78**: 360-365.
- ARUGA, Y. (1966): Ecological studies of photosynthesis and matter production of phytoplankton III. Relationship between chlorophyll amount in water and primary productivity. *Bot. Mag. Tokyo*, **79**: 20-27.
- ARUGA, Y. and S. ICHIMURA (1968): Characteristics of photosynthesis of phytoplankton and primary production in the Kuroshio. *Bull. Misaki Mar. Biol. Inst. Kyoto Univ.*, (12): 3-20.
- ARUGA, Y. and M. MONSI (1962): Primary production in the northwestern part of the Pacific off Honshu, Japan. *J. Oceanogr. Soc. Jap.*, **18**: 85-94.
- ARUGA, Y. and M. MONSI (1963): Chlorophyll amount as an indicator of matter productivity in bio-communities. *Plant & Cell Physiol.*, **4**: 29-39.
- FUNAKOSHI, M. (1973): Pollution and red tide occurrence in inland bay. *J. Rikkyo Jyogakuin*, **2**: 35-52. (in Japanese)
- FUNAKOSHI, M., N. NAKAMOTO and K. HOGETSU (1974): Primary production and the role of red tide in Tokyo Bay. *Ann. Rep. Special Project Res. Environment & Human Survival, Ministry Educ.*, p. 115-128. (in Japanese)
- HOGETSU, K., M. SAKAMOTO and H. SUMIKAWA (1959): On the high photosynthetic activity of *Skeletonema costatum* under the strong light intensity. *Bot. Mag. Tokyo*, **72**: 421-422.
- ICHIMURA, S. (1956): On the ecological meaning of transparency for the production of matter in phytoplankton community of lake. *Bot. Mag. Tokyo*, **69**: 219-226.
- ICHIMURA, S. (1967): Environmental gradient and its relation to primary productivity in Tokyo Bay. *Rec. Oceanogr. Works Jap.*, **9**: 115-128.
- ICHIMURA, S. and Y. ARUGA (1964): Photosynthetic natures of natural algal communities in Japanese waters. *K. Sugawara Fest. Vol. "Recent Researches in the Fields of Hydrosphere, Atmosphere and Nuclear Geochemistry"* (ed. Y. MIYAKE and T. KOYAMA). Maruzen, Tokyo. p. 13-37.
- ICHIMURA, S. and H. KOBAYASHI (1964): Primary production in Tokyo Bay. *Inform. Bull. Planktol. Jap.*, **11**: 6-8. (in Japanese)
- ICHIMURA, S., Y. SAIJO and Y. ARUGA (1962): Photosynthetic characteristics of marine phytoplankton and their ecological meaning in the chlorophyll method. *Bot. Mag. Tokyo*, **75**: 212-220.
- LORENZEN, C. J. (1967): Vertical distribution of chlorophyll and phaeo-pigments: Baja California. *Deep-Sea Res.*, **14**: 735-745.
- MAEDA, O., M. ZAMMA and S. ICHIMURA (1973): Photosynthetic response of estuarine phytoplankton to salinity variations in their habitat. *La mer*, **11**: 137-140.
- MARUMO, R. and M. MURANO (1973): Succession of plankton diatoms in Tokyo Bay. *La mer*, **11**: 70-82. (in Japanese)
- MARUMO, R., A. SANO and M. MURANO (1974): Further study on succession of plankton diatoms in Tokyo Bay. *La mer*, **12**: 145-156. (in Japanese)
- MATSUDAIRA, Y. (1964): Cooperative studies on primary productivity in the coastal waters of Japan 1962-63. *Inform. Bull. Planktol. Jap.*, **11**: 24-73.
- MCALLISTER, C. D. (1961): Observations on the variation of planktonic photosynthesis with light intensity, using both the O₂ and C¹⁴ method. *Limnol. Oceanogr.*, **6**: 483-484.

- NAKANISHI, M. and M. MONSI (1965): Effect of variation in salinity on photosynthesis of phytoplankton growing in estuaries. J. Fac. Sci., Univ. Tokyo, Sec. III, **9**: 19-42.
- RYTHER, J.H. (1956): Photosynthesis in the ocean as a function of light intensity. Limnol. Oceanogr., **1**: 61-70.
- RYTHER, J.H. and D.W. MENZEL (1959): Light adaptation by marine phytoplankton. Limnol. Oceanogr., **4**: 492-497.
- RYTHER, J.H. and C.S. YENTSCH (1958): Primary production of continental shelf waters off New York. Limnol. Oceanogr., **3**: 327-235.
- SAIJO, Y. and S. ICHIMURA (1960): Primary production in the northwestern Pacific Ocean. J. Oceanogr. Soc. Jap., **16**: 139-145.
- SAITOH, S., J. IISAKA and O. ASAOKA (1979): Marine pollution analysis in Tokyo Bay by LANDSAT 1 and 2. Proc. 13th Internat. Symp. Remote Sensing Environ. (Apr. 23-27, 1979, Ann Arbor, Michigan). p. 1657-1679.
- SCOR-Unesco W. G. 17 (1966): Determination of photosynthetic pigments. Unesco Monogr. Oceanogr. Methodol., **1**: 9-18.
- SHIMURA, S., Y. YAMAGUCHI, Y. ARUGA, Y. FUJITA and S. ICHIMURA (1978): Extracellular release of photosynthetic products by pelagic blue-green alga, *Trichodesmium thiebautii*. J. Oceanogr. Soc. Jap., **34**: 181-188.
- SHIMURA, S., H. SHIBUYA and S. ICHIMURA (1979): Growth and photosynthesis properties of some planktonic marine diatoms at various salinity. La mer, **17**: 149-155.
- STRICKLAND, J.D.H. and T.R. PARSONS (1972): A Practical Handbook of Seawater Analysis (2nd ed.). Fish. Res. Bd. Canada Bull. No. 167. Ottawa. 310 pp.
- TERADA, T. and S. ICHIMURA (1979a): Environmental properties and the distribution of phytoplankton biomass and photosynthesis in a small eutrophic estuary of Shimoda Bay. La mer, **17**: 137-144.
- TERADA, T. and S. ICHIMURA (1979b): Phytoplankton photosynthesis in a eutrophic estuary with special reference to salinity gradient. La mer, **17**: 171-177.
- TERADA, T., H. SEKI and S. ICHIMURA (1974): An areal distribution of microbial biomass in Tokyo Bay at summer stagnation period. La mer, **12**: 192-196.
- YAMAGUCHI, Y. and S. ICHIMURA (1976): Changes in primary production with eutrophication of Tokyo Bay. Preprint Oceanogr. Soc. Jap. Spring Meet. p. 120. (in Japanese)
- YAMAGUCHI, Y. and Y. SHIBATA (1979): Recent status of primary production in Tokyo Bay. Bull. Coast. Oceanogr., **16**: 106-111. (in Japanese)

東京湾における植物プランクトンのクロロフィル量 と光合成活性の変動

柴田 佳明, 有賀 祐勝

要旨: 植物プランクトン現存量(クロロフィル a)といくつかの環境要因を、東京湾内湾、浦賀水道および館山沖の定点を中心に、1975年12月から1978年12月までの3年間にわたって調べた。また、同時期に羽田沖の表面水を用いて光合成と呼吸の活性を種々の照度と温度の下で測定した。

通常、クロロフィル a 濃度は内湾北西部で高く、南東部で低かった。また浦賀水道以南では、クロロフィル a 濃度は内湾に比べて明白に低かった。光合成活性とクロロフィル a 濃度の季節変化は10年もしくはそれ以前に比べ大きく異なっており、両者とも1年を通じて高く、最大値は夏季に得られたが、春季および秋季の増殖は顕著でなかった。水温と塩分は植物プランクトンの現存量および光合成活性の変動に大きな役割を果しているようであり、植物プランクトンの現存量およびその分布の変化は栄養塩濃度等の化学的要因よりも、むしろ潮汐や強風によってもたらされる吹送流等の物理的もしくは気象的要因に依るところが大きいと考えられる。東京湾では、植物プランクトン群集の高い生産力は通年維持され、物理的環境が好適であれば、栄養塩等によって制限されることはないようである。

コイ目 (Cypriniformes) 魚類 46 種の 尾舌骨 (Urohyal) の形状*

草 下 孝 也**

On the Urohyal of Forty-Six Species of Fishes of the Order Cypriniformes*

Takaya KUSAKA**

Abstract: Urohyals of 46 species of fishes of the order Cypriniformes were observed and compared. The features of urohyals are remarkably characteristic of genera and families. The common feature of urohyals in this order is the vertical plate of main body developed commonly, and the ventral edge is remarkably expanded horizontally in various grades like a triangle or quadrate shape representatively. The frontal top as the part connected to the hypohyal is commonly developed, and on the other hand, the anterodorsal part connected to the basibranchial is entirely undeveloped. In the suborders *Characoidei* and *Cyprinidei*, the urohyals resemble in shape an aeroplane tail without a few example. In the suborder *Siluroidei*, the urohyal is commonly taking a flat shape as laterally viewed and a remarkably expanded shape as dorsally viewed.

著者は硬骨魚類の尾舌骨の形状を観察比較しているが(草下 1969, 1970, KUSAKA and THUC 1972, KUSAKA 1974, 草下 1975, 1977), 今回は観察したコイ目の 4 亜目, 14 科, 39 属の 46 種について結果を報告する。この目に属する魚類の尾舌骨の形状は, 2, 3 の例外を除けば, いずれも下辺の左右への拡りが非常によく発達しており, 垂直部は大體普通で, 中には垂直部がかなり狭小になっているものもある。いずれにしても前連部は比較的発達しているが, 鰓連部は発達せず, その部分の隆起や肥厚も全く見られない。下辺の拡りは極端な場合は長さよりも幅の方が大きいものさえある。拡り方は前方から後方にかけて徐々に拡りを増し, 後端近くで狭小になるか, 後端で急に消失する形のものもあり, 中には拡りの左右の後

端が棒状に尖っているものもある。下辺の拡りが本目でよく発達していることは本目の魚類が発達した内顎歯をもち, 雑食性で, この内顎で食物を噛みくだくために下顎を自由に動かし, 操縦性をもたせるために必要な形状と考えられる。例えば, やはり雑食性のキスや特殊な食性のソメワケベラの尾舌骨もやはり下辺拡り形をしていることでもうなずける (KUSAKA 1974)。

この目に含まれる各々の分類単位について, それぞれ形状に特徴が見られるが, 以下順を追って記述する。

コイ目 *Cypriniformes*

前連部はかなり肥厚しているが, 鰓連部は全く発達していない。垂直部は普通で, 下辺の拡りがよく発達する。尾舌骨形各部の割合を概括すると, 尾舌骨長は頭長の 5% のものから 50% のものもあり, 変化が大きい, 平均すれば 26% で,

* 1981年12月2日受理 Received December 2, 1981

** 〒154 東京都世田谷区若林 1-37-14
Wakabayashi 1-37-14, Setagaya-ku, Tokyo, 154
Japan

硬骨魚全体の標準よりはやや小さいといえる。骨高の骨長比は 18% から 260% で、やはり範囲が広く、平均値は 49% で、かなり高い値を示している。骨幅は 8% から 156% で変化が著しく、平均すれば 47% で、かなり幅広いといえる。

1. カラシン (Characin) 亜目 *Characoidei*

前連部発達・下辺折り型で、他にとりたてて特徴はない。尾舌骨長の頭長比は 12% ないし 46%、平均 29% で僅かに大きめである。

骨高の骨長比は 22% ないし 66%、平均 43% で、かなり高さは高い。骨幅の骨長比は 8% ないし 37%、平均 23% で、本目中では折りは狭い方である。

1.1 カラシン科 *Characidae*

垂直部は大体標準形であるが、短形のものも多い。下辺の折りはいずれも発達しているが、その程度はいろいろである。尾舌骨長の頭長比は 16% ないし 37% と範囲が広く、平均値は約 30% である。骨高の骨長比は 22% ないし 66%、平均値は約 46% で、かなり短形である。骨幅の骨長比は 8% ないし 37%、平均値は 23% で、下辺の折りは比較的少ない。

1.1-1 ピラニア (Piranha) 属 *Serrasalmus*

垂直部は発達し、骨高は高い。下辺の折りは次第に折り、中央部が幅広く、後方でせばまっているので、上面形は紡錘形をしている。

1.1-1.1 ピラニア・ナツレリ *Serrasalmus nattereri* (KNER)

尾舌骨長の頭長比は 30%、骨高の骨長比は 51% と著しく高く、骨幅の骨長比は 30% と標準的である。

1.1-2 メチネス属 *Metynnis*

垂直部はよく発達し、ほぼ正三角形を呈し、下辺折りもよく発達するが、その折りが下方にのびて、あたかも鞍状をしている。この形状は極めて特徴的である。

1.1-2.1 メチネス *Metynnis schreitmulleri* AHL

尾舌骨長の頭長比は 37% で、本科中ではかなり大きな方である。骨高の骨長比は 66% と本科

中で最高である。骨幅の骨長比も 36% で、やはり本科中で幅広いものの一つである。

1.1-3 ミロソマ属 *Mylossoma*

垂直部も下辺の折りも共によく発達し、折りの後縁はほぼ截形をしている。コイ目を代表する典型的な形をしているものの一つである。

1.1-3.1 ミロソマ *Mylossoma aureum* (AGASSIZ)

尾舌骨長の頭長比は 25% でやや小さく、骨高の骨長比は 61% とかなり大きく、骨幅の骨長比は 37% と本科中最も幅広い。

1.1-4 コンゴウ・テトラ (Congo tetra) 属 *Phenacogrammus*

垂直部は普通で、前連部がかなり肥大している。下辺の折りは下方にたれさがり、前方から後方まで一様な折り具合である。

1.1-4.1 コンゴウ・テトラ *Phenacogrammus interruptus* (BOULENGER)

尾舌骨長の頭長比は 16% と著しく小さく、本科中最小である。骨高の骨長比は 50% と大きい方であるが、骨幅の骨長比は 19% とかなり狭小である。

1.1-5 レポリナス属 *Leporinus*

垂直部は後上方によく発達している。一方、下辺の折りは発達が悪く、僅かに認められる程度である。

1.5-5.1 ブラック・ラインド・レポリナス (Black-lined leporinus) *Leporinus striatus* KNER

尾舌骨長の頭長比は 26%、骨高の骨長比は 50% といずれも標準であるが、骨幅の骨長比は 13% と本科中の最小値に近い。

1.1-6 キロダス属 *Chilodus*

前連部が肥厚している。垂直部は上辺がかなりそりあがっている。下辺の折りはよく発達し、上面形は細長い菱形をしている。

1.1-6.1 キロダス・プンクタータス *Chilodus punctatus* MUELLER & TROSCHEL

尾舌骨長の頭長比は 46% と本科中で最大であり、他科の魚類に比してもかなり大である。骨高の骨長比は 36% と割合に低く、骨幅の骨長比は

23% と普通である。

1.1-7 プリステラ属 *Pristella*

垂直部は直角三角形に発達している。前連部は比較的細い。下辺の広がりも僅かで細長く、上面からみてペン軸様の形状をしている。

1.1-7.1 プリステラ・リッドレイ *Pristella riddlei* (MEEK)

尾舌骨長の頭長比は 33%、骨高の骨長比は 30% といずれも小さい。さらに、骨幅の骨長比は 8% と本科中最小である。

1.1-8 モンクハウシア属 *Moenkhausia*

垂直部は細長く後方にのびる。下辺は短く、その後半に左右の広がりが発達し、その上面形は楕円形を呈する。

1.1-8.1 モンクハウシア・オリゴレピス *Moenkhausia oligolepis* (GÜNTHER)

尾舌骨長の頭長比は 23%、骨高の骨長比は 22%、骨幅の骨長比は 16% といずれも小さな値を示している。特に骨高は本科中最低である。

1.2 ヘミオダス (Hemiodus) 科 *Hemiodidae*

垂直部および下辺の広がり共によく発達し、コイ科の尾舌骨とよく似ている。

1.2-1 ヘミオダス属 *Hemiodus*

垂直部はほぼ直角三角形をなし、下辺の広がり著しく広く左右に広がり、あぶみ形を呈している。

1.2-1.1 ヒトツボシヘミオダス *Hemiodus semitaeniatus* KNER

尾舌骨長の頭長比は 37% と割合に大きい。

骨高の骨長比は 33% と普通であり、骨幅の骨長比は 29% とやや大きい。

1.3 ハチェット (Hatchet) 科 *Gasteropelecidae*

尾舌骨は著しく退化的で、単純な形状をしている。

1.3-1 ハチェット属 *Gasteropelecus*

前連部は肥厚している。垂直部は狭く後方にのびているだけで、下辺の広がり全く見られない、側面形は一見、把手の様な形状である。

1.3-1.1 シルバー・ハチェット (Silver hatchet) *Gasteropelecus levis* (EIGENMANN)

尾舌骨長の頭長比は 12% と極めて小さい。

骨高の骨長比は 30%、骨幅の骨長比は 17% と

共に小さ目の値である。

2. デンキウナギ亜目 *Gymnotoidei*

特別な特徴はみられない。

2.1 ランフィクタイ (Rhamphichthyi) 科 *Rhamphichthyidae*

2.1-1 ヒポポムス属 *Hypopomus*

垂直部の上辺が著しく後方に延長している。下辺は短かく、その部分に左右への広がり、ほぼ菱形に発達している。

2.1-1.1 トランスルーセント・ナイフ・フィッシュ (Translucent knife-fish) *Hypopomus artedii* KAUP

尾舌骨長の頭長比は 42% とかなり大きい。

骨高は骨長の 29%、骨幅は骨長の 26% と共に普通である。

3. コイ亜目 *Cyprinoidei*

前連部、垂直部、下辺の広がりといずれもよく発達し、標準的な形状は航空機の尾翼を思わせる形状をしている。中には例外的な形状のものもあるが、概して前述のカラシン亜目のそれと著しく類似している。

3.1 コイ科 *Cyprinidae*

尾舌骨長の頭長比は 30% ないし 50%、平均値は 36% と標準よりやや大である。骨高の骨長比は平均 35% で標準値を示す。骨幅の骨長比は平均 31% と下辺の広がりかなり発達している。

3.1-1 バラタナゴ属 *Rhodeus*

前連部は小さな二股になり、垂直部はよく発達し、下辺の左右の広がりもよく発達していて、コイ・フナのそれとよく似た形をしている。

3.1-1.1 バラタナゴ *Rhodeus ocellatus* (KNER)

尾舌骨長の頭長比は 37% で、標準値であり、骨高の骨長比は 42%、骨幅の骨長比は 40% と、いずれもかなり大きな値である。

3.1-2 モツゴ属 *Pseudorasbora*

骨長、骨高、骨幅のいずれもかなり大きめである。垂直部は後方にのび、そり上っており、下辺の広りは前方でよく発達して、全体形があぶみ状

Table 1. List of specimens examined, with measurements (in mm)

Species name (or common name)	Locating and date of collecting (* Obtained from a market in Tokyo, Japan)
1. 1-1. 1	<i>Serrasalmus nattereri</i> South America;* Sept. 1971.
1. 1-2. 1	<i>Metynnis schreitmulleri</i> South America;* Mar. 1969.
1. 1-3. 1	<i>Mylosoma aureum</i> South America;* Oct. 1971.
1. 1-4. 1	<i>Phenacogrammus interruptus</i> Congo, Africa;* Feb. 1971.
1. 1-5. 1	<i>Leporinus striatus</i> South America;* Oct. 1971.
1. 1-6. 1	<i>Chilodus punctatus</i> South America;* Oct. 1971.
1. 1-7. 1	<i>Pristella riddlei</i> South America;* Oct. 1971.
1. 1-8. 1	<i>Moenkhausia oligolepis</i> South America;* Oct. 1971.
1. 2-1. 1	<i>Hemiodus semitaeniatus</i> South America;* Feb. 1971.
1. 3-1. 1	<i>Gasteropelcus levis</i> South America;* Feb. 1971.
2. 1-1. 1	<i>Hypopomus artedii</i> Guiana, South America;* Oct. 1971.
3. 1-1. 1	<i>Rhodeus ocellatus</i> Saitama, eastern Central Japan, July 1971.
3. 1-2. 1	<i>Pseudorasbora parva</i> Southwest Tokyo, Japan, Feb. 1970.
3. 1-2. 2	<i>Pseudorasbora pumila</i> Saitama, eastern Central Japan, Aug. 1969.
3. 1-3. 1	<i>Gnathopogon caeruleus</i> Chiba, southeastern Central Japan, Aug. 1972.
3. 1-4. 1	<i>Tribolodon hakonensis</i> Chiba, southeastern Central Japan, Nov. 1971.
3. 1-5. 1	<i>Zacco platypus</i> Tokyo, Japan, May 1966.
3. 1-6. 1	<i>Ctenopharyngodon idellus</i> Saitama, eastern Central Japan, Nov. 1968.
3. 1-7. 1	<i>Hypophthalmichthys moritrix</i> Tokyo, Japan, Apr. 1969.
3. 1-8. 1	"Ganges dace" Mymensingh, Ganges River, South Asia, Jan. 1971.
3. 1-9. 1	<i>Carrassius carrassius</i> Saitama, eastern Central Japan, July 1969.
3. 1-9. 2	<i>Carrassius auratus</i> Tokyo, Japan, July 1970.
3. 1-10. 1	<i>Cyprinus carpio</i> Saitama, eastern Central Japan, July 1966.
3. 1-11. 1	<i>Barbus tetrazona</i> Southeast Asia;* Oct. 1971.
3. 1-11. 2	<i>Barbus oligolepis</i> Southeast Asia;* Oct. 1971.
3. 1-12. 1	<i>Labeo bicolor</i> Southeast Asia;* Feb. 1971.
3. 1-13. 1	<i>Brachydanio rerio</i> India and Burma;* Oct. 1971.
3. 2-1. 1	<i>Misgurnus anguillicaudatus</i> Saitama, eastern Central Japan, Nov. 1968.
3. 2-1. 2	"White loach" Southeast Asia;* Oct. 1971.
3. 2-1. 3	"Ganges loach" Mymensingh, Ganges River, South Asia, Jan. 1971.
3. 2-2. 1	<i>Acanthopthalmus semicinctus</i> Southeast Asia;* Oct. 1971.
3. 2-3. 1	<i>Botia macracanthus</i> Borneo, Southeast Asia;* Nov. 1970.
3. 2-4. 1	"Red-fin shark-like loach" Southeast Asia;* Oct. 1971.
3. 3-1. 1	<i>Gyrinocheilus ayonieri</i> Thailand, Southeast Asia;* Aug. 1971.
4. 1-1. 1	<i>Parasilurus asotus</i> Saitama, eastern Central Japan, Dec. 1971.
4. 1-2. 1	<i>Kryptopterus bicirrhus</i> Southeast Asia;* Oct. 1971.
4. 2-1. 1	<i>Plotosus anguillaris</i> Sagami Bay, Southeast Japan, May 1966.
4. 3-1. 1	"Kaiyan" South America;* Aug. 1967.
4. 3-2. 1	"Kaiyan resembling" South America;* Feb. 1971.
4. 3-3. 1	"Ganges bagrus" Mymensingh, Ganges River, South Asia, Jan. 1971.
4. 3-4. 1	"Dotted dorsalfin bagrus" Mymensingh, Ganges River, South Asia, Jan. 1971.
4. 4-1. 1	<i>Corydrus paleatus</i> South America;* Oct. 1971.
4. 4-1. 2	<i>Corydrus paleatus</i> Albino South America;* Oct. 1971.
4. 5-1. 1	<i>Clarias lazera</i> Africa;* May 1972.
4. 6-1. 1	<i>Loricaria parva</i> South America;* Oct. 1971.
4. 7-1. 1	"Ganges chaca" Mymensingh, Ganges River, South Asia, Jan. 1971.

of total length, body length, body height, head length, etc.

Total length	Measurements in mm						Proportion in percentage		
	Body length	Body height	Head length	Urohyal length	Urohyal height	Urohyal width	Head length of urohyal length	Urohyal length of urohyal height	Urohyal length of urohyal width
88	76	36	24	7.3	3.7	2.2	30%	51%	30%
135	121	72	25	9.2	6.0	3.3	37	66	36
85	79	47	22	5.6	3.0	2.0	25	54	36
84	72	19.0	19.5	3.2	1.6	0.6	16	50	19
166	146	30	38	10.0	5.0	1.3	26	50	13
56	48	14.0	13.5	6.2	2.2	1.4	46	36	23
34	28	8.4	6.0	2.0	0.65	0.25	33	33	8
34	27	11.4	7.7	1.8	0.40	0.28	23	22	16
108	93	19	23	8.5	2.8	2.5	37	33	29
45	41	19	10	1.2	0.36	0.20	12	30	17
88	80	8.0	9.0	3.8	1.1	1.0	42	29	26
71	59	26	13	4.8	2.0	1.9	38	42	40
73	63	14.0	13.5	5.7	2.3	2.4	39	40	40
45	39	7.7	8.4	3.7	1.7	1.8	40	46	49
62	53	12	13	4.7	1.5	1.4	36	32	30
195	162	36	38	11.8	4.3	3.7	31	36	31
121	101	24.0	24.5	7.3	3.3	1.6	30	40	22
172	143	36	32	11.8	2.6	3.8	37	27	32
170	142	40	39	19.5	6.0	4.0	50	31	31
106	94	21	20	6.0	2.3	1.2	30	38	20
82	70	27	21	7.7	2.8	3.8	36	36	49
118	92	38	27	10.7	3.5	4.6	39	33	43
347	302	89	79	28.0	7.2	13.6	35	26	48
39	30	9.0	9.5	3.0	1.2	0.4	32	40	13
81	65	18	17	6.0	1.7	1.5	35	28	25
45	37	8.1	9.5	2.8	1.0	0.6	30	36	21
23.7	19.3	4.0	4.3	1.3	0.40	0.35	30	31	27
114	100	14.0	15.5	2.5	1.4	1.1	16	56	43
90	80	11	13	1.7	0.8	0.8	13	47	47
92	79	16	16	1.08	0.86	0.40	8	80	37
56	52	3.4	7.5	0.68	0.37	0.13	9	54	18
58	45	12	16	1.05	2.76	0.65	7	260	62
34	25	5.8	8.3	0.4	0.7	0.3	5	175	75
112	95	17.0	18.5	4.8	3.3	4.0	27	69	83
400	365	73	85	17.7	7.2	11.0	22	30	63
55	46	9.0	8.0	0.7	0.7	0.3	10	100	43
180	166	27	35	6.6	3.5	6.0	19	53	91
110	98	21	25	5.0	1.8	3.7	20	36	74
71	63	12	15	3.5	1.2	2.4	24	34	69
127	107	22	22	4.4	1.34	1.42	20	31	32
125	110	20	20	4.1	1.75	1.42	21	43	35
35	27	8.0	8.0	2.0	0.5	2.0	25	25	100
30	23	7.0	8.0	1.4	0.4	1.6	18	29	114
324	307	45	62	12.0	3.2	13.5	19	27	112
95	82	7.0	12.0	2.8	0.5	4.2	23	18	150
146	125	20	44	6.2	1.5	9.7	14	24	156

であるのが特徴である。

3.1-2.1 モツゴ *Pseudorasbora parva*

(TEMMINCK & SCHLEGEL)

尾舌骨長の頭長比は 39%、骨高の骨長比は 40%、骨幅の骨長比も 40% といずれもかなり大きな値を示している。

3.1-3 モロコ属 *Gnathopogon*

垂直部も下辺の拡りも共によく発達するが、全体に長さが長く、側面形はへら状を呈する。

3.1-3.1 ホンモロコ *Gnathopogon caerulescens* (SAUVAGE)

尾舌骨長の頭長比は 36% と標準であり、骨高の骨長比は 32% とやや低く、骨幅の骨長比は 30% でほぼ標準である。

3.1-4 ウグイ属 *Tribolodon*

前連部は小さく二股になり、垂直部と下辺の拡りはよく発達し、側面は下辺後端がとがっている。上面形は矢羽根状を呈する。

3.1-4.1 ウグイ *Tribolodon hakonensis* (GÜNTHER)

尾舌骨長の頭長比は 33% とやや小さい。骨高の骨長比は 32%、骨幅の骨長比は 29% といずれも標準より僅かに小さい。

3.1-5 オイカワ属 *Zacco*

垂直部は後上方によく延長する。下辺の拡りは全く水平に発達しているので、側面形は完全に一直線をしている。下辺の拡りの後縁は深く切れこんでいる。

3.1-5.1 オイカワ *Zacco platypus* (TEMMINCK & SCHLEGEL)

尾舌骨長の頭長比は 30% とやや小さい。骨高の骨長比は 40% とかなり大きい、骨幅の骨長比は 22% とかなり小さい値である。

3.1-6 ソウギョ属 *Ctenopharyngodon*

全体にやや細形で上辺が緩くそり上っている点と下辺の拡りの後縁が深く切れこんでいるのが特徴的である。

3.1-6.1 ソウギョ *Ctenopharyngodon idellus* (CUVIER & VALENCIENNES)

尾舌骨長の頭長比は 37% と標準であるが、骨高の骨長比は 27% とかなり小さく、骨幅の骨長

比は 32% とやや小さい値を示す。

3.1-7 ハクレン属 *Hypophthalmichthys*

やや細形で、左右への拡りの後縁が切れこんでいるため、上面形は矢羽根状を呈する。下辺前方が、側面からみて竜骨状にそりだしているのが特徴である。

3.1-7.1 ハクレン *Hypophthalmichthys*

moritrix (CUVIER & VALENCIENNES)

尾舌骨長の頭長比は 50% に達し、本科中の最大値を示している。骨高の骨長比は 31%、骨幅の骨長比は 21% といずれも小さい値である。

3.1-8 (Genus undetermined)

下辺の側面形が直線的で、前記オイカワに似ているが、下辺の拡りが狭小なことで、その後縁が極めて深く鋭角的に切れこんでいる点異なる。

3.1-8.1 ガンジス・ワタカ “Ganges dace”

尾舌骨長の頭長比は 30% とかなり小さい。骨高の骨長比は 38% と標準に近く、骨幅の骨長比は 20% と著しく狭小である。

3.1-9 フナ属 *Carrassius*

下辺の左右への拡りが著しく発達し、上面形はほぼ正三角形を呈する程である。

3.1-9.1 フナ *Carrassius carrassius* LINNÉ

尾舌骨長の頭長比は 36% と標準であり、骨高の骨長比も 36% と標準値を示すが、骨幅の骨長比は 49% に達し、拡りの発達していることを示している。

3.1-9.2 キンギョ *Carrassius auratus* LINNÉ

上記フナのそれと酷似しているが、尾舌骨長の頭長比が 39% と少しであるが大きく、一方、骨高の骨長比が 32% であり、骨幅の骨長比が 35% といずれもフナの場合より小さい値を示している。

3.1-10 コイ属 *Cyprinus*

尾舌骨形はフナ属のそれに似ているが、前端部のくびれた部分が短いこと、下辺の拡りの側縁が曲線状であること、および、垂直部が後方にやや延長し骨高が低い点異なっている。

3.1-10.1 コイ *Cyprinus carpio* LINNÉ

尾舌骨長の頭長比は 35% と標準値である。骨高の骨長比は 26% とかなり低い。骨幅の骨長比

は 48% でかなり幅広い形状である。

3.1-11 バルブス属 *Barbus*

全体的にやや細長い、特別に変った点はなく、ただ垂直部の上辺が僅かに上方に凸のゆるい曲線であることが特徴といえる。

3.1-11.1 スマトラ (Sumatra) *Barbus tetrazona* BLEEKER

尾舌骨長の頭長比は 32% とやや小さい。垂直部はよく発達し、骨高の骨長比は 40% を示す。下辺は長く、左右の拡りは狭く細長く、上面形はペン軸状で、骨幅の骨長比は 13% と著しく小さい。

3.1-11.2 バルブス オリゴレピス *Barbus oligolepis* (BLEEKER)

尾舌骨長の頭長比は 35% で普通である。垂直部はよく発達するが、上記スマトラのそれよりも高さがかなり低く、骨高の骨長比は 28% にすぎない。下辺の拡りは左右によく発達し、その後端は上方から見て截形をしており、骨幅の骨長比は 25% と上記スマトラのそれよりかなり大である。

3.1-12 ラベオ属 *Labeo*

上記バルブス属に似てやや細いが、前連部がやや肥大し、上辺は極めてゆるい曲線で、前半が凹、後半が凸になっている。下辺の拡りは後縁が截形である。

3.1-12.1 レッドテイル ブラック シャーク (Red tail black shark) *Labeo bicolor* SMITH

尾舌骨長の頭長比は 30% と比較的小さい。骨高の骨長比は 36% と高く、骨幅の骨長比は 21% とかなり狭小である。

3.1-13 ブラキイダニオ属 *Brachydanio*

垂直部が発達し、後上方にのびているので、上辺の方が下辺よりかなり長さが長いのが特徴である。

3.1-13.1 ゼブラ ダニオ (Zebra danio) *Brachydanio rerio* (HAMILTON-BUCHANAN)

尾舌骨長の頭長比は 30% とやや小さい。骨高の骨長比は 31% と普通であり、骨幅の骨長比は 27% でやはり普通である。

3.2 ドジョウ科 *Cobitidae*

本科のものは尾舌骨が著しく短小で、尾舌骨長

の頭長比が 7% から 16%、平均約 10% しかない。短形ながら垂直部と下辺の拡りは発達しているものが多い。骨高の骨長比は 70% 前後を示して著しく高く、中には高さの方が骨長の倍以上のものもある。骨幅の骨長比は 18% から 62% と多様で、平均値は 48% である。

3.2-1 ドジョウ属 *Misgurnus*

この属のものはいずれも前連部が発達し、二股になっている。下辺部の拡りはよく拡っている。尾舌骨長の頭長比は 8% から 16%、骨高の骨長比は 56% から 80%、骨幅の骨長比は 37% から 50% を示す。

3.2-1.1 ドジョウ *Misgurnus anguillicaudatus* (CANTOR)

垂直部は普通に発達し、ほぼ正三角形をしている。下辺の拡りは前半部のみであるが顕著に拡っている。尾舌骨長の頭長比は 16%、骨高の骨長比は 56%、骨幅の骨長比は 43% である。

3.2-1.2 シロドジョウ “White loach”

Misgurnus sp. Type A

上記ドジョウのそれに似ているが、下辺が上辺より著しく短かく、垂直部の後下の部分が欠けているのが特徴である。尾舌骨長の頭長比は 12%、骨高の骨長比は 69%、骨幅の骨長比は 50% であって、いずれも上記種のそれらと大差はない。

3.2-1.3 ガンジスドジョウ “Ganges loach”

Misgurnus sp. Type B

前連部は上記 2 種と同様よく発達するが、垂直部の上辺は発達がわるく下辺より長さが短い。下辺の拡りはあまり発達していない点が上記 2 種との明確な相違といえる。尾舌骨長の頭長比は 8% と著しく小さく、骨高の骨長比は 80% と大きい、骨幅の骨長比は 37% と比較的であるが狭い。

3.2-2 クーリーローチ (Kuhli loach) 属

Acanthopthalmus

垂直部は後上方に発達し、上辺は下辺より著しく長く、側面形はほぼ直角三角形をなす。下辺の拡りは僅かである。

3.2-2.1 クーリーローチ *Acanthopthalmus semicinctus* FRASER-BRUNNER

骨長の頭長比は 9% と著しく小さい。骨高の

骨長比は 54%, 骨幅の骨長比は 18% と狭い。

3.2-3 クラウンローチ(Clown loach)属 *Botia*
垂直部は上方のみ発達しているので、長さは極めて短かく、典型的な縦長形である。下辺は短かく左右への拡りが認められる。

3.2-3.1 クラウンローチ *Botia macracanthus*
(BLEEKER)

尾舌骨長の頭長比は 7% と極めて小さい。骨高の骨長比は 260% と極端に大であり、骨幅の骨長比は 62% という値を示す。

3.2-4 (Genus undetermined)

3.2-4.1 レッドフィンシャーク似ドジョウ
“Red-fin shark-like loach”

垂直部は全く発達しない。前連部のみが発達し、下辺の拡りは全く認められずたんに下方のびて縦長の形状をしている。尾舌骨長の頭長比は 5% と極端に小さい。骨高の骨長比は 175% と極めて大きく、骨幅の骨長比は 75% とかなり大きい値を示す。

3.3 ジリノケイルス (*Gyrinocheilus*) 科
Gyrinocheilidae

垂直部は細長く後方に延長し、下辺は左右後方に細長く延長しており、全体形が飛んでいる鳥の様な形状で、極めて特異形である。

3.3-1 ジリノケイルス属 *Gyrinocheilus*

3.3-1.1 アルジーター (Algetar)

Gyrinocheilus aymonieri (TIRANT)

尾舌骨長の頭長比は 27% とやや小さい。骨高の骨長比は 69% と大きく、骨幅の骨長比は 83% と顕著に大きい。

4. ナマズ亜目 *Siluroidei*

いずれも左右への拡りがよく発達し、全体形が幅広いものが多いが、また、特異な形状をするものもかなりある。尾舌骨長の頭長比は 10% ないし 24% と比較的小型で、骨高の骨長比は 18% から 175% と変化が大きい。一方、骨幅の骨長比は 32% から 156% と幅が広く、2, 3 のものを除けば、他の魚類にみられぬ幅広形が特徴である。

4.1 ナマズ科 *Siluridae*

特に特徴はない。

4.1-1 ナマズ属 *Parasilurus*

前連部は肥厚し、垂直部は発達せず狭い。下辺は後方にのび、左右への拡りは充分に発達し、上面形は菱形をしている。

4.1-1.1 ナマズ *Parasilurus asotus* (LINNÉ)

尾舌骨長の頭長比は 22% と本亜目の標準に近い。骨高の骨長比は 36% で、骨幅の骨長比は 63% と大きい。

4.1-2 グラス キャット フィッシュ (Glass cat fish) 属 *Kryptopterus*

垂直部は上下に発達し、上辺は短かく下辺の方が長い。下辺の拡りは比較的になく狭小で、上面形は紡錘形をしている。

4.1-2.1 グラス キャット フィッシュ

Kryptopterus bicirrhus (CUVIER & VALENCIENNES)

尾舌骨長の頭長比は 10% とこの亜目の中で最も小さい。骨高の骨長比は 100% と大きく、この亜目中では最高である。骨幅の骨長比は 37% と比較的狭い。

4.2 ゴンズイ科 *Plotosidae*

前記ナマズの尾舌骨に似て、前端が厚く発達し、垂直部はゆがんだ梯形を呈し、下辺の拡りは上面形がゆがんだ菱形をしている。

4.2-1 ゴンズイ属 *Plotosus*

4.2-1.1 ゴンズイ *Plotosus anguillaris*

LACÉPÈDE

尾舌骨長の頭長比は 19% とナマズのそれとほぼ同じである。骨高の骨長比は 53%, 骨幅の骨長比は 91% と下辺の拡りは広い。

4.3 ギギ科 *Bagridae*

前端部が肥厚している点は前記ナマズ科のそれとよく似ている。垂直部および下辺の拡りもよく発達している。尾舌骨長の頭長比は 20% ないし 24%, 骨高の骨長比は 32% ないし 44%, 骨幅の骨長比は小さいものと大きなものと二様で、30% から 74% と範囲が大きい。

4.3-1 (Genus undetermined)

4.3-1.1 カイヤン “Kaiyan”

垂直部は高さが低く、下辺の拡りはよく発達し、上面形はほぼ正三角形をしている。尾舌骨長の頭

長比は 20%, 骨高の骨長比は 36% であり, 骨幅の骨長比は 74% と極めて大きい。

4.3-2 (Genus undetermined)

4.3-2.1 カイヤン似 “Kaiyan resembling”

前種のそれによく似ているが, 垂直部が後方に延長し, その後端がとがっている点が相違している。尾舌骨長の頭長比は 24%, 骨高の骨長比は 34%, 骨幅の骨長比は 69% と上記種とほぼ変らない。

4.3-3 (Genus undetermined)

4.3-3.1 ガンジスギギ “Ganges bagrus”

前端部が肥厚し, 下辺の拡りが発達している。垂直部は前後でほぼ同じ高さをしており, 下辺の拡りは前方で狭く, 後方で菱形に拡っている。尾舌骨長の頭長比は 20%, 骨高の骨長比は 31%, 骨幅の骨長比は 32% で, 全体に細長いことを示す。

4.3-4 (Genus undetermined)

4.3-4.1 セブレナシギギ “Dotted dorsalfin bagrus”

上記種に似ているが垂直部の高さが前方で高く, 後方で低くなっている点と下辺の拡りの形がへら状を呈する点が異なる。尾舌骨長の頭長比は 21%, 骨高の骨長比は 43%, 骨幅の骨長比は 35% といずれの値も上記種より僅かに大である。

4.4 カリクタイ (Callichthyi) 科 *Callichthyidae*

4.4-1 コリドラス属 *Corydoras*

前端部は肥大しているが, 垂直部はほとんどなく, 左右への拡りが発達した平板状で, 上面形は変形な五角形をしている。骨高は著しく低く, 骨幅は骨長と同じか, それ以上と幅広い。

4.4-1.1 コリドラス・パレアタス *Corydoras paleatus* (JENYNS)

下辺の側縁, 左右の後縁は共にほぼ直線状で, 側端, 後端部の角はいずれも丸味をおびている。尾舌骨長の頭長比は 25%, 骨高の骨長比は 25%, 骨幅の骨長比は 100% である。

4.4-1.2 アルビノ・コリドラス *Corydoras paleatus* (JENYNS) Albino

上記種に比して, 側縁, 後縁は共に僅かに内に湾曲している。そのため, 拡りの左右の端および

後縁の後端部は鋭角にとがっている。尾舌骨長の頭長比は 18%, 骨高の骨長比は 29%, 骨幅の骨長比は 114% と拡りが顕著で, 上記種と数値的にかなり異なっている。

4.5 クララ (Clara) 科 *Clariidae*

4.5-1 クララ属 *Clarias*

前端部は幅広く肥厚し, 垂直部は全くなく, 左右の拡りは突起となって側方に突出しているので, 全体形は先端は截形であるがやじりの形状をしている。

4.5-1.1 アルビノ・クララ *Clarias lazera*

CUVIER & VALENCIENNES Albino

尾舌骨長の頭長比は 19%, 骨高の骨長比は 27% で, 骨幅の骨長比は 112% と幅の方が大である。

4.6 ロリカリア科 *Loricariidae*

4.6-1 ロリカリア属 *Loricaria*

前端部は幅広く発達し, その両端は前方への小突起となっている。垂直部はほとんどなく, 中心線が僅かに隆起しているにすぎない。左右への拡りは極めてよく発達している。

4.6-1.1 ロリカリア *Loricaria parva*

BOULENGER

尾舌骨長の頭長比は 23%, 骨高の骨長比は 18% と極めて低い。骨幅は骨長の 150% と極めて幅広い。

4.7 イワナマズ科 *Chacidae*

4.7-1 イワナマズ属 *Chaca*

前端部は肥大していない。垂直部は全くなく, 上面, 下面共ほぼ平板である。左右の拡りは極めてよく発達し, 側縁後半は棒状となって, 側方後方に延長している。したがって, 極めて奇異な形状で, あたかもジェット機のような形状をしている。

4.7-1.1 ガンジスチャカ (Ganges chaca)

Chaca sp.

尾舌骨長の頭長比は 14% と小さく, 骨高の骨長比は 24% で, 骨幅の骨長比は 156% と極めて大である。

以上のごとく, カラシン亜目 *Characoidei* とコイ亜目 *Cyprinoidei* との尾舌骨はデンキウナギ亜

目 *Gymnotoidei* を含め、いずれも 2, 3 の例外を除くと、垂直部と下辺の拡りが発達した形状で、各亜目の間に特に相異点は見られず、系統分類上も極めて密接な関係にあるものと考えられる。ナマズ亜目 *Siluroidei* の尾舌骨においては、前連部が発達肥厚し、垂直部はやや低いものから次第に狭小になっており、それらでの下辺の拡りは一段と発達して尾舌骨長を越える骨幅のものが多い。いずれにしてもコイ亜目からナマズ亜目へと派生進化した尾舌骨形といえる。

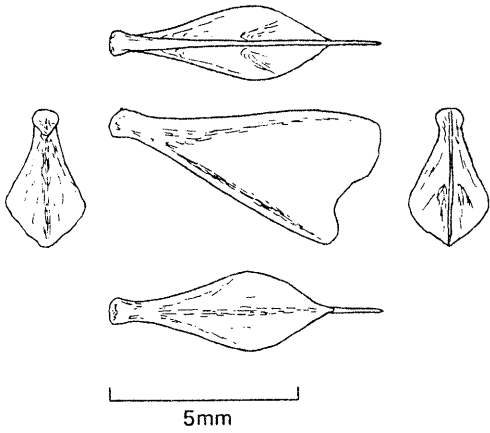
科、属、種の配列は尾舌骨形の上から、類形的なものを順に並べてみたが、これが系統分類学上の配置とどの程度適合するのかが焦点であり、諸賢の御意見を戴ければ幸いと存ずる次第であります。

尚、尾舌骨の観察図については、既刊、魚類の尾舌骨 (KUSAKA 1974) の原図を再使用したもので、その転用を御諒承下さった東京大学出版会の御好意に対し、感謝申し上げます。

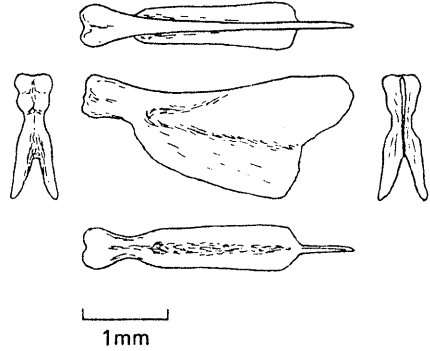
文 献

- GOSLINE, W. A. (1971): Functional Morphology and Classification of Teleostean Fishes. The Univ. Press of Hawaii, Honolulu. 208 pp.
- 草下孝也 (1969): 魚類の顔面骨の研究-I. うみ, 7, 126-143.
- 草下孝也 (1970): 魚類の顔面骨の研究-II. うみ, 8, 149-170.
- KUSAKA, T. (1974): The Urohyal of Fishes. Univ. of Tokyo Press, Tokyo. 320 pp. 10 textfigures and 700 figures.
- 草下孝也 (1975): ニシン亜目 (Clupeoidei), ウナギ亜目 (Anguilloidei) の尾舌骨の形状. うみ, 13, 134-149.
- 草下孝也 (1977): サケ目 (Salmoniformes) の尾舌骨の形状. うみ, 15, 21-36.
- KUSAKA, T. and N. tri THUC (1972): Regarding feature of urohyal, parasphenoid, hyomandibular and pelvic bone of the Japanese lanternfishes (Family Myctophidae, Teleostei). La mer, 10, 145-155.

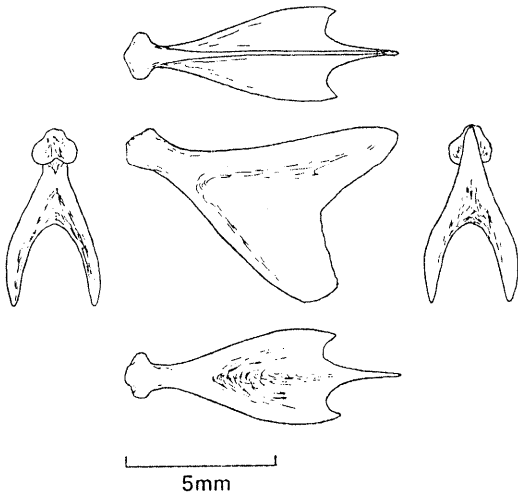
PLATE 1



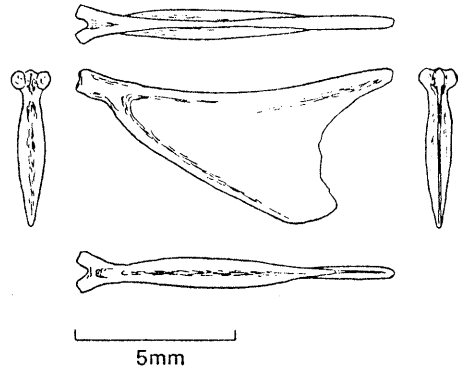
1.1-1.1 SERRASALMUS NATTERERI



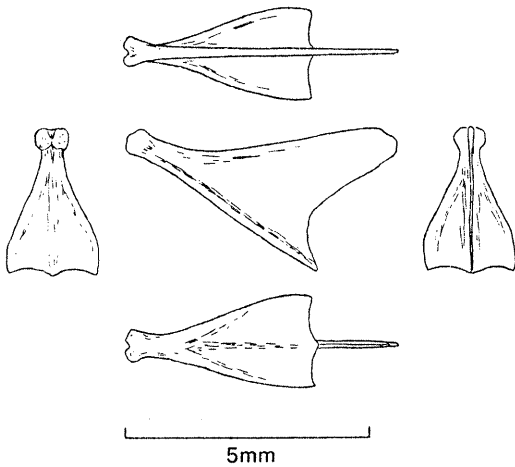
1.1-4.1 PHENACOGRAMMUS INTERRUPTUS



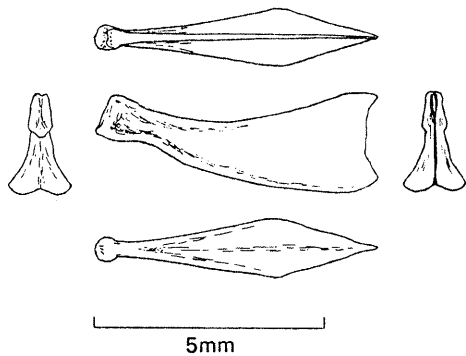
1.1-2.1 METYNNIS SCHREITMULLERI



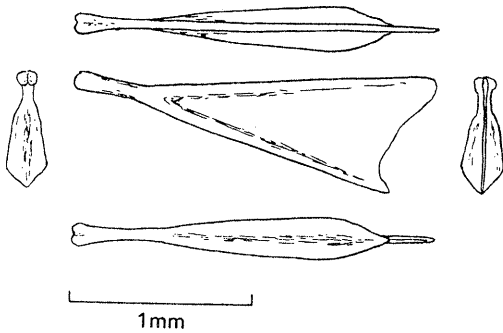
1.1-5.1 LEPORINUS STRIATUS



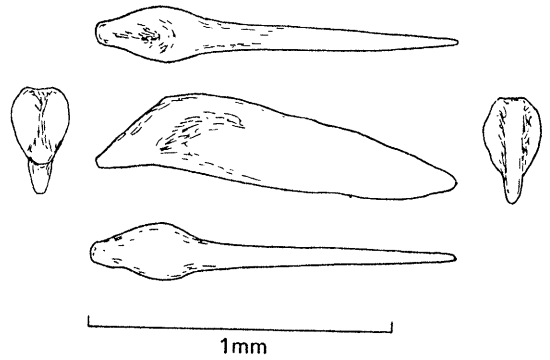
1.1-3.1 MYLOSOMA AUREUM



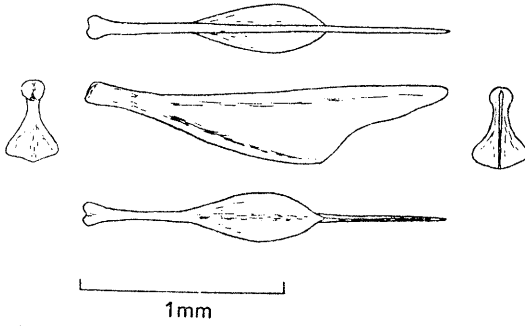
1.1-6.1 CHILODUS PUNCTATUS



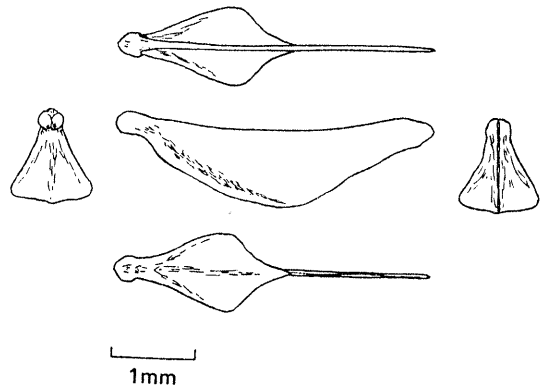
1.1-7.1 PRISTELLA RIDDLEI



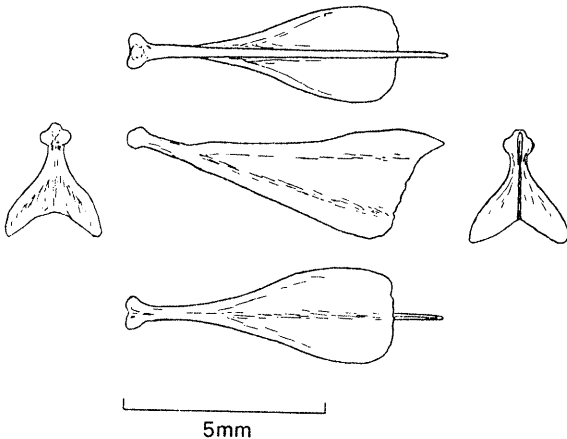
1.3-1.1 GASTROPELCUS LEVIS



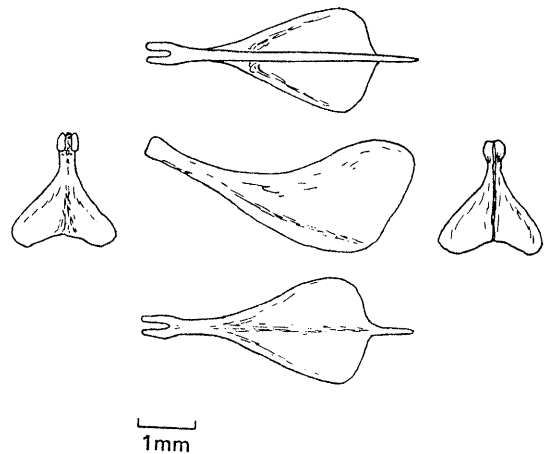
1.1-8.1 MOENKHAUSIA OLIGOLEPIS



2.1-1.1 HYPOPOMUS ARTEDII

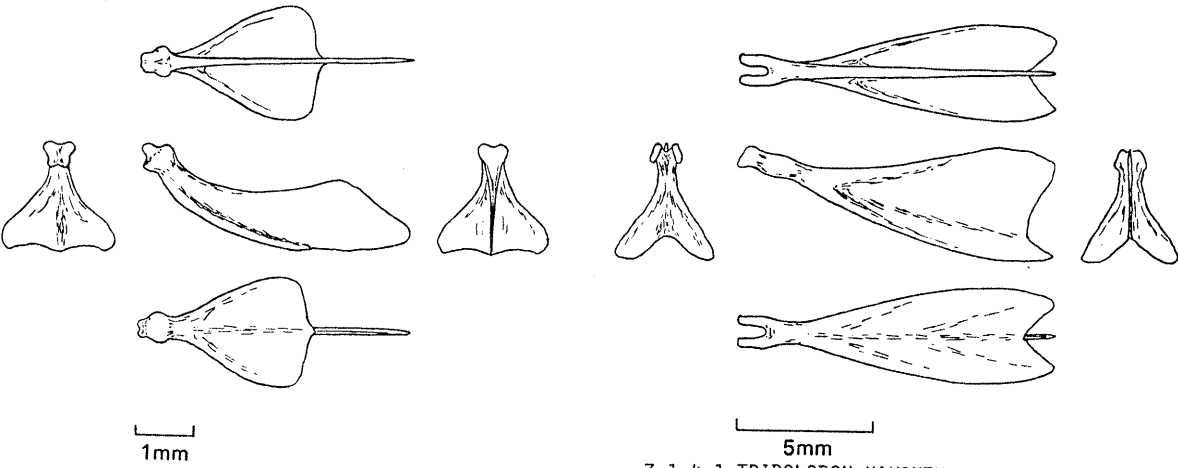


1.2-1.1 HEMIODUS SEMITAENIATUS



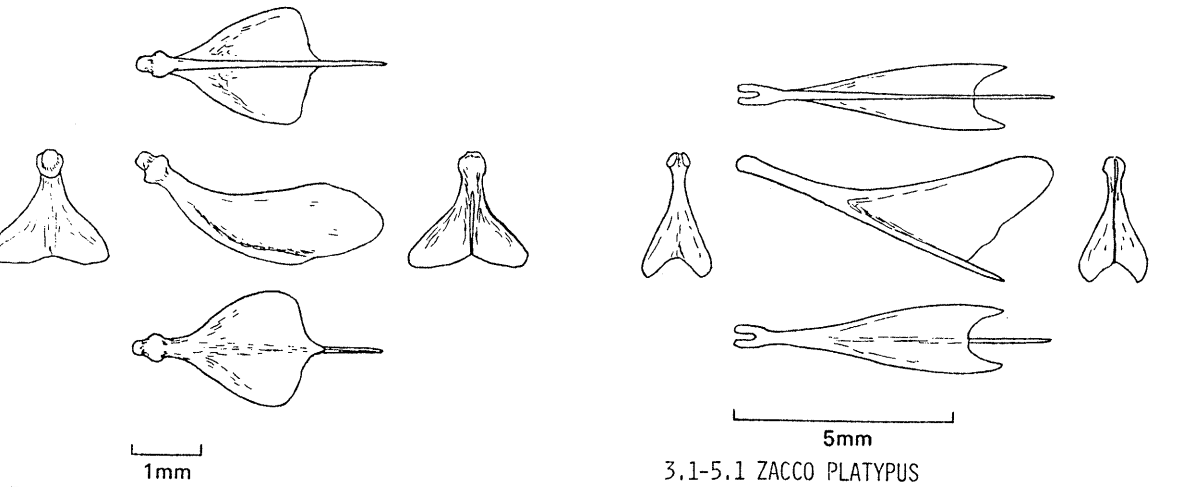
3.1-1.1 RHODEUS OCELLATUS

PLATE 3



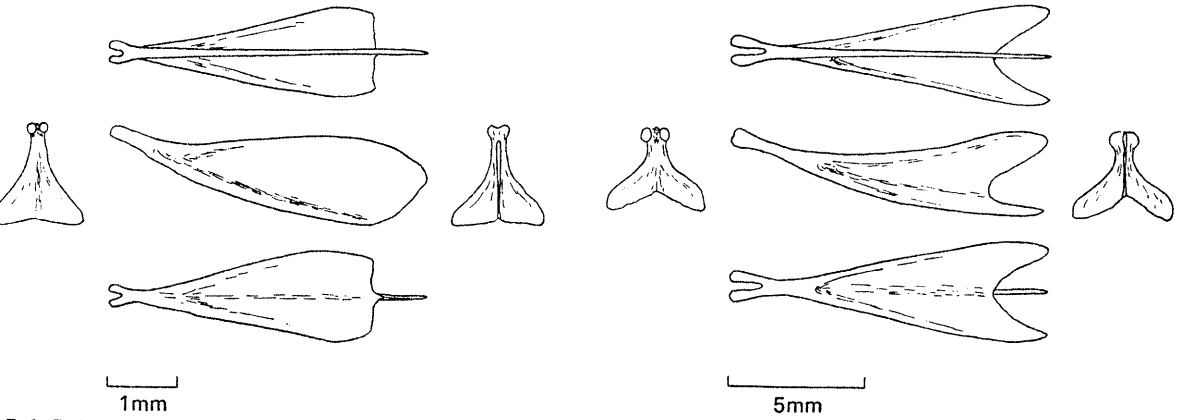
3.1-2.1 *PSEUDORASBORA PARVA*

3.1-4.1 *TRIBOLODON HAKONENSIS*



3.1-2.2 *PSEUDORASBORA PUMILA*

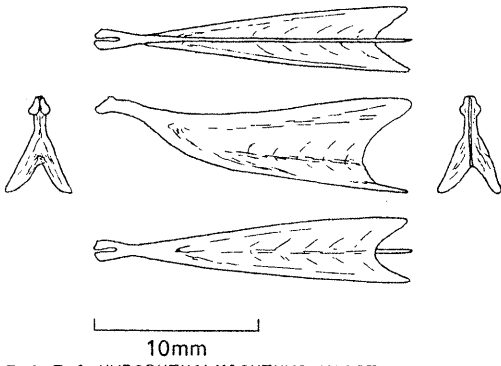
3.1-5.1 *ZACCO PLATYPUS*



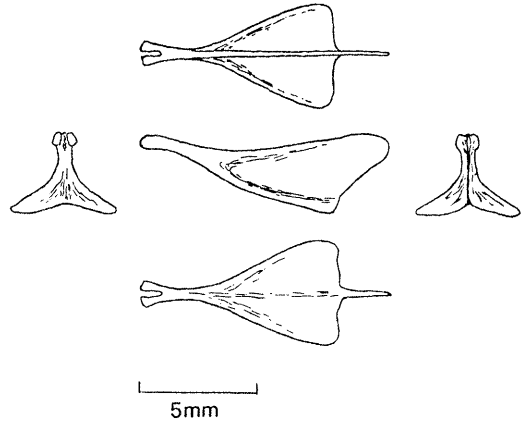
3.1-3.1 *GNATHOPOGON CAERULESCENS*

3.1-6.1 *CTENOPHARYNGODON IDELLUS*

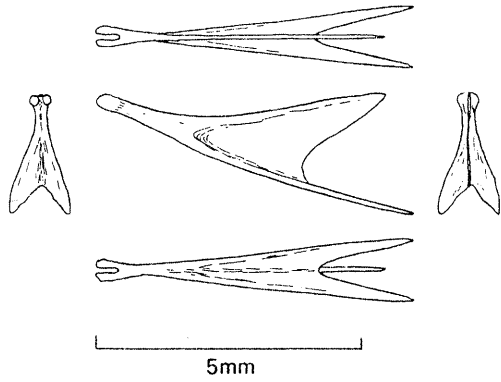
PLATE 4



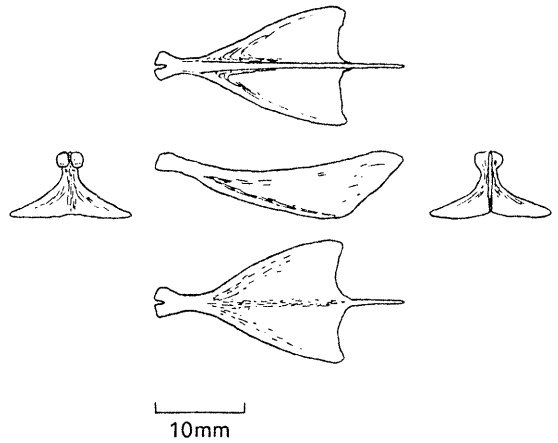
3.1-7.1 HYPOPHTHALMICHTHYS MORITRIX



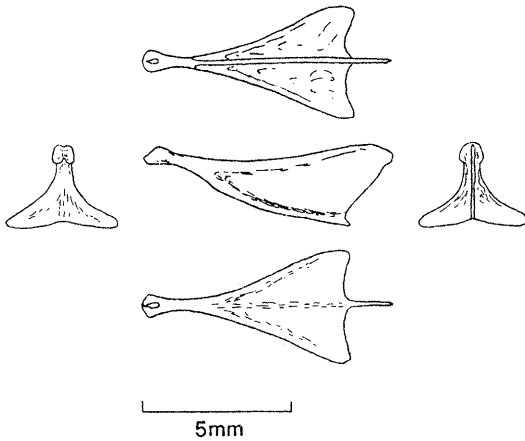
3.1-9.2 CARRASSIUS AURATUS



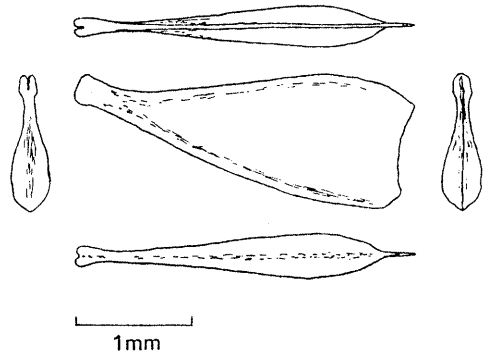
3.1-8.1 "GANGES DACE"



3.1-10.1 CYPRINUS CARPIO

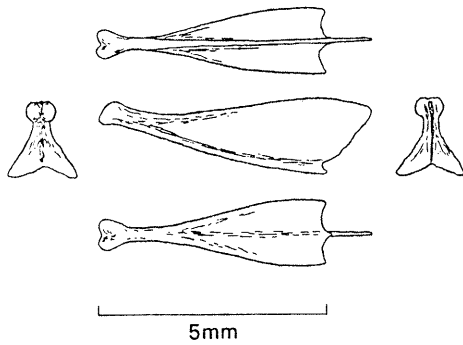


3.1-9.1 CARRASSIUS CARRASSIUS

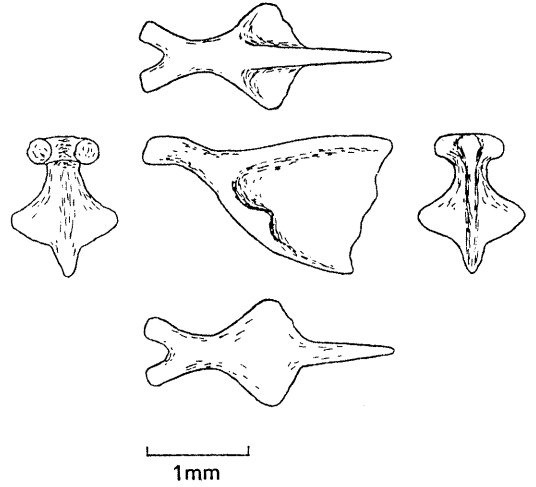


3.1-11.1 BARBUS TETRAZONA

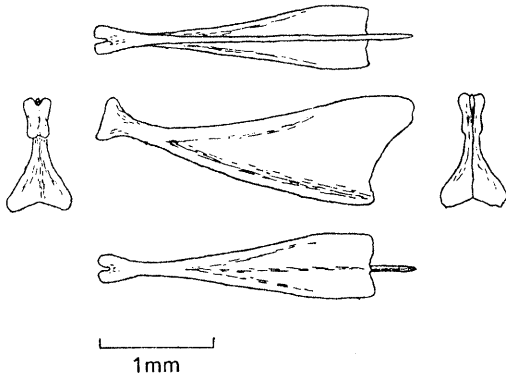
PLATE 5



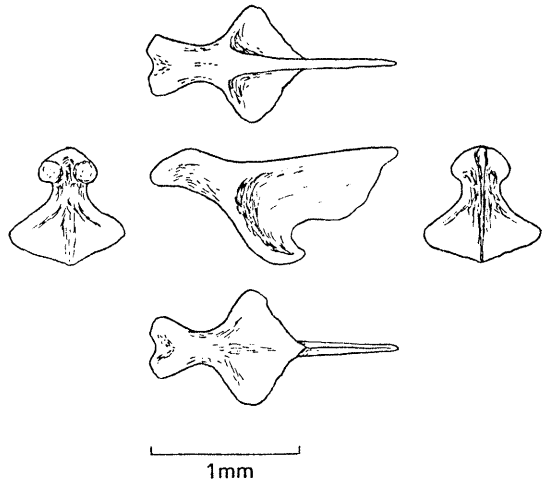
3.1-11.2 BARBUS OLIGOLEPIS



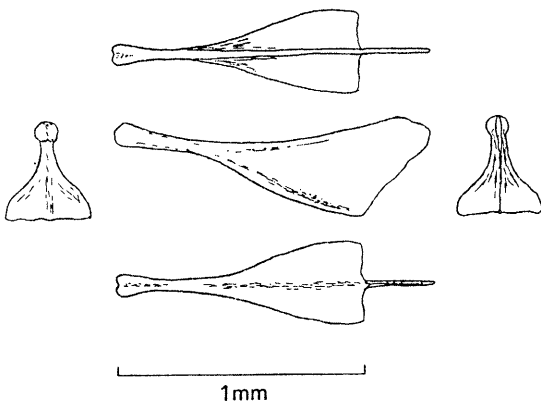
3.2-1.1 MISGURNUS ANGUILLICAUDATUS



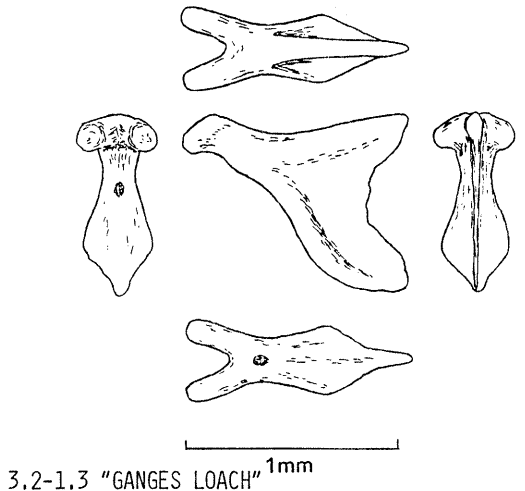
3.1-12.1 LABEO BICOLOR



3.2-1.2 "WHITE LOACH"

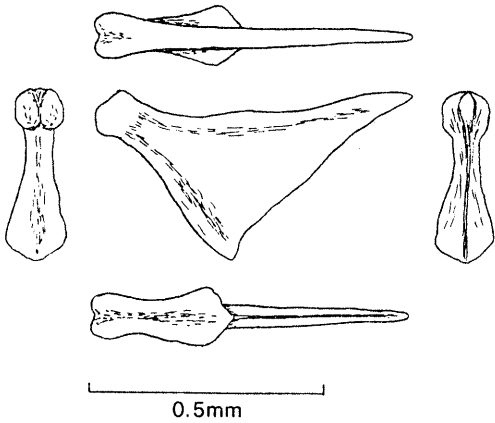


3.1-13.1 BRACHYDANIO RERIO

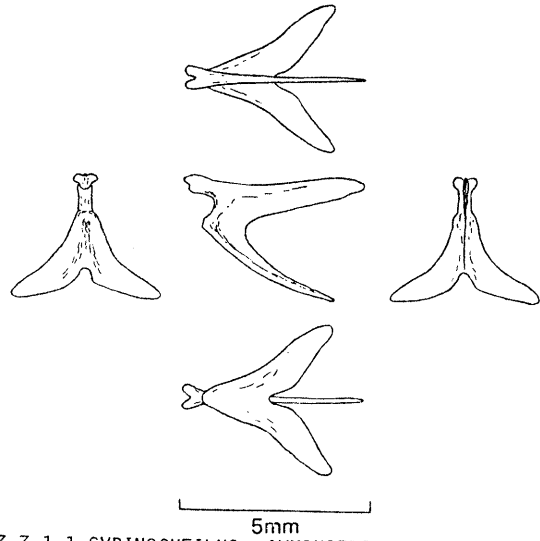


3.2-1.3 "GANGES LOACH" 1mm

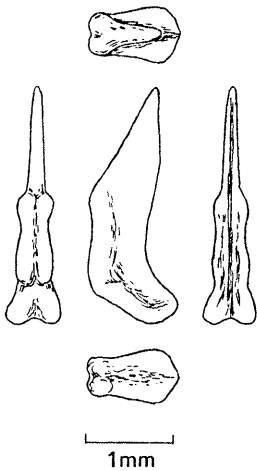
PLATE 6



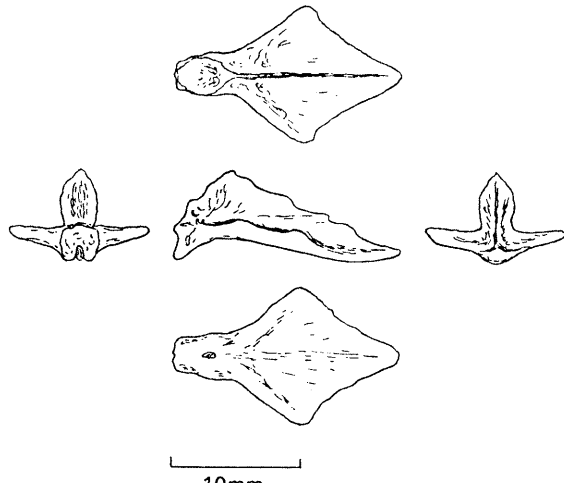
3.2-2.1 ACANTHOPHTHALMUS SEMICINCTUS



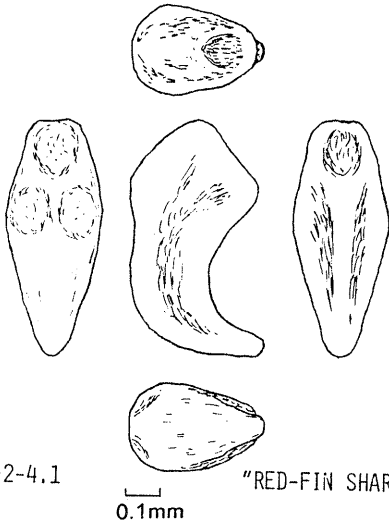
3.3-1.1 GYRINOCHEILUS AYMONIERI



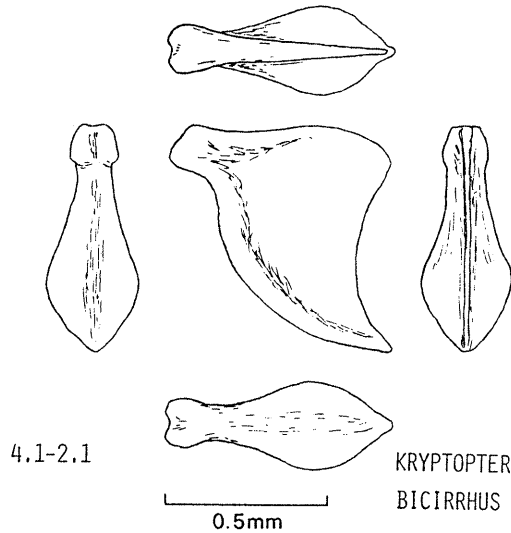
3.2-3.1 BOTIA MACRACANTHUS



4.1-1.1 PARASILURUS ASOTUS



3.2-4.1 "RED-FIN SHARK-LIKE LOACH"



4.1-2.1 KRYPTOPTERUS BICIRRHUS

PLATE 7

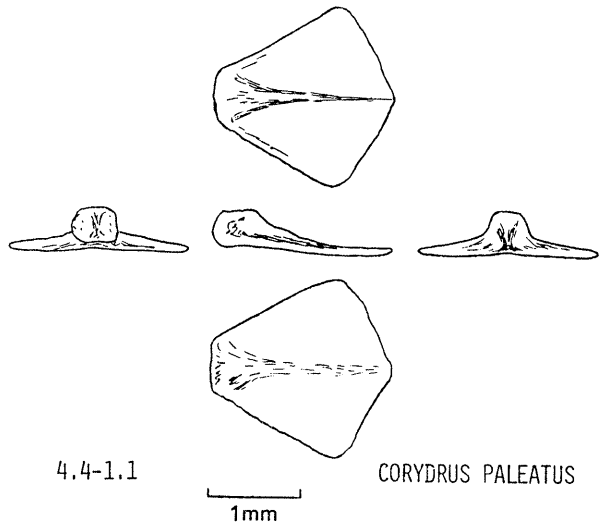
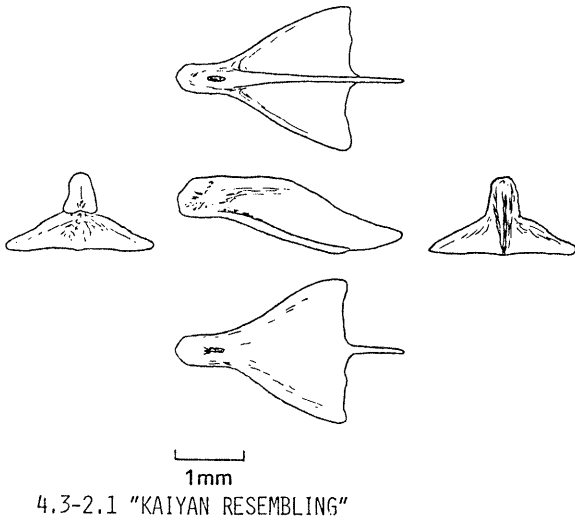
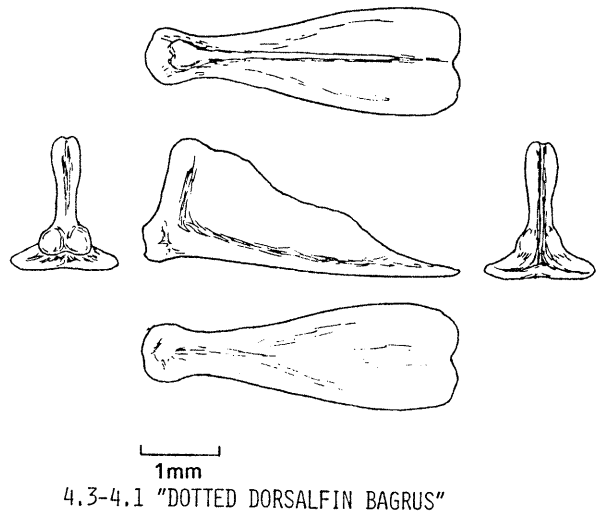
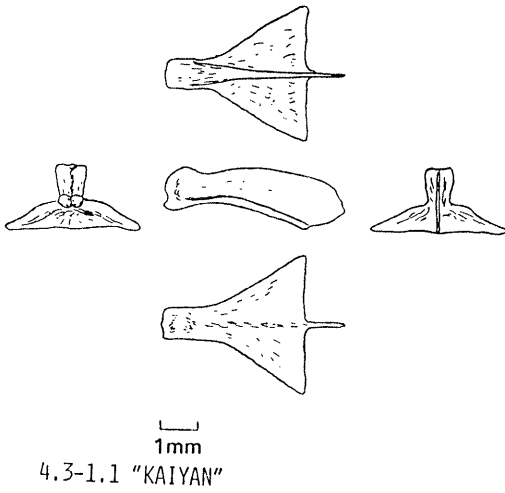
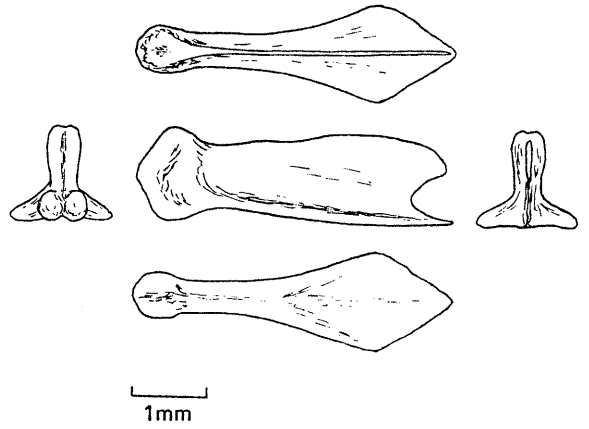
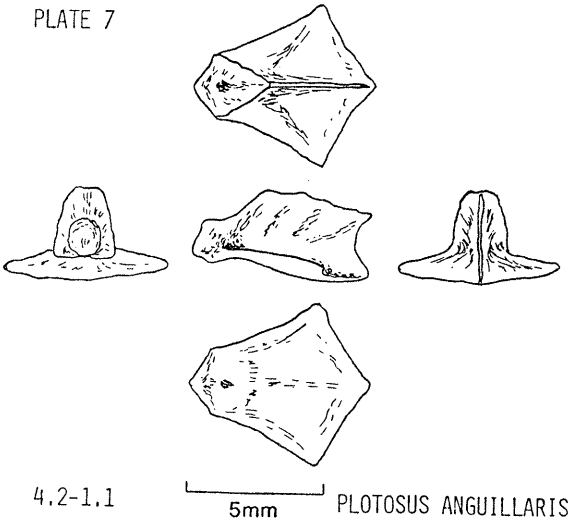
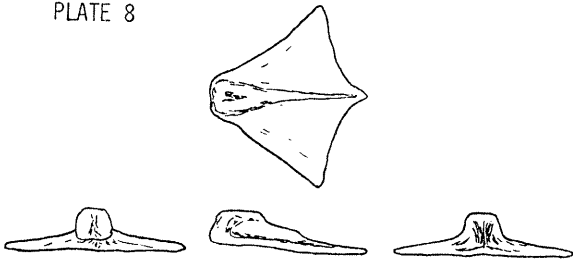
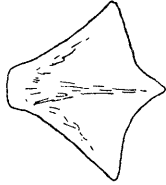


PLATE 8

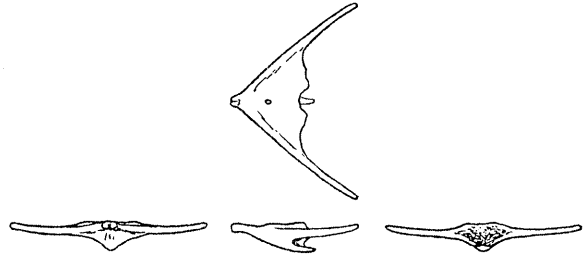


4.4-1.2



1mm

CORYDRUS PALEATUS ALBINO

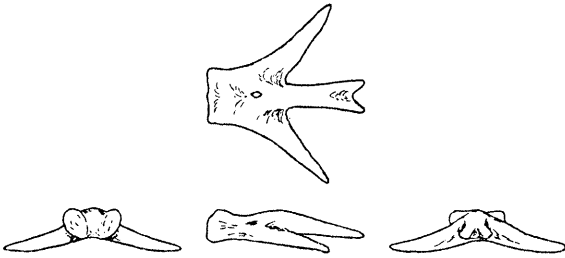


4.7-1.1

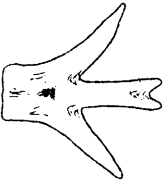


5mm

"GANGES CHACA"

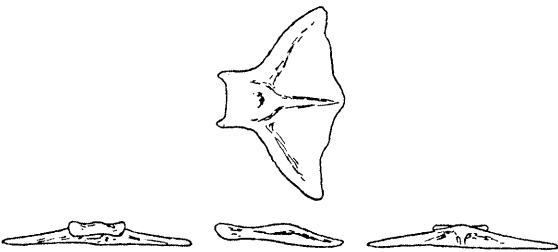


4.5-1.1

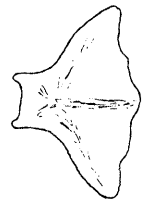


10mm

CLARIAS LAZERA



4.6-1.1



1mm

LORICARIA PARVA

大槌湾における毛顎類の性状と海況変動との関係*

寺崎 誠**, 丸茂 隆三***

Seasonal Distribution of Pelagic Chaetognaths in Relation to Variation of Water Masses in Otsuchi Bay, Northern Japan*

Makoto TERAZAKI** and Ryuzo MARUMO***

Abstract: A plankton sampling was carried out at three stations in Otsuchi Bay once monthly over the period of one year, May 1978-May 1979. On the basis of analyses of 35 samples taken by a Norpac net with 0.33 mm in mesh-opening, studies were made on the monthly variation in number of pelagic chaetognaths and the breeding seasons and the relationship between the distribution of indicator species and the water masses was discussed.

There is a large variation of chaetognath number ranging from $1/m^3$ (in March) to $78/m^3$ (in October). Three genera and 9 species 1 form of chaetognaths were identified. The species composition in Otsuchi Bay was similar to that in the open sea off Otsuchi Bay. *Sagitta minima* was the most common and abundant species, followed by *S. nagae*, *S. enflata*, *S. elegans* and *S. crassa* f. *naikaiensis*. The breeding season of these species in the bay was June-October in *S. crassa* f. *naikaiensis*, April in *S. elegans*, August-October in *S. enflata*, October-November in *S. nagae* and August-December and February-May in *S. minima*. *S. crassa* including *S. crassa* f. *naikaiensis*, and *S. minima* have finished their life history in Otsuchi Bay. *S. elegans* and *Eukrohnia hamata* were carried by the Oyashio cold current and on the other hand, the occurrence of *S. enflata*, *S. ferox*, *S. regularis* and *Pterosagitta draco* had close connection with the Kuroshio warm current.

1. 緒言

大槌湾は、南北 2 km、東西 8 km の、東側が太平洋に開いた細長い湾であり (Fig. 1)、水深は、湾口部 70~80 m、湾奥部 10~20 m である。湾内の水は、湾奥部に開く大槌川、小釜川、鶴住居川から供給される河川水と、沖合から流入する外洋水によって形成される。大槌湾の沖合は年によ

て変動があるが、一般に 3~4 月には南下した親潮第一分枝、5~6 月には津軽暖水、6~2 月には黒潮北上分派が卓越する複雑な海域である (岩手県水産試験場先定地点観測資料)。

大槌湾に出現する毛顎類については、これまで著者の 1 人、丸茂 (1977) が出現種と海況との関係について報告している。本研究はさらにこれを発展させ、年間を通して大槌湾に出現する毛顎類各種の分布・消長および本湾に流入する水塊とその指標種との関連について解析することを目的とした。このため、1978 年 5 月より 1979 年 4 月まで、毎月 1 回、湾口、湾中央、湾奥の 3 定点で水温・塩分の観測、プランクトン採集を実施した。

本研究を行なうにあたり、種々の助言をいただいた東京大学海洋研究所大槌臨海研究センター主任 沼知健一助教授、および試料採集にあたり協力

* 1981年10月9日受理

Received October 9, 1981

** 東京大学海洋研究所大槌臨海研究センター、〒028-11 岩手県上閉伊郡大槌町赤浜 2-106-1 Otsuchi Marine Research Center, Ocean Research Institute, University of Tokyo, Akahama, Otsuchi, Iwate, 028-11 Japan

*** 東京大学海洋研究所、〒164 東京都中野区南台 1-15-1 Ocean Research Institute, University of Tokyo, Minamidai, Nakano-ku, Tokyo, 164 Japan

をいただいた同センター 川村忠技官, 東京大学海洋研究所 山下洋氏に深く感謝の意を表する。

この研究は文部省科学研究費特定研究の補助を得て行なわれた。

2. 材料と方法

1978年5月から1979年4月までの1年間にわたり, 毎月1回下旬に Fig. 1 に示す大槌湾内の A (水深 35 m), B (水深 47 m), C (水深 75 m) の3定点で, 網目 0.33 mm の Norpac ネットを用いて, 底から表面までの鉛直曳採集を行なった。汲水量はネットの口部に取付けられたフローメーターの回転数より算出した。採集試料はただちに 10% 中性ホルマリン溶液で固定した。試料から毛類類を選別した後, 種を同定し, 各種について個体数を算定した。標本の体長測定は実体顕微鏡に取付けたマイクロメーターを用いて行なった。量的に多い *Sagitta minima*, *S. elegans*, *S. enflata*, *S. nagae*, *S. crassa* forma *naikaiensis* の4種1型については, 湾内で再生産が行なわれているかどうかを知るため, THOMSON (1947) の方法に基づいて成熟度を調べた。

また大槌湾内外の *S. elegans* の出現頻度を比べるため, 1979年5月10日, 東京大学海洋研究所研究船淡青丸で ORI-100 ネット (OMORI 1965) を用い, 湾内6点, 湾外3点で傾斜曳採集を実施した。

3 定点 A, B, C ではプランクトン採集と同時にマーテック STD メーターを用い, 表面から底までの水温, 塩分の観測を行なった。この観測結果に基づき, 大槌湾の水塊構造の変化を追跡するため湾中央の測点 B での T-S ダイアグラムを作成した。しかし 5 m 以浅の表層は河川水の影響を受け (寺崎・四竈 1979), きわめて低塩分の特殊な層であるので, T-S ダイアグラムの解析から除外した。

3. 結果

(1) 大槌湾の水温と塩分

Fig. 2 に示すように, 測点 B における T-S ダイアグラムによると 2~4 月は大槌湾は 7°C 以下, 34‰ 以下の低温低塩分水によって占められ, 親潮水域 (44°N, 154°E) での水温・塩分構造 (HATTORI 1973) に近いが, 5 月に入ると水温, 塩分の上昇が始まり, これは 8 月まで続く。8 月は T-S ダイアグラムは黒潮水域 (34°N, 136°50'E) の水温・塩分構造 (YAMAMOTO and HORIKOSHI 1979) と近く, この時期に湾内水が黒潮水の強い影響下にあったことが示される。9 月に入ると降温が始まり, これは 3 月まで続くが, 塩分は 9 月, 10 月を除き 1 月まで 34‰ 以上である。9 月, 10 月の低塩分は, この時期に多量の降雨があり (寺崎・四竈 1979), 湾内水が河川の影響を強く受けたためである。

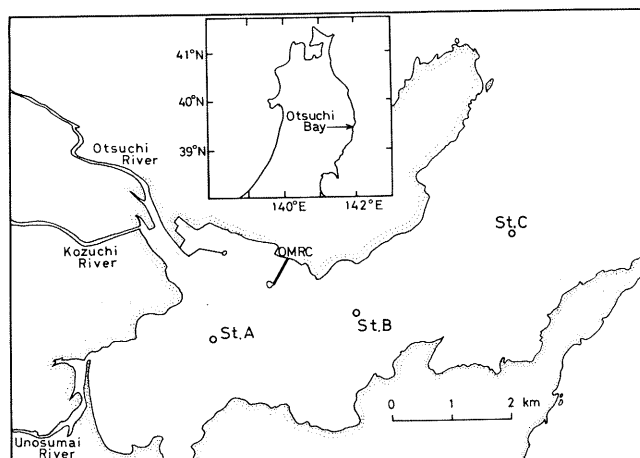


Fig. 1. Map showing Otsuchi Bay. Stns. A-C are routine sampling locations.

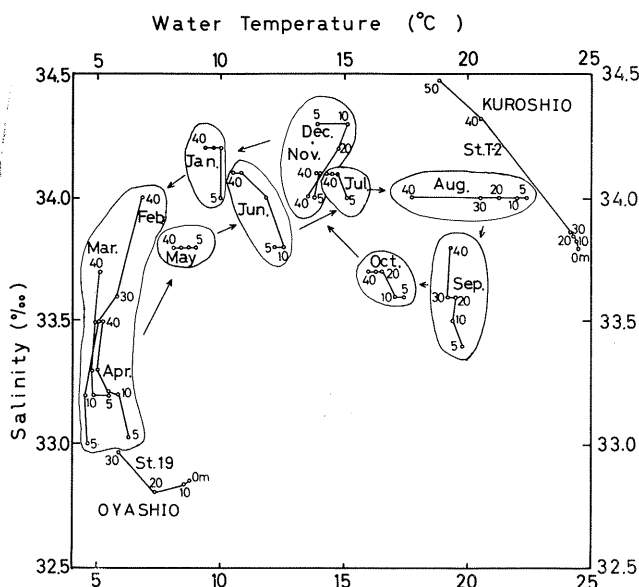


Fig. 2. Seasonal variation of T-S diagrams at Stn. B in Otsuchi Bay. Stns. 19 (44°N, 154°E) and T-2 (34°N, 136°50'E) are located in the Oyashio area (HATTORI 1973) and the Kuroshio area (YAMAMOTO and HORIKOSHI 1979) respectively.

(2) 出現種

大槌湾では、1978年5月から1979年5月までの間に3属9種1型が出現し、その種類は *Sagitta crassa*, *S. crassa* forma *naikaiensis*, *S. elegans*, *S. enflata*, *S. ferox*, *S. minima*, *S. nagae*, *S. regularis*, *Pterosagitta draco*, *Eukrohnia hamata* である。

3定点 A, B, C の毛顎類総個体数の周年変動は類似した傾向を示した。個体数はどの点でも10月が最も多く60/m³以上で、1~3月は少なく5/m³以下であった (Fig. 3)。

以下に各種の出現状況について述べる。

Sagitta crassa と *S. crassa* f. *naikaiensis*: 大槌湾では *S. crassa* は11~3月および5月に、*S. crassa* f. *naikaiensis* は6~10月の高温期に出現し (Fig. 4), 両者が同じ月に採集されることはなかった。村上 (1959) が瀬戸内海で報告している両者の中間型は今回の調査では検出されなかった。*S. crassa* は湾全域に出現したが、個体数はどの月も1/m³前後と少なかった。一方、*S. crassa* f. *naikaiensis* は湾奥の測点Aから多く採集され、

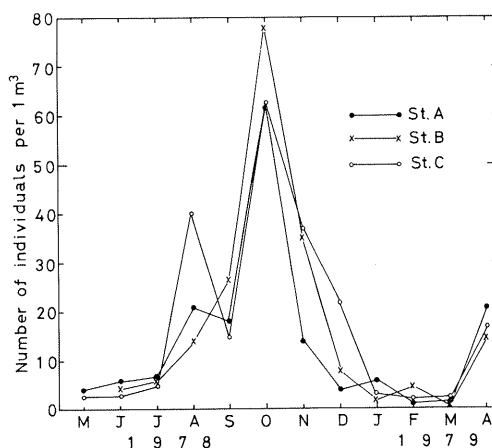


Fig. 3. Seasonal variation of total individual number of chaetognaths in Otsuchi Bay.

この点における出現個体数は1~18/m³ (平均7/m³), 測点B, Cではどの月も3/m³以下であった。

S. crassa の体長は4.0~15.3 mmで、5月のみ完熟個体 (体長13 mm以上) が出現した。*S. crassa* f. *naikaiensis* の体長は3.0~8.5 mmであり、完熟個体 (体長6 mm以上) は何れの月

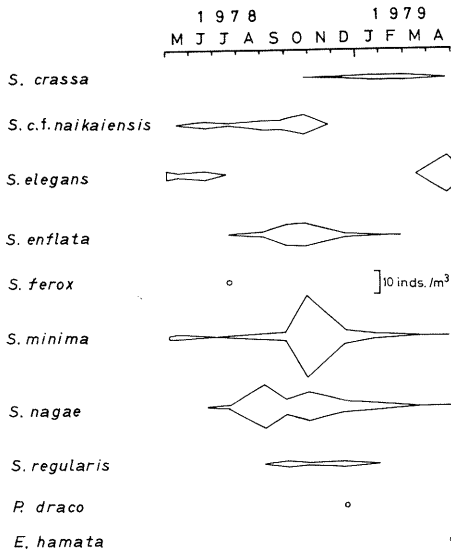


Fig. 4. Seasonal distribution of individual number of chaetognath species in Otsuchi Bay.

にも出現した。

Sagitta elegans: 本種は4~6月に採集されたが、量的には4月が最も多く13~20個体/m³であり(Fig. 4)、完熟個体は4月のみ認められた(Fig. 5)。1979年5月のORIネットによる傾斜曳では、本種が湾内の6点から0.001~0.028個体/m³採集されたが、沖合の3点のうち1点では採集されず、他の2点でもいずれも0.001個体/m³以下と低い値であった。

Sagitta enflata: 本種は8~1月に出現したが量的には9~10月が多い(Fig. 4)。8~10月には体長10mm以上の大型個体が多く、完熟個体もかなり認められたが、11月には12mm以上、12月には8mm以上の個体は出現せず、この両月には6mm未満の小型個体が多く見られた(Fig. 6)。

Sagitta ferox: 本種は7月に測点A, Bからそれぞれ1個体ずつ採集されたが、他の月には出現しなかった。

Sagitta minima: 本種は大槌湾の卓越種であり、6月を除く各月に全測点で採集された。10月が最も多く27~45個体/m³、1~7月は少なく3個体/m³以下であった(Fig. 4)。10月に見られる毛顎類総個体数の極大(Fig. 3)は本種の大量出現に起因する。

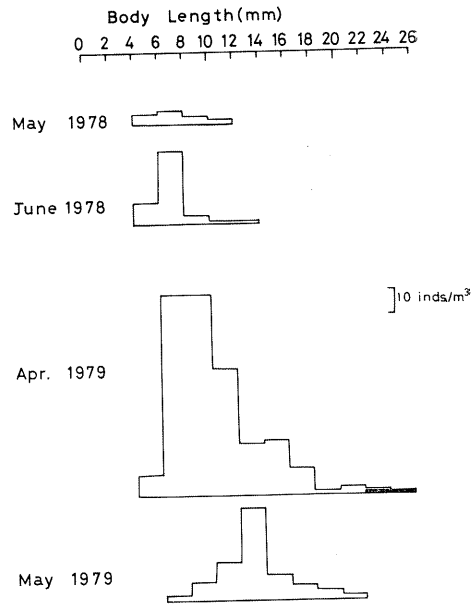


Fig. 5. Size frequency of *Sagitta elegans* collected in different months. Shaded areas show the number of fully matured individuals.

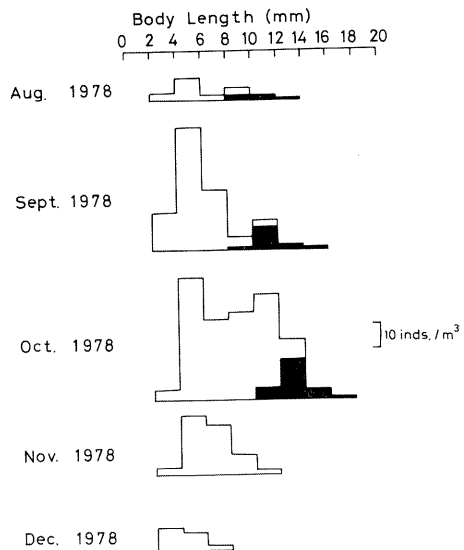


Fig. 6. Size frequency of *Sagitta enflata* collected in different months. Shaded areas show the number of fully matured individuals.

2~5月の低温期には体長8mm以上の大型個体が出現するが、7~1月の高温期には8mm未満の個体のみが検出され、完熟個体は1月、6月、7月を除く各月に出現した(Fig. 7)。

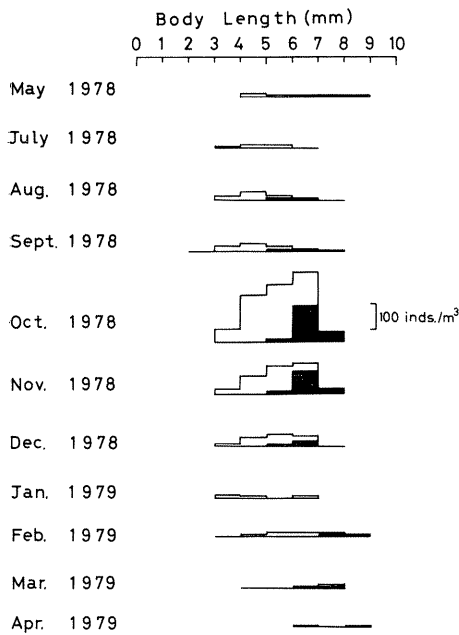


Fig. 7. Size frequency of *Sagitta minima* collected in different months. Shaded areas show the number of fully matured individuals.

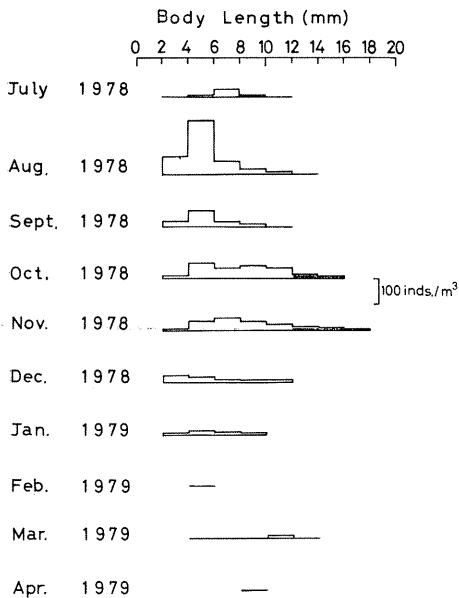


Fig. 8. Size frequency of *Sagitta nageae* collected in different months. Shaded areas show the number of fully matured individuals.

Sagitta nageae: 本種は5月、6月を除く各月に出現し、*S. minima* に次いで量的に多い。個体数

は8月が最も多く $8\sim 30/m^3$ 、2~4月の低温期には $1/m^3$ 以下であった。10月、11月の採集試料中には多くの完熟個体が含まれており、12月、1月に体長6mm未満の小型個体の占める割合が大きかった (Fig. 8)。

Sagitta regularis: 本種は9~12月に出現したが、個体数は少なく $1/m^3$ 以下で、測点Aから採集されたのは9月のみであった。

Pterosagitta draco: 本種は12月に測点B、Cから各々1個体ずつ採集された。

Eukrohnia hamata: 本種は4月に測点Cから1個体採集されたのみである。

4. 考 察

(1) 大槌湾に出現する毛顎類の特色

1978年5月から1979年4月までの1年間にわたる調査で、大槌湾から採集された毛顎類3属9種1型のうち、*S. crassa*、*S. crassa* forma *naikaiensis* は暖海の内湾 (村上, 1957, 1959, 丸茂 1977)、*S. enflata*、*S. ferox*、*S. nageae*、*S. regularis*、*P. draco* は黒潮水域 (KURODA 1976, 1977)、*S. minima* は親潮と黒潮の遭遇する混合水域 (鬼頭 1974)、*S. elegans*、*E. hamata* は亜寒帯水域 (ALVARIÑO 1964, KOTORI 1972) に多く出現する種類である。

鬼頭 (1974) が1955~1960年の間、2月、5月、8月、11月に三陸沖でOネットを用いて行なった0~100mの鉛直採集では、毛顎類20種が出現したが、周年出現頻度が高いのは *S. minima* のみであり、その他は季節的に出現し、*S. nageae* は春から秋にかけて高い頻度を示した。また毛顎類総個体数は2月が最も低く $2.4/m^3$ で、その後は徐々に増加し、5月が $8/m^3$ 、8月が $15.3/m^3$ 、11月が $27.7/m^3$ であった。三陸沖と大槌湾を比べると、毛顎類総個体数は大槌湾の方が多いが、総個体数の周年変動の傾向および各種の季節的出現状況は極めてよく類似している。三陸沖からは報告されているが、本研究で大槌湾から採集されなかった種類は、*Sagitta bipunctata*、*S. delicata*、*S. hexaptera*、*S. lyra*、*S. neglecta*、*S. pacifica*、*S.*

pseudoserratodentata, *S. robusta*, *Krohnitta pacifica*, *K. subtilis* の 10 種で、いずれも暖海性の表層種であり、今後、大槌湾に出現する可能性もある。

S. crassa, *S. crassa* f. *naikaiensis* は、東京湾や瀬戸内海などの内湾では卓越種であるが（村上 1957, 1959, 丸茂 1977）、大槌湾では両者とも個体数は $7/m^3$ 以下と極めて少なく、その分布も主に湾奥部に限られていた。これは大槌湾が東京湾や瀬戸内海に比較して、外洋に直接面しているため外洋水との交換がよく行なわれることを意味し、物理的な解析結果（蓮沼他 1977, 四竈私信）とよく一致する。

(2) 出現種と水塊との関連

S. ferox, *S. regularis*, *P. draco* はそれぞれ 7 月, 9~12 月, 12 月に出現したが、それぞれ 1 個体得られただけである。上記 3 種は黒潮水域、日本海に分布することが知られており、黒潮北上分派もしくは津軽暖水によって大槌湾まで運ばれたものと考えられる。これまでの日本海の調査では、上記 3 種は 2 個体/ m^3 以下で、かつ採集される頻度も少なかった（鬼頭 1974）。また、本研究で 7 月から 12 月にかけての沖合は、南から張り出した黒潮北上分派の勢力が強かった（岩手県水産試験場地先定点観測資料）、これらは津軽暖水

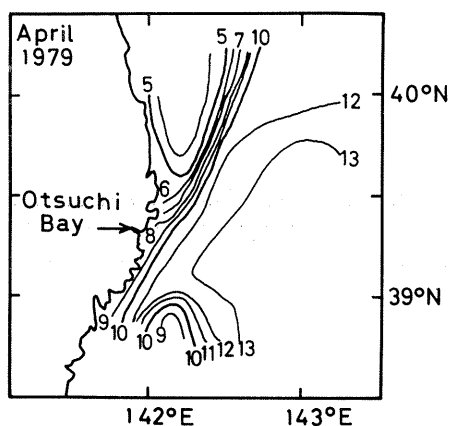


Fig. 9. Distribution of the surface water temperature ($^{\circ}C$) in neighboring water of Otsuchi Bay in April 1979 (Data from the Iwate Prefecture Fisheries Experimental Station).

よりむしろ黒潮系水によって運ばれたものと考えられる。

4 月には *S. elegans*, *E. hamata* など亜寒帯水域に生息する種類が採集された。この時期は親潮第一分枝の南下が著しく、湾口から沿岸域一帯は $8^{\circ}C$ 以下の冷水に覆われており (Fig. 9)、また、湾内からは *Calanus plumchrus*, *Eucalanus bungii*, *Tortanus discaudata* などの冷水性かいあし類がかなり多く採集された（寺崎 1980）こととも相俟って上記 2 種は親潮によって運ばれてきたと推定できる。*S. elegans* の場合、5 月, 6 月にも出現したが、完熟個体は認められず、個体数は $2\sim 3/m^3$ で、4 月の $13\sim 20/m^3$ と比べてかなり少なくなった。5 月に行なった ORI ネットによる湾内外調査では沖合からはほとんど採集されなかったため、この時期には湾外からの補給はなく、4 月に大量に流入した個体が、湾内に拡散し 6 月まで生残したものと考えられる。

S. enflata は大槌湾では 8 月から出現したが、量的には 9 月, 10 月が多く、その後は徐々に減少し、1 月には測点 A で 1 個体採集されたのみであった。1 月の湾内の水温は $10^{\circ}C$ 前後で、本種の出現下限水温 $10^{\circ}C$ （浜田 1967）あるいは $11^{\circ}C$ （鬼頭 1974）と一致していた。水温は 12 月から 1, 2 月にかけて急激に下降し (Fig. 2)、2 月は全層で $7^{\circ}C$ 以下になった。このため、これまで湾内に生息していた *S. enflata* はこの低水温に適応できずに死滅したと推定できる。この考え方は、2 月に暖海種が全く採集されていないことから裏付けされる。*S. enflata* は黒潮水域では通年、日本海では夏に少し分布するので（鬼頭 1974）、黒潮北上分派、または津軽暖水によって大槌湾に運ばれたと考えられるが、本研究においては、この時の湾沖合の海況から考えて、*S. ferox*, *S. regularis*, *P. draco* の場合同様、黒潮による可能性が高い。*S. enflata* では 8 月から 10 月にかけて完熟個体が出現し、9 月以降に小型個体が増加すること (Fig. 6) から、本種は湾内では秋に産卵すると考えられる。しかし、前述の理由により低温期に死滅してしまうので、湾内では生活史を繰り返すことができない。

S. minima と *S. nagae* は、大槌湾に出現する毛顎類の中では量的に多く、*S. minima* では6月、*S. nagae* では5月、6月を除く、すべての月に採集された。両種は三陸沖の混合水域と日本海に多く出現し、また親潮水域からも報告されており(鬼頭1974)、分布が普遍的であるので水塊の指標種としては適当でない。*S. minima* は完熟個体の出現状況から見て8~12月、2~5月が産卵期であると考えられ、前者の期間すなわち高温期には6mm前後の小型個体、後者では8mm前後の個体で産卵する。大槌湾内での*S. nagae* の産卵期は10~11月で、12月以降に幼虫の出現が認められる。しかし、2月以降は出現個体数も極端に減少し、ついに5、6月には採集されなかった。過去にも1977年5月に湾内の15点でNorpacネット鉛直曳によるプランクトン採集が実施されたが、この時にも出現しておらず(丸茂1977)、*S. nagae* はこの時期に大槌湾に生息していない可能性がある。さらに1978年7、8月に採集された*S. nagae* は体長14mm未満の個体ばかりで、11~12月に生まれ越冬した世代を含むとは考えられない。これらの事からも*S. nagae* が大槌湾で生活史を繰り返す可能性は極めて少ない。また、5月には沖合の混合水域では*S. nagae* は卓越種である(鬼頭1974)にもかかわらず、湾内には出現しないというのは興味深い事で、この時期に湾内外の水の交換があまりないため本種や他の暖海種が湾内に流入できないと考えられる。しかし、この点を明らかにするためには将来流速測定などによって大槌湾内の水の動向を正確に知る必要がある。

文 献

- ALVARINO, A. (1964): Bathymetric distribution of chaetognaths. *Pacific Science*, **18**, 64-82.
- 浜田尚雄 (1967): 播磨灘、大阪湾における Chaetognatha, 特に *Sagitta enflata* の分布について. 日本水産学会誌, **33**, 98-103.
- 蓮沼啓一, 永江英雄, 平野敏行 (1977): 大槌湾での流れの測定. 大槌臨海研究センター報告, **3**, 21-23.
- HATTORI, A. (1973): Preliminary Report of the Hakuho Maru Cruise KH-71-3 (IBP Cruise). *Ocean Res. Inst. Univ. Tokyo, Tokyo*. 69 pp.
- 鬼頭正隆 (1974): 毛顎類. 丸茂隆三編, 海洋学講座10「海洋プランクトン」, 東京大学出版会, 東京. p. 65-85.
- KOTORI, M. (1972): Vertical distribution of chaetognaths in the northern North Pacific Ocean and Bering Sea. In: A. Y. TAKENOUCI *et al.* (eds.), *Biological Oceanography of the Northern North Pacific Ocean*. Idemitsu Shoten, Tokyo. p. 291-308.
- KURODA, K. (1976): Chaetognatha in the Kuroshio area south of Japan. I. Selection of important species. *Bull. Kobe Mar. Obs.*, **192**, 42-49.
- KURODA, K. (1977): Chaetognatha in the Kuroshio area south of Japan. II. Revision of indicator species. *Bull. Kobe Mar. Obs.*, **194**, 26-33.
- 丸茂隆三 (1977): 動物プランクトンの指標性. 堀部純男編, 「環境科学としての海洋学」, 東京大学出版会, 東京. p. 91-94.
- 村上彰男 (1957): 内湾・内海に於ける浮遊性毛顎類の出現 (1) 東京湾及び瀬戸内海中西部海域に於ける出現状況. 水産学集成, 東京大学出版会, 東京. p. 357-384.
- 村上彰男 (1959): 瀬戸内海産浮遊性毛顎類に関する海洋生物学的研究. 内海区水研研究報告, **12**, 1-186.
- OMORI, M. (1965): A 160-cm opening-closing plankton net. I. Description of the gear. *J. Oceanogr. Soc. Japan*, **21**, 20-26.
- 寺崎 誠, 四竈信行 (1979): 大槌湾の3定点における水温, 塩分の周年変動. 大槌臨海研究センター報告, **5**, 9-14.
- 寺崎 誠 (1980): 大槌湾の動物プランクトン. 大槌臨海研究センター報告, **6**, 1-5.
- THOMSON, J. M. (1947): The chaetognaths of south-eastern Australia. *Bull. Coun. Sci. Ind. Res. Melb.*, **222**, 1-43.
- YAMAMOTO, G. and M. HORIKOSHI (1979): Preliminary Report of the Hakuho Maru Cruise KH-74-3. *Ocean Res. Inst. Univ. Tokyo, Tokyo*. 74 pp.



A Review of Sea Conditions in the Japan Sea*

Kenzo SHUTO**

Abstract: Sea conditions in the Japan Sea are briefly reviewed. Flow patterns in upper and deeper layers are described together with prevailing water masses.

1. Bottom topography

Figure 1 is a bathymetric chart of the Japan Sea, which is connected with the East China Sea, the Pacific Ocean and the Sea of Okhotsk through the Straits of Tsushima, Tsugaru, Soya

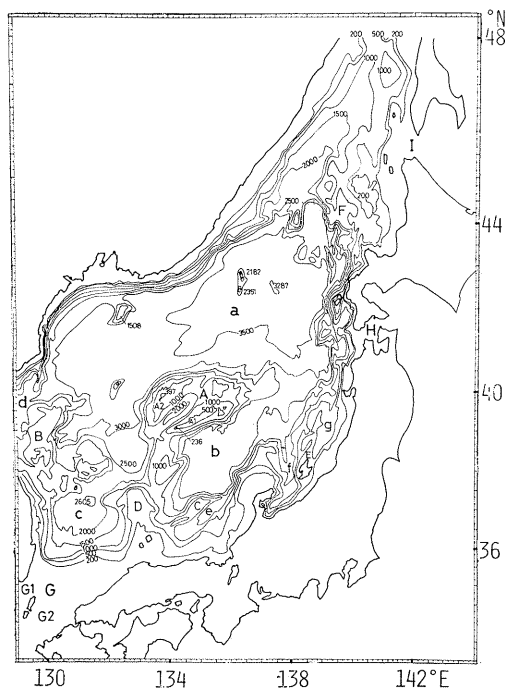


Fig. 1. Bathymetric chart of the Japan Sea. G, the Straits of Tsushima; H, the Straits of Tsugaru; I, the Straits of Soya; A, Yamato Rise; a, Japan Basin; b, Yamato Basin; c, Tsushima Basin.

and Mamiya, respectively. There is Yamato Rise which consists of Yamato Tai and Kita-Yamato Tai in the central part of the Japan Sea. It divides the Japan Sea into three basins: Yamato Basin, Tsushima Basin and Japan Basin.

2. Flow conditions in the Straits of Tsushima

According to the velocity sections constructed by MIITA (1976) on the basis of current measurements, the Tsushima Current is split into two branches in the west of Goto Islands; one is the eastern branch passing through the East Channel of the Tsushima Strait and the other is the western branch passing through the West Channel. Figure 2 shows a velocity section immediately after the Tsushima Current passed through the Straits of Tsushima. The western branch flows away along the Korean Peninsula. The eastern branch flows at a maximum speed of about one half of that in the western branch. Compared with the western branch, the eastern branch is unstable and does not reach deep layers. It is to be noted that a countercurrent extending from the surface to the bottom between both branches flows at a maximum speed of 25 cm/s. The volume transport of the western branch is 3.0 sv and that of the eastern branch is 1.9 sv.

The velocity in the upper layer in the West Channel, obtained by YI (1970) from the difference of the sea level between Izuhara of Tsushima and Pusan at the southern coast of Korea, becomes maximum in October and minimum in March. Its annual mean is 48 cm/s.

3. East Korea Warm Current

The western branch passing through the West Channel flows northward, as the East Korean

* Received October 27, 1981

** Oceanographical Division, Japan Meteorological Agency, Otomachi 1-3-4, Chiyoda-ku, Tokyo, 100 Japan

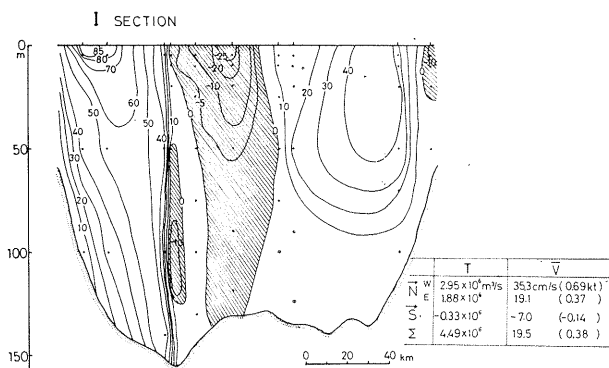


Fig. 2. Velocity section immediately after the Tsushima Current passed through the Straits of Tsushima (MIITA, 1976). Velocity in cm/s. The right is Japan side and the left is Korea side.

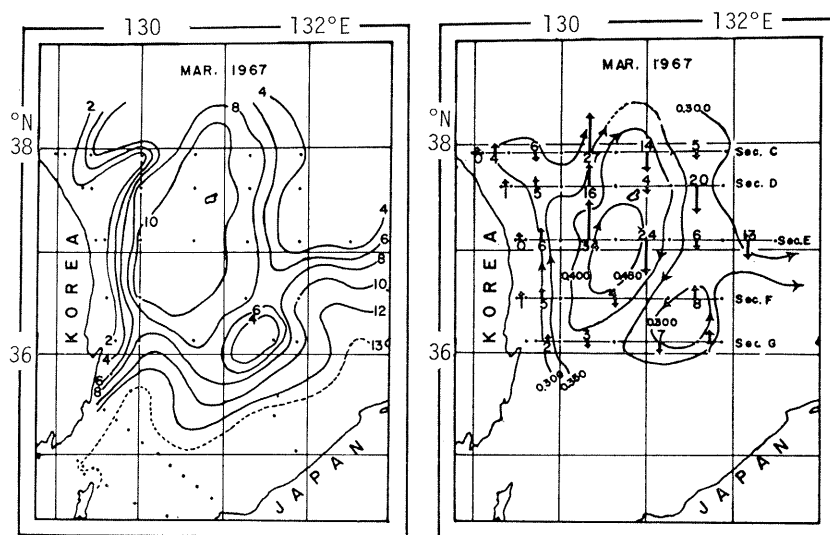


Fig. 3. Water temperature ($^{\circ}\text{C}$) at 100 m depth (left) and dynamic topography (right) of the sea surface referred to 300 db surface in March, 1967 (TANIOKA, 1968).

Warm Current, along the eastern coast of Korean Peninsula. It turns along the north side of a warm water region which is formed on the east side of it, whose location varies to a great extent from year to year. As an example, Fig. 3 shows the Korean Warm Current in March, 1967 (TANIOKA, 1968). The left is the distribution of water temperature at 100 m depth and the right is the dynamic topography of the sea surface referred to 300 db surface. The warm water region is particularly large. It extends from 36°N to 38°N .

The northward volume transport of the East Korean Warm Current varies seasonally, with its maximum in October. The average of the yearly mean geostrophic transport referred to 200 db surface is 1.09 sv, while the volume transport of the southward countercurrent flowing along the east side of the warm water region is 80 to 90 % of that of the northward flowing East Korean Warm Current.

In May 1963 the warm water region was located extremely south and its extent was particularly limited.

4. Flow conditions in the interior region

Figure 4 is a schematic representation of surface currents in summer (NAGANUMA, 1972). After passing through the Straits of Tsushima, the Tsushima Current is split into three branches: the first one flows northeastward along the coast of Japan main island, the second one flows from the north of the Oki Islands to the west of Cape Nyudozaki off the Noto Peninsula and Sado Island, and the third one flows northward along the east coast of Korea, turns to the right at about 38°N, passes by the vicinity of Yamato Rise and reaches the west of Cape Nyudozaki. These three branches meet one another in the west of Cape Nyudozaki. There are southward and northward currents between the second and third branch, and warm and cold water regions are developed there.

The volume transport of the Tsushima Current between the west of Cape Nyudozaki at 40°N and the west of the Shakotan Peninsula at 43°N varies seasonally. Its maximum appears in August in the south, and in October in the north delaying northward. The northward geostrophic volume transport of the Tsushima Current referred to 400 db varies greatly from year to year, particularly in summer, in the

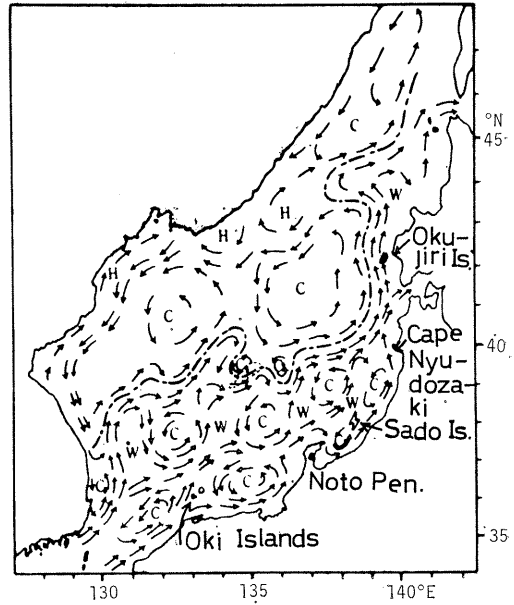


Fig. 4. Schematic representation of the surface currents in summer (NAGANUMA, 1972).

west of Cape Nyudozaki. For example, it ranges from 2.0 sv to 6.5 sv in August.

The outflow transport through the Straits of Tsugaru is evaluated by subtracting the north-

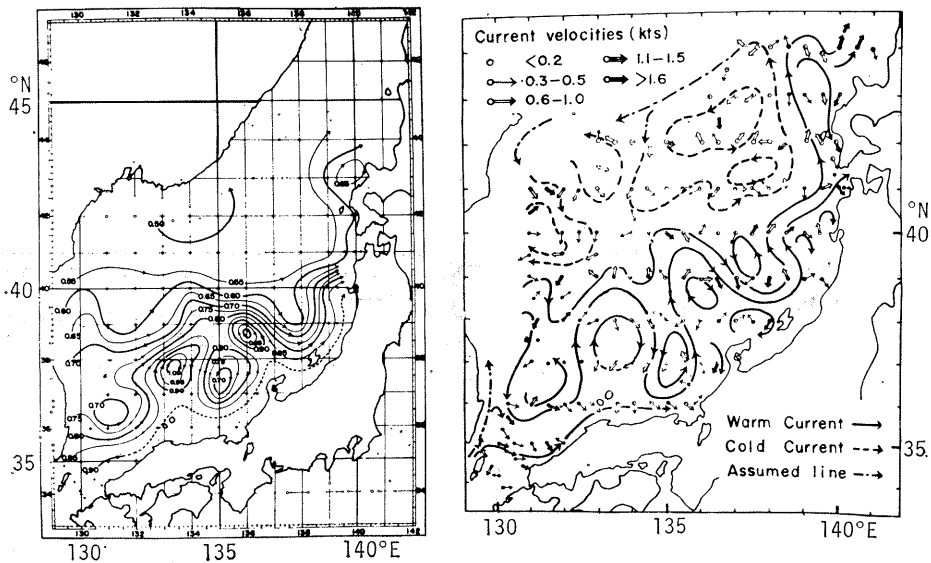


Fig. 5. Dynamic topography (left) of the sea surface referred to 600 db surface and surface currents (right) measured with GEK (OHWADA and TANIOKA, 1971).

ward transport near Okujiri Island at 42°N from that in the west of the Tsugaru Peninsula at 41°N. Its year-to-year variation is large, particularly in August when it ranges from 1.0 to 4.1 sv. The ratio of the outflow transport through the Straits of Tsugaru to the northward transport at 41°N is 80% on the average. It becomes larger in the year when many strong depressions pass through the central part of the Japan Sea and reach Oshima Peninsula (HATA, 1962, 1973).

Figure 5 shows one of the results of a cooperative survey made by five research vessels of Japan Meteorological Agency in October 1969 (OHWADA and TANIOKA, 1971). The left is the dynamic topography of the sea surface referred to 600 db, and the right is the surface current measured with GEK. The Tsushima Current meanders and makes a detour around cold water regions in the north of Sado Island, and around warm water regions in the north of the Oki Islands and in the northwest of Noto

Peninsula. Also seen are weak currents along the coast of Japan and the polar front as well. There is a cyclonic gyre in the northern part and a smaller anticyclonic gyre in the western part of the Liman Current region.

NAGANUMA (1973) pointed out that the Tsushima Current has the above-mentioned characteristics such as its splitting into three branches in summer and in warm years, meandering in winter and in cold years.

Figure 6 shows a dynamic topography of 1,200 db surface referred to 2,000 db in October, 1969 (OHWADA and TANIOKA, 1971). There is a cyclonic gyre in Japan Basin and another one in Tsushima Basin with the maximum speed of about 2.8 cm/s. There is an anticyclonic gyre in Yamato Basin, and another one is in the west of Yamato Rise with a speed of about 0.9 cm/s. The above-mentioned cyclonic gyre in Japan Basin is also found on the dynamic topography of 1,500 db surface referred to 3,000 db (NITANI, 1972).

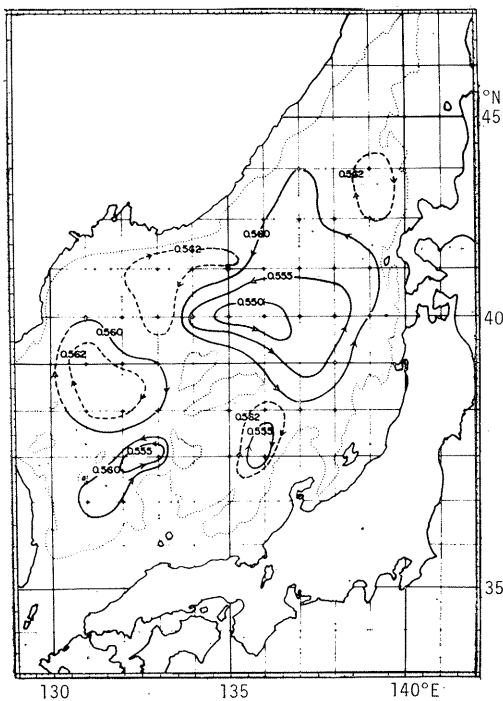


Fig. 6. Dynamic topography of 1,200 db surface referred to 2,000 db surface in October, 1969 (OHWADA and TANIOKA, 1971).

5. Proper Water in the Japan Sea

The name of "Proper Water in Japan Sea" was given by UDA (1934) to a water mass characterized by temperatures of 0 to 1°C, salinity of about 34.1‰ and dissolved oxygen of 5.4 to 5.9 ml/l. According to YASUI *et al.* (1967), the water mass of 0 to 1°C and of 33.96 to 34.15‰ extends predominantly over the Japan Sea (84% of the total volume). This is the Proper Water.

Figure 7 gives the vertical distribution of potential temperatures averaged over the Liman Current and the Tsushima Current region (NITANI, 1972). Three straight lines intersect each other at two points; one is at 1,000 to 1,100 m depth and the other is at 2,000 to 2,300 m depth. The water shallower than the former is called deep water, the water deeper than the former but shallower than the latter is called upper bottom water, and the water deeper than the latter is called lower bottom water. The potential temperature is decreased exponentially with depth in the deep and upper bottom water, but is constant in the lower bottom water.

There is a cold, saline region of temperature lower than 0.06°C and salinity higher than

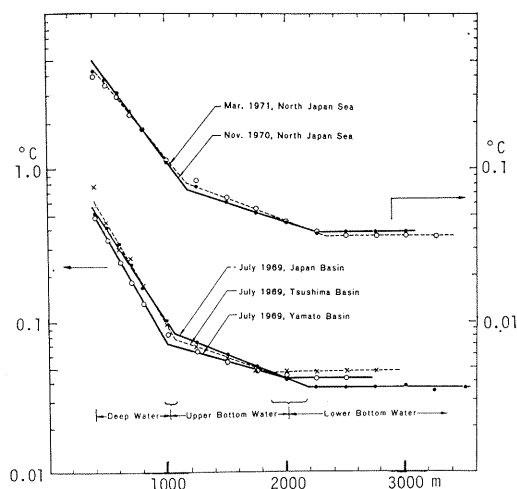


Fig. 7. Several examples of vertical distribution of the averaged potential temperatures in the Liman Current and the Tsushima Current regions (NITANI, 1972).

34.075‰ off the Siberian coast at 1,500m depth, depth of the upper bottom water. This region is also rich in dissolved oxygen (more than 5.3 ml/l). In the central part of Japan Basin there is a warm region of temperature higher than 0.05°C at 2,500m depth, depth of the lower bottom water. A saline water of salinity higher than 34.075‰ extends eastward from the Straits of Tsugaru. A rich dissolved oxygen water (more than 5.5 ml/l) extends along the northern side of Yamato Rise.

Figure 8 shows the horizontal distribution of σ_t at the sea surface in winter. A belt of high σ_t denser than 27.30 lies in the distance of 45 nautical miles from the Siberian coast. The thickness of the surface mixed layer becomes maximum (550 m) near this belt, which suggests an active sinking at the surface and subsurface layer.

Figure 9 gives a zonal-vertical section of the potential σ_t in the west of the Straits of Tsugaru in March, 1971. Near the continent, a homogeneous water of the potential σ_t equal to 27.36 occupies the whole layer from the surface to the depth of 450 m. The equipotential surface of $\sigma_t=27.36$ reaches a depth of 800 m in the central part. The potential σ_t of the lower bottom water is higher than 27.375.

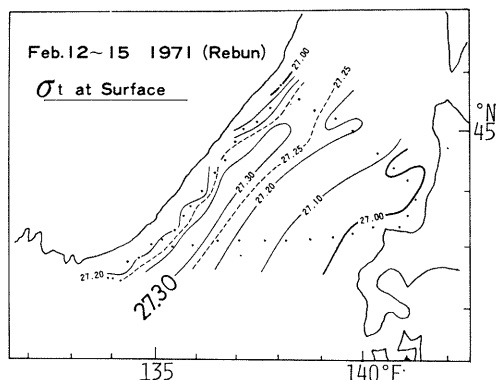


Fig. 8. Sigma-t at the sea surface obtained by the patrol ship Rebun in mid February 1971 (NITANI, 1972).

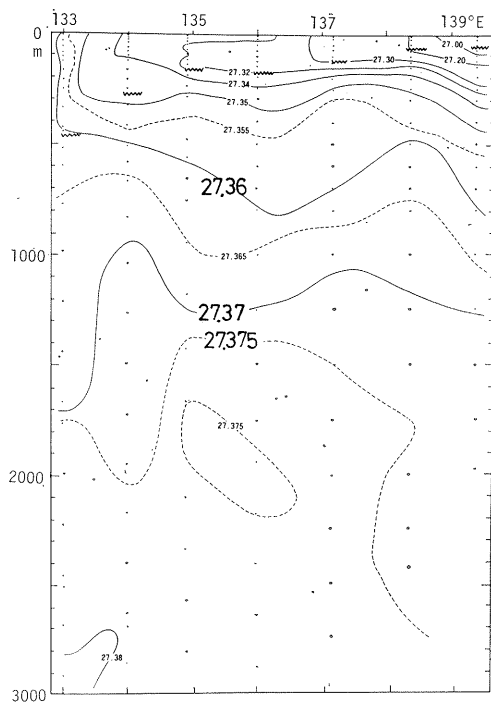


Fig. 9. Latitudinal vertical section of potential sigma-t west of the Straits of Tsugaru in March, 1971 (NITANI, 1972).

These observational results should indicate that the sinking at the belt of high σ_t forms the deep water as well as the upper bottom water in the Japan Sea. However, it is not so strong as to form the lower bottom water, which should result from ice formation. SUDA

(1932) showed that the bottom water of the Japan Sea is formed in the central and northern part of the Liman Current. A dense water formed near the Siberian coast as a result of ice formation could sink down to deep layers to form the bottom water.

References

- HATA, K. (1962): Seasonal variation of the volume transport in northern part of the Japan Sea. *J. Oceanogr. Soc. Japan*, 20th Anniv. Vol., 168-179. (in Japanese)
- HATA, K. (1973): Variation in hydrographic conditions in the seas adjacent to the Tsugaru Straits. *J. Meteorol. Res.*, **25**, 467-479. (in Japanese)
- MIITA, T. (1976): Current characteristics measured with current meters at the fixed stations. *Bull. Jap. Soc. Fish. Oceanogr.*, **28**, 33-58. (in Japanese)
- NAGANUMA, K. (1972): The oceanographical conditions in the Japan Sea. *Gyokaiyo Handobukku* (Handbook of Fish. Oceanogr.), Zengyoren Gyokaiyo Center, 32-38. (in Japanese)
- NAGANUMA, K. (1973): A discussion on the existence of Tsushima Current third sub-branch. *Nihonkaiku Suisan Shiken Kenkyu Renraku News* (News for Fish. Res. Japan Sea), No.266. (in Japanese)
- NITANI, H. (1972): On the deep and the bottom water in the Japan Sea. *Researches in Hydrography and Oceanography* (ed. D. SHOJI), Hydrogr. Dept. Japan, 151-201.
- OHWADA, M. and K. TANIOKA (1971): Multiple ship survey of the Japan Sea. *Nihonkai ni kansuru Sogo Hokokusho* (Rept. Oceanogr. Survey of the Japan Sea), Science and Technology Agency, 51-72. (in Japanese)
- SUDA, K. (1932): On the bottom water of the Japan Sea (Preliminary report). *Kaiyo Jiho*, **4**, 221-240. (in Japanese)
- TANIOKA, K. (1968): On the East Korean Warm Current (Tōsen Warm Current). *Oceanogr. Mag.*, **20**, 31-38.
- UDA, M. (1934): The results of simultaneous oceanographical investigations in the Japan Sea and its adjacent waters in May and June, 1932. *J. Imp. Fish. Exp. Sta.*, **5**, 57-190. (in Japanese)
- YASUI, M., Y. YASUOKA, K. TANIOKA and O. SHIOTA (1967): Oceanographic studies of the Japan Sea — water characteristics —. *Oceanogr. Mag.*, **19**, 177-192.
- YI, S. (1970): Variations of oceanic condition and mean sea level in the Korean Strait. *The Kuroshio — A symposium on the Japan Current —*. (ed. J. D. MARR), East-West Center Press, Honolulu, 125-141.

日本海 の 海 況 (総 説)

周 東 健 三

要旨: 日本海の海況について簡単にまとめた。対馬海峡通過直後の流速断面において、東西 2 つの流速コアの中間に西向きの反流があるのが注目される。朝鮮半島沿いに北上する東鮮暖流の東側には暖水域が形成されるが、その位置と規模は年によってかなり変化する。日本海における対馬暖流が 3 分枝状態をとる場合と蛇行流路が顕著な場合を示したが、これは季節もしくは長期変動の現われであると指摘されている。

津軽海峡からの平均流出量は、北上する対馬暖流の流量の約 80% であるが、顕著な低気圧が日本海中央部を通過して渡島半島に達する回数が多い年は、流出量も多い。

深層では、日本海盆と対島海盆に反時計まわりの循環、大和海盆には時計まわりの循環が存在すると思われる。

日本海全体積の約 80% を占める最大の水塊である日本海固有水は、低温で均質であるが、この水塊は、冬季における海面の冷却による鉛直対流だけでは生成されそうにもなく、生成には結氷作用が必要なようである。

A Commentary Note on the Paper "On the Outflow Modes of the Tsugaru Warm Current" by D. M. CONLON*

Takashi ICHIYE**

Abstract: CONLON (1982) proposed that there are two modes of the Tsugaru Warm Current outflowing from Tsugaru Strait; one is the gyre mode with the outflow turning around an anticyclonic gyre during the warm season and the other is the coastal mode with the outflow moving southward along the east coast of the Japanese mainland during the cold season. Seasonal change of these two modes is confirmed by the seasonally averaged surface current measured with GEK from 1953 through 1977. The month-to-month change of the isotherms at 100 m and GEK data from November 1975 through January 1976 agreed with the mode change suggested by currents measured directly at two mooring stations. The mode change may be dependent on the ratio of the internal Froude number to the Rossby number of the two-layer strait, though its dependency on the Rossby radius of deformation as proposed by Conlon cannot be dismissed.

1. Introduction

CONLON's paper (1982, hereafter referred as C) is both interesting and provocative in interpreting the flow pattern of the Tsugaru Warm Current which has been studied by a number of Japanese oceanographers for decades. He recognizes its two modes, the gyre and coastal modes based on two hydrographic data collected by Hakodate Marine Observatory in October 1975 and February 1976. The two modes seem to be substantiated by currents measured directly at two mooring stations which were operated from November 1975 to January 1976. Then he compared the two modes with the hydraulic experiment by WHITEHEAD and MILLER (1979, hereafter referred to as WM) and concluded that the coastal and gyre modes are related to smaller or larger Rossby radius of deformation in colder or warmer seasons, respectively, since the radius changes seasonally mainly due to density differences between the upper and lower layers.

2. Additional data

C used the hydrographic data of 1949-1952 for monthly mean values of the upper layer density in calculation of the Rossby radius of

deformation. His result can be compared to the seasonal change in the Tsugaru Warm Current. The Marine Environmental Atlas (JODC, 1979) shows the seasonal charts of the vectorial averaged surface current measured with GEK from 1953 through 1977 in each square of half degree longitude and latitude (Fig. 1). In this atlas, winter, spring, etc. are defined as Jan.-Mar., Apr.-June and so on. It is clearly seen that from January through June the current just east of Tsugaru Straits flows south or southeastwards, whereas in summer and fall the current there flows eastwards with speed exceeding 0.5 knots and then turns to the southeast of 143°W. Particularly in summer an anticyclonic eddy of about 60 n. miles diameter can be recognized with a center at about 41.3°N and 142°W. Although the period of statistics for this figure is different from the one used by C for the upper layer density, this seasonal change seems to match the internal Rossby radius in his Table 1, as the gyre and coastal modes correspond to large or small density difference and thus the Rossby radius, respectively. Lack of the anticyclonic gyre in the fall may be due to the coarse grid for statistics and smallness and shifting nature of the gyre.

In order to fill gaps in the flow patterns

* Received February 5, 1982

** Department of Oceanography, Texas A & M University, College Station, Texas 77843, USA

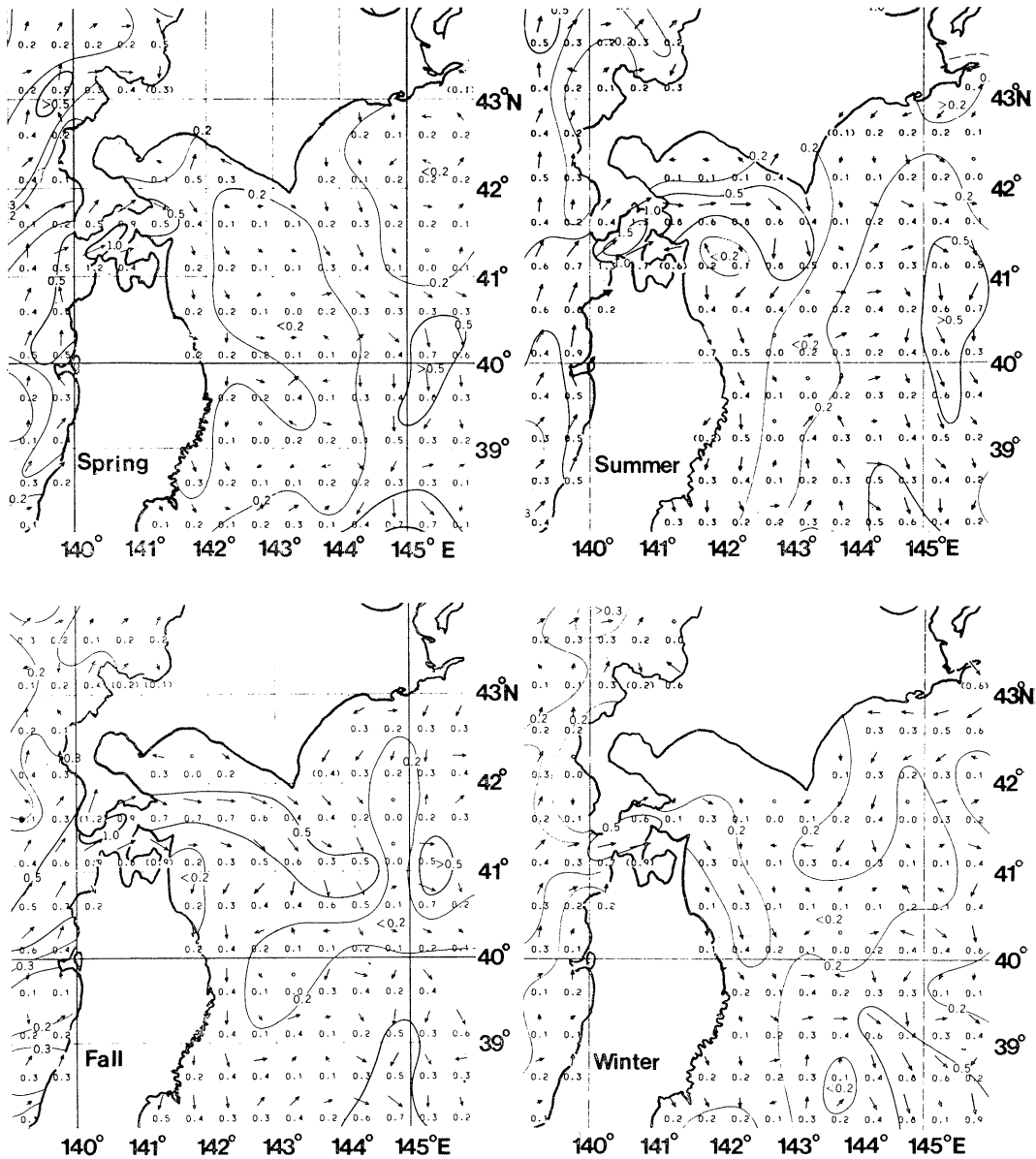


Fig. 1. Vectorially averaged surface current from GEK data obtained from 1955 through 1977, based on "The Marine Environmental Atlas" of JODC (1979).

between October 1975 and February 1976 shown by Figures 2 and 3 of C, the temperature distributions at 100 m depth in months between these two months are shown based on Ten-Day Marine Report (JMA, 1975 and 1976) in Fig. 2. The isotherms are modified to limit the data within an interval stated, instead of the whole month. Selected vectors of the surface current

determined with GEK are also plotted in this figure.

It is seen that in mid-November the surface current just east of Tsugaru Strait was mainly eastwards and there was still the warm water in late November, though its maximum temperature decreased by about 2°C from October and its area also shrunk. This corresponds with

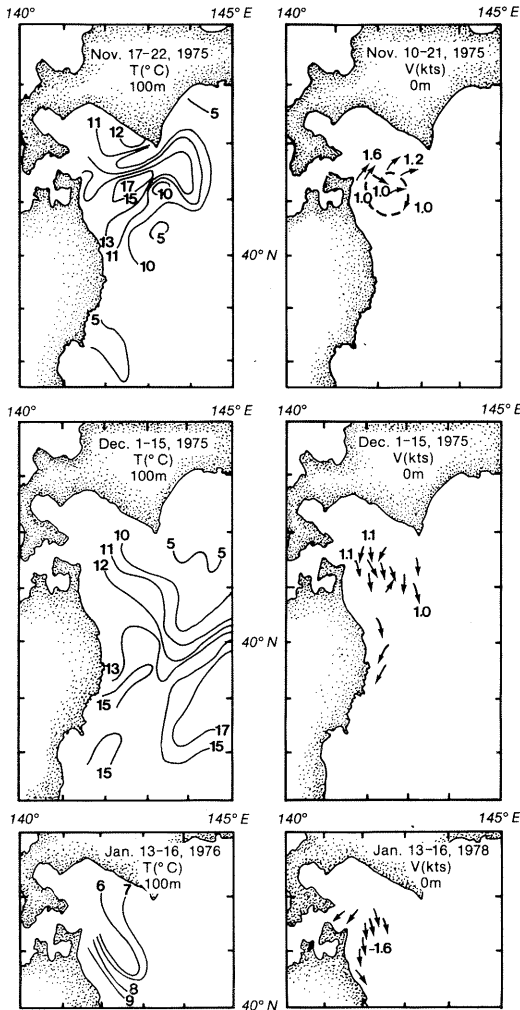


Fig. 2. The temperature at 100 m depth in °C (left panel) and surface current measured with GEK (right panel, speed in knots shown only for above 1 knot) modified from the Ten-day Marine Report of JMA (1975-1976).

the current meter data in Figure 4 of C. In December, the surface current east of Tsugaru Strait started to flow southwards and the temperature at 100 m depth showed no isolated warm water there, although both GEK and hydrographic data were collected over the early half of the month and the exact time of mode change could not be determined. In January both GEK and hydrographic data are insufficient compared to previous months but suggested that the flow pattern immediately east of Tsugaru

Strait was southerly without the anticyclonic gyre.

3. Compared with theoretical and experimental models

C compared his two modes of the Tsugaru Warm Current with the experiment of WM. The latter indicates that the gyre is apt to form to the right of the outflow when the Rossby radius of deformation is beyond a certain critical number, whereas the outflow turns to the right along the wall as a jet for the radius within a certain range. Also the flow becomes unstable for the radius below another critical number. Therefore the experimental result agrees qualitatively at least with the mode change observed in the Tsugaru Warm Current. However, the experiment was made with two-layer fluid (bottom layer with salted water) and the radius is calculated from density difference of these layers, whereas in the Tsugaru Warm Current the pycnocline is not so sharp, particularly in the cold seasons as considered to form the two-layer system. It may be interpreted that Tsugaru Strait is shallow and the outflow moves over the underlying water without mixing, thus virtually forming a two-layer system, in order to apply the experimental result.

It is out of scope in this note to discuss details of dynamics of the outflow from the strait or to criticize experimental and theoretical modeling. However it seems that the result of WM may be applicable to the Tsugaru Current only in a qualitative sense, particularly since the topography and vertical stratification of the prototype are quite different from the model and also since the critical parameter of the model is the Rossby radius of deformation only and does not include the velocity of the flow in the strait.

A numerical model of NOF (1978) may have some relevancy to the present case, though the topography is extremely simplified. The potential vorticity equation and the Bernoulli integral of the upper layer in the two-layer model are dependent on the Rossby number $R = V/fB$ and the internal Froude number $F = V^2/g'H$, respectively, and both are dependent on F/R , where V is a characteristic velocity of the current in the strait, f is the Coriolis co-

Table 1. Characteristic speeds V and $(g'H)^{1/2}$, the Rossby number R , and internal Froude number F .

Months	Mar.	June	July	Aug.	Sept.	Oct.	Nov.
V (m/s)	0.027	0.11	0.13	0.19	0.32	0.27	0.19
$(g'H)^{1/2}$ (m/s)	0.45	1.21	1.78	2.24	3.25	2.19	1.71
R	0.0093	0.083	0.045	0.066	0.111	0.093	0.066
F	0.0036	0.038	0.053	0.072	0.097	0.015	0.012
F/R	0.39	0.22	0.12	0.11	0.09	0.16	0.19

The characteristic speed of the Tsugaru Strait, V , is determined from the mean transport by TOBA *et al.* (1982) divided by 3.73 km^2 , and $(g'H)^{1/2}$ is calculated from Table 1 of CONLON (1982). The Rossby and Froude numbers are determined from $F=V^2/g'H$, $R=V/fB$, where g' , f , B , and H are reduced gravity, Coriolis coefficient, width of the Strait and the mean depth of the upper layer, respectively.

efficient, B is the width of the strait, g' is the reduced gravity and H is the unperturbed thickness of the upper layer. For a horizontally uniform current in the strait, NOF (1978) obtained the flow pattern which shows the outflow being narrow and veering to the right close to the wall for a higher value of F/R , whereas the outflow becomes more straight but broader for lower F/R .

Since $F/R=VfB/g'H=VB/fR_d^2$, where R_d is the Rossby radius of deformation, this ratio increases for a decreasing R_d . Thus, if V is constant, this ratio becomes larger in the colder seasons and thus the behavior of the Tsugaru Current corresponds to both WM and NOF. However as indicated by TOBA *et al.* (1982) V is smaller in spring and winter and larger in summer and fall. Therefore seasonal change of V and R_d may counteract each other to keep F/R constant. In order to check this effect, V is determined by dividing the monthly mean transport of the geostrophic current through an eastern section of Tsugaru Strait (TOBA *et al.*, 1982) by the cross-sectional area of 3.73 km^2 . In Table 1, V is listed for months where the mean transport was determined by TOBA *et al.* (1982) and $(g'H)^{1/2}$ computed from Table 1 of C is also listed with F , R and F/R . The table indicates that the ratio F/R is largest in March but not so large as by an order of magnitude compared to the minimum in September as Nof's example of numerical modeling suggests. The Rossby and Froude numbers reach both minimum in March but maximum in September and October, respectively. Thus it seems that the observed patterns agree qualitatively at least with Nof's model, too.

4. Conclusion

The flow pattern of the Tsugaru Warm Current definitely shows two different modes as C first pointed out. The mode change may be dependent on the critical Rossby radius of deformation as he suggested or on the ratio of the Froude to the Rossby number. The definite conclusion should wait for more elaborate work on theoretical or experimental modeling. Most significant contribution by C is that the direct current measurement is useful even at two mooring stations if these stations are located at a strategically important place and if the conventional hydrographic measurement is carried out frequently enough within a limited area.

This work is supported by the Office of Naval Research.

References

- CONLON, D. M. (1982): On the outflow modes of the Tsugaru Warm Current. *La mer*, **20**: 60-64.
- JMA (Japan Meteorological Agency) (1975-1976): The Ten-day Marine Report No. 1047-1055.
- JODC (Japanese Oceanographic Data Center) (1979): The Marine Environmental Atlas.
- NOF, D. (1978): On geostrophic adjustment in sea straits and wide estuaries: theory and laboratory experiments. Part II, Two-layer system. *J. Phys. Oceanogr.* **8**: 861-872.
- TOBA, Y., K. TOMIZAWA, Y. KURASAWA and K. HANZAWA (1982): Seasonal and year-to-year variability of the Tsushima-Tsugaru Warm Current System with its possible cause. *La mer*, **20**: 41-51.
- WHITEHEAD, J. A. and A. R. MILLER (1979): Laboratory simulation of the gyre in the Alboran Sea. *J. Geophys. Res.*, **84**(C), 3733-3742.

学 会 記 事

- 昭和57年3月10日, 日仏会館会議室において日仏会館と共催でセミナーを開催した。
アンドレ・モレル「海の色のリモートセンシング」
橘高二郎「甲殻類の養殖と放流」
- 昭和57年5月1日, 東京水産大学において編集委員会が開かれ, La mer 第20巻第2号の編集を行った。
- 新入会員 (正会員)

氏 名	所 属	紹介者
Yves Henocque	北里大学	
島本 信夫	兵庫県立水産試験場	宇野 寛
上原 研吾	ウシオ電機㈱	森永 勤
André Morel	パリ第6大学	佐々木忠義
中村 陽一	東京大学海洋研究所	高野 健三

- 退会者
(正会員) 結城了伍, 小長谷史郎, 伊藤 隆,
蓮沼啓一
(賛助会員) ㈱大林組, ㈱ビデオ・プロモーション,
㈱日本プレスコンクリート, ㈱オルガノ
- 逝 去
安田富士郎, 長谷川秀治, 田畑忠司, 菅原 健,
宇田道隆
- 会員の住所・所属の変更

氏 名	新住所または新所属
岩渕義郎	〒104 中央区築地 5-3-1 海上保安庁水路部
赤松英雄	〒790 松山市北持田町 102 松山地方気象台
岩佐欽司	〒104 中央区築地 5-3-1 海上保安庁水路部海洋研究室
中村保昭	〒420 静岡市追手町 9-6 静岡県農業水産部水産課
松本 勝	〒270-11 千葉県我孫子市白山3-8-1-102
倉田 亮	〒520 大津市京町3丁目滋賀会館内 滋賀県琵琶湖研究所

- 交換および寄贈図書
 - 「太平洋における海洋科学技術協力」第6回国際海洋シンポジウム報告書
 - 国立科学博物館彙報 第14号
 - 国立科学博物館研究報告 Vol. 7, No. 4

- 地盤水理実験施設年報 第7号
- 海洋産業研究資料 Vol. 13, Nos. 1, 2, 3
- 日本プランクトン学会報 第28巻第2号
- 地質調査所 クルーズレポート No. 17
- 研究実用化報告 Vol. 31, Nos. 3, 4
- 海洋時報 第24号
- 新海洋法条約の締結に伴う国内法制の研究 第1号
- 船舶の通航権をめぐる海事紛争と新海洋法秩序 第2号
- 広島日仏協会報 No. 81
- なつしま
- 昭和53年水産試験研究機関海洋観測資料
- 湖沼実習施設論文集 No. 20
- 海洋法と海洋政策 第5号
- 養殖研究所研究報告 第2号
- 養殖研ニュース No. 3
- RESTIC 8号
- 千葉県水産試験場研究報告 第40号
- A Phylogenetic and Biogeographic Analysis of Cyprinodontiform Fishes Vol. 168-4
- Novitates 2719
- 科学通報 Vol. 27, Nos. 2, 3
- Annals de l'institut océanographique Tome 57-2
- IOLR Collected Reprints Vol. 4
- Boletín do INIP N° 5
- Revue des travaux de l'institut des pêches maritimes Tome 44, Fasc.2, 3

日仏海洋学会役員

- 顧問 ユベール・ブロッシェ ジャン・デルサル
ジャック・ロペール アレクシス・ドラン
ール ペルナル・フランク ミシェル・ル
サージュ ロペール・ゲルムール ジャック・
マゴ
- 名誉会長 レオン・ヴァンデルメルシュ
会 長 佐々木忠義
副 会 長 黒木敏郎, 國司秀明
常任幹事 阿部友三郎, 有賀祐勝, 富永政英, 松生 治,
三浦昭雄
庶務幹事 佐伯和昭
編集幹事 村野正昭

幹 事 石野 誠, 井上 実, 今村 豊, 岩下光男,
宇野 寛, 川原田 裕, 神田献二, 菊地真一,
草下孝也, 斎藤泰一, 佐々木幸康, 高木和徳,
高野健三, 高橋 正, 辻田時美, 奈須敬二,
根本敬久, 半沢正男, 丸茂隆三, 森田良美,
山中麿之助 (五十音順)

監 査 久保田 穰, 岩崎秀人

評 議 員 青山恒雄, 赤松英雄, 秋山 勉, 阿部宗明,
阿部友三郎, 新崎盛敏, 有賀祐勝, 石野 誠,
石渡直典, 市村俊英, 井上 実, 今村 豊,
入江春彦, 岩崎秀人, 岩下光男, 岩田憲幸,
宇野 寛, 大内正夫, 小倉通男, 大村秀雄,
岡部史郎, 岡見 登, 梶浦欣二郎, 加藤重一,
加納 敬, 川合英夫, 川上太左英, 川村輝良,
川原田 裕, 神田献二, 菊地真一, 草下孝也,
楠 宏, 國司秀明, 久保田 穰, 黒木敏郎,
小泉政美, 小林 博, 小牧勇藏, 西条八東,
斎藤泰一, 斎藤行正, 佐伯和昭, 坂本市太郎,

佐々木忠義, 佐々木幸康, 猿橋勝子, 柴田恵司,
下村敏正, 庄司大太郎, 関 文威, 多賀信夫,
高木和徳, 高野健三, 高橋淳雄, 高橋 正,
谷口 旭, 田村 保, 千葉卓夫, 辻田時美,
寺本俊彦, 鳥羽良明, 富永政英, 鳥居鉄也,
中井基二郎, 中野猿人, 永田 正, 永田 豊,
奈須敬二, 奈須紀幸, 西沢 敏, 根本敬久,
野村 正, 半沢正男, 半谷高久, 樋口明生,
菱田耕造, 日比谷 京, 平野敏行, 深沢文雄,
深瀬 茂, 福島久雄, 淵 秀隆, 増沢謙太郎,
増田辰良, 松生 治, 丸茂隆三, 三浦昭雄,
三宅泰雄, 村野正昭, 元田 茂, 森川吉郎,
森田良美, 森安茂雄, 安井 正, 柳川三郎,
山路 勇, 山中麿之助, 山中一郎, 山中 一,
吉田多摩夫, 渡辺精一 (五十音順)

マルセル・ジュグラリス, ジャン・アンクテ
イル, ロジェ・ペリカ

賛 助 会 員

旭化成工業株式会社
株式会社内田老鶴園新社 内田梧
株式会社 オーシャン・エージ社
株式会社 オセアノート
小樽船舶電機株式会社
社団法人 海洋産業研究会
協同低温工業株式会社
小松川化工機株式会社
小 山 康 三
三信船舶電具株式会社
三洋水路測量株式会社
シュナイダー財団極東駐在事務所
昭和電装株式会社
新日本気象海洋株式会社
株式会社 鶴見精機
株式会社 東京久栄
東京製網繊維ロープ株式会社
株式会社 東邦電探
中川防蝕工業株式会社
日本アクアラング株式会社
日本テトラポッド株式会社
社団法人 日本能率協会
深田サルベージ株式会社
藤 田 峯 雄
古野電気株式会社
丸文株式会社
三井海洋開発株式会社
宮 本 悟
株式会社ユニオン・エンジニア
ング 佐野博持
吉野計器製作所
株式会社 読売広告社
株式会社 離合社
株式会社 渡部計器製作所

東京都千代田区有楽町 1-1-2 三井ビル
東京都千代田区九段北 1-2-1 蜂谷ビル
東京都千代田区神田美土代町 11-2 第1東英ビル
東京都世田谷区北沢 1-19-4-202
小樽市色内町 3-4-3
東京都港区新橋 3-1-10 丸藤ビル
東京都千代田区神田佐久間町 1-21 山伝ビル
東京都千代田区岩本町 1-10-5 TMMビル5F
東京都文京区本駒込 6-15-10 英和印刷社
東京都千代田区神田 1-16-8
東京都港区新橋 5-23-7 三栄ビル
東京都港区南青山 2-2-8 DFビル
高松市寺井町 1079
東京都世田谷区玉川 3-14-5
横浜市鶴見区鶴見中央 2-2-20
東京都中央区日本橋 3-1-15 久栄ビル
東京都中央区日本橋室町 2-6 江戸ビル
東京都杉並区宮前 1-8-9
東京都千代田区神田鍛冶町 2-2-2 東京建物ビル
神奈川県厚木市温水 2229-4
東京都港区新橋 2-1-13 新橋富士ビル9階
東京都港区芝公園 3-1-22 協立ビル
東京都千代田区神田錦町 1-9-1 天理教ビル8階
茨城県北相馬郡藤代町大字毛有 850 株式会社 中村鉄工所
東京都中央区八重洲 4-5 藤和ビル
東京都中央区日本橋大伝馬町 2-1-1
東京都千代田区一ツ橋 2-3-1 小学館ビル
東京都中央区かちどき 3-3-5 かちどきビル (株)本地郷
神戸市中央区海岸通 3-1-1 KCCビル4F
東京都北区西ヶ原 1-14
東京都中央区銀座 1-8-14
東京都千代田区神田鍛冶町 1-10-4
東京都文京区向丘 1-7-17

Exploiting the Ocean by...

T.S.K. OCEANOGRAPHIC INSTRUMENTS

REPRESENTATIVE GROUPS OF INSTRUMENTS AND SYSTEMS

T.S- 塩分計 DIGI-AUTO

《新製品》

本器は電磁誘導方式による卓上塩分計として画期的な T.S-E シリーズを全自動化した新製品です。その取扱いには熟練を必要とせず、誰にでも迅速・容易・正確に塩分値を計測する事が出来ます。

- ◎ 資料の海水ビンにチューブを入れてスタートボタンを押すだけで自動的に作動し塩分値を表示し又速かに試水は元にもどります。
- ◎ 大型 LED デジタル表示
- ◎ 高精度・高安定度
- ◎ 検出部にサンプルの吸入速度を自動的にコントロールしているのでセル部への気泡付着に気をを使う必要はありません。
- ◎ 電極式ではないため洗浄等のメンテナンスも容易です。
- ◎ 二重の安定装置によりポンプの寿命がのびました。



測定範囲	0~36 ‰ S
精度	±0.01 ‰ S
分解能	0.001 ‰ S
自動温度補償範囲	5~30°C
所要試水量	約 60 cc
電源	AC 100V 50/60Hz
重量	約 15 kg
寸法	450×250×400m/m

株式会社 鶴見精機

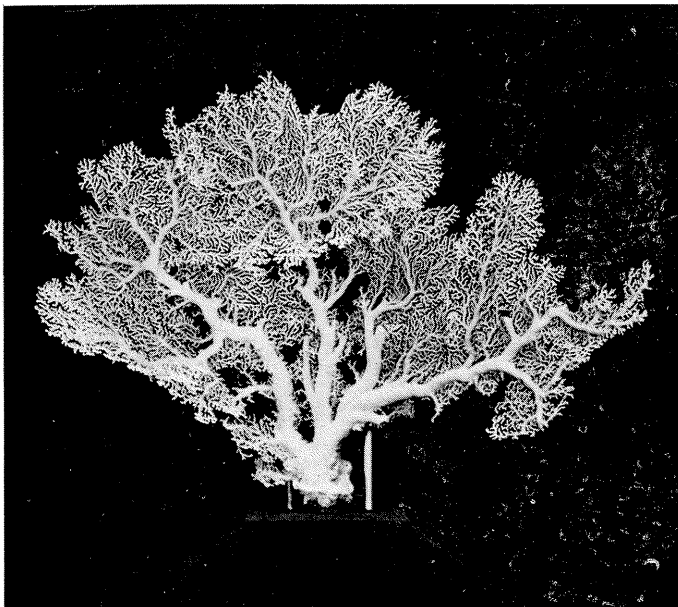
横浜市鶴見区鶴見中央2丁目2番20号 〒230 TEL; 045-521-5252

CABLE ADDRESS; TSURUMISEIKI Yokohama, TELEX; 3823750 TSKJPN J

OVERSEAS OFFICE; TSK-AMERICA INC. Seattle WASHINGTON

IWAMIYA INSTRUMENTATION LABORATORY

珊瑚美術館

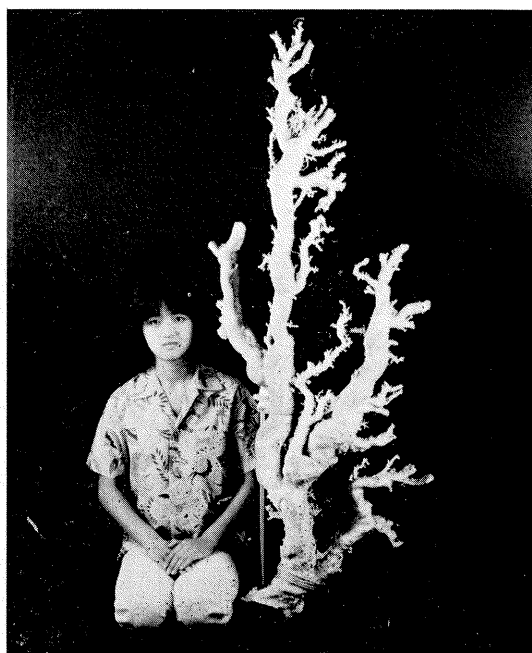


「クイーン・コーラル」 ↑
深海潜水艇“はくよう”により採集された、世界で一番美しい珊瑚。

高さ 1m 幅 1.2m 重さ 12kg

採集場所 徳之島近海

採集年月日 昭和54年7月4日



世界最大の珊瑚 →
高さ 1.6m、重さ 35kg の歴史上最大といわれる“ジャンボサンゴ”

採集場所 沖縄近海

採集年月日 昭和49年5月

花とさんごと美術館



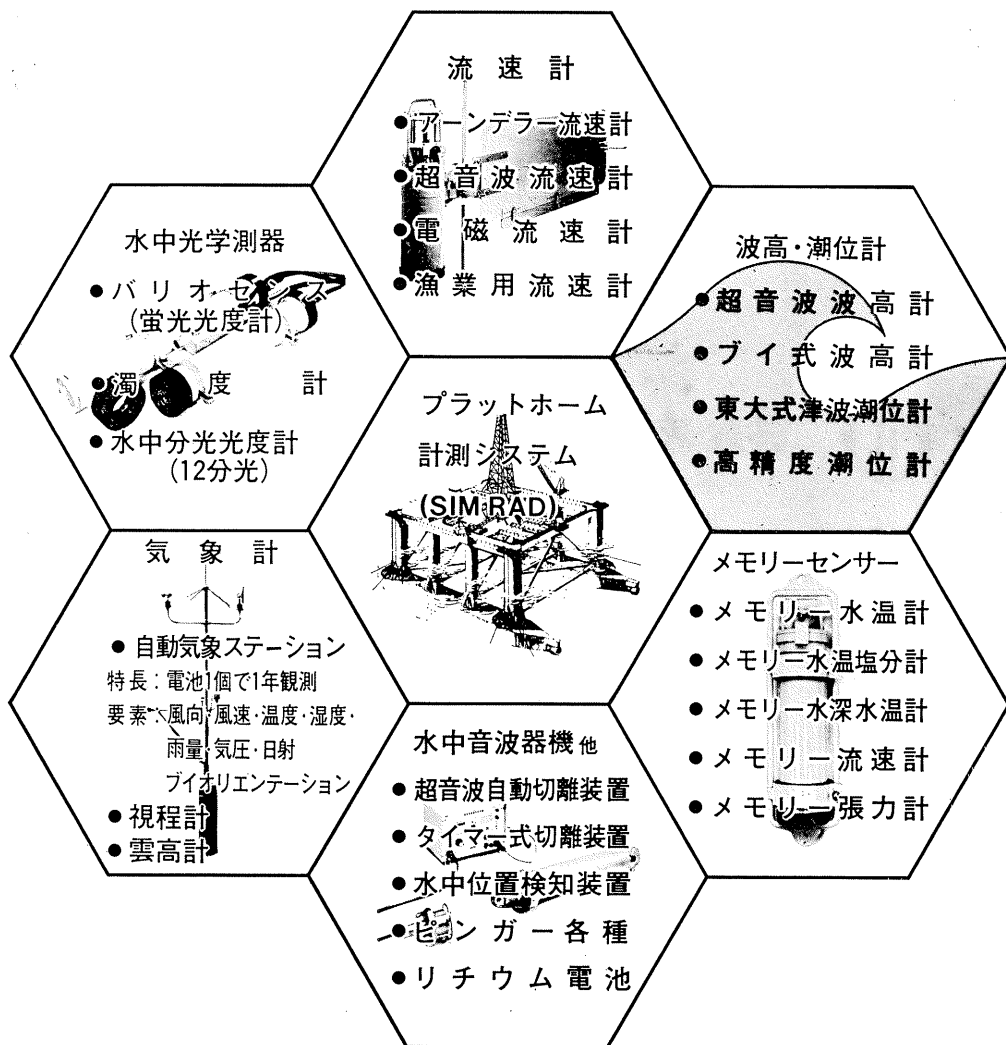
沖縄さんご園

本社 / 〒903 那覇市首里金城町 3-5 ☎ (0988) 86-3535 (代)
さんご園事業所 / 〒901-003 糸満市字摩文仁 1102 ☎ (09899) 7-3535 (代)
ホテル店事業所 / 〒903 那覇市首里山川町 1-132-1 ☎ (0988) 84-3535 (代)

ユニオン・エンジニアリングが
パーフェクトな観測をお約束する

海象・気象計測器

優れた精度・取扱い容易・世界的な実績・豊富な部品在庫・迅速確実なメンテナンス



株式会社 **ユニオン・エンジニアリング**
 本社 神戸市中央区海岸通3丁目1-1
 〒650 KCCビル4F TEL078-332-3381(代)
 東京支店 東京都中央区銀座7丁目18
 〒104 銀座スカイハイツ602号 TEL03-543-5399

Murayama

計 濁 度 中 水
計 照 度 中 水
計 導 度 電



株式会社 村山電機製作所

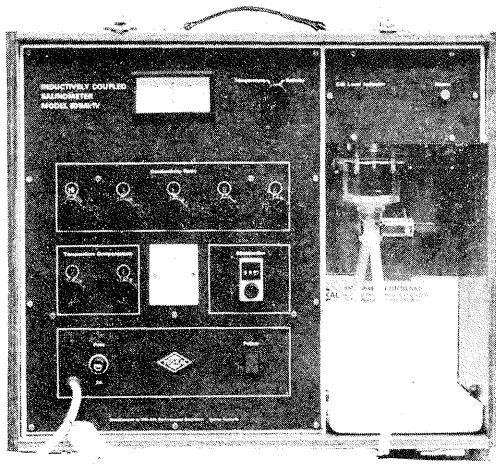
本社 東京都目黒区五本木2-13-1
出張所 名古屋・大阪・北九州

7IL は無限の可能性に挑戦する

- ◆ 漁撈電子機器
- ◆ 航海計器
- ◆ 海洋開発機器
- ◆ 航空機用電子機器
- ◆ 各種制御機器
- ◆ コンピュータ端末機器
- ◆ 各種情報システム



INDUCTIVE SALINOMER MODEL 601 MK IV



海水の塩分測定の標準器として、既に定評のあるオート・ラブ 601 MK III の改良型で、小型・軽量・能率化した高精密塩分計です。試料水を吸上げる際に、レベル検出器により吸引ポンプと攪拌モーターとが自動的に切換えられます。温度はメーター指針により直示されます。

測定範囲	0~51 ‰ S
感 度	0.0004 ‰ S
確 度	±0.003 ‰ S
所要水量	約 55 cc
電 源	AC 100 V 50~60 Hz
消費電力	最大 25 W
寸 法	52(幅)×43.5(高)×21(奥行)cm

営 業 品 目

転倒温度計・水温計・湿度計・
採水器・採泥器・塩分計・
水中照度計・濁度計・S-T計・
海洋観測機器・水質公害監視機器



株式 渡部計器製作所

東京都文京区向丘1の7の17
TEL (811) 0044 (代表) ☎ 113

昭和 57 年 5 月 25 日 印刷
昭和 57 年 5 月 28 日 発行

う み 第 20 卷
第 2 号

定価 円 1,200

編集者 富 永 政 英
発行者 佐 々 木 忠 義
発行所 日 仏 海 洋 学 会
財団法人 日仏会館内
東京都千代田区神田駿河台2-3
郵便番号: 1 0 1
電話: 03(291)1141
振替番号: 東京 5-96503

印刷者 小 山 康 三
印刷所 英 和 印 刷 社
東京都文京区本駒込 6-15-10
郵便番号: 1 1 3
電話: 03(941)6500

Tome 20 N° 2

SOMMAIRE

Notes originales

- Estimation of the Kuroshio Mass Transport Flowing out of the East China Sea
to the North PacificJunichi NISHIZAWA, Eturo KAMIHIRA, Kumio KOMURA,
Ryoji KUMABE and Masamori MIYAZAKI 55
- On the Outflow Modes of the Tsugaru Warm CurrentDennis M. CONLON 60
- Note on Currents Driven by a Steady Uniform Wind Stress on the Yellow
Sea and the East China SeaByung Ho CHOI 65
- Variations of Chlorophyll *a* Concentration and Photosynthetic Activity of
Phytoplankton in Tokyo BayYoshiaki SHIBATA and Yusho ARUGA 75
- On the Urohyal of Forty-Six Species of Fishes of the Order Cypriniformes
(in Japanese)Takaya KUSAKA 93
- Seasonal Distribution of Pelagic Chaetognaths in Relation to Variation of
Water Masses in Otsuchi Bay, Northern Japan (in Japanese)Makoto TERAZAKI and
Ryuzo MARUMO 111

Compte rendu

- A Review of Sea Conditions in the Japan SeaKenzo SHUTO 119

Miscellanées

- A Commentary Note on the Paper "On the Outflow Modes of the Tsugaru
Warm Current" by D. M. CONLONTakashi ICHIYE 125

- Procès-Verbaux 129

第 20 卷 第 2 号

目 次

原 著

- 東シナ海から北太平洋へ流出する黒潮流量の見積り (英文)西沢純一, 上平悦朗, 小村久美男,
隈部良司, 宮崎正衛 55
- 津軽暖流の流出モード (英文)Dennis M. CONLON 60
- 黄海と東シナ海で定常均一風によってひきおこされる海流 (英文)Byung Ho CHOI 65
- 東京湾における植物プランクトンのクロロフィル量と光合成活性の変動 (英文)柴田佳明, 有賀祐勝 75
- コイ目 (Cypriniformes) 魚類46種の尾舌骨 (Urohyal) の形状草下 孝也 93
- 大槌湾における毛顎類の性状と海況変動との関係寺崎 誠, 丸茂隆三 111

総 説

- 日本海の海況 (英文)周東 健三 119

寄 稿

- D. M. CONLON 著「津軽暖流の流出モード」に対するコメント (英文)市栄 誉 125

- 学会記事 129